GEORGIA DOT RESEARCH PROJECT 17-27

FINAL REPORT

# HYDRAULIC EFFECTS OF TEMPORARY BRIDGE CONSTRUCTION ACTIVITIES


**OFFICE OF PERFORMANCE-BASED MANAGEMENT AND RESEARCH**

**600 WEST PEACHTREE NW**
**ATLANTA, GA 30308**

# TECHNICAL REPORT DOCUMENTATION

| | | |
|---|---|---|
| **1. Report No.**<br>FHWA-GA-21-1727 | **2. Government Accession No.**<br>N/A | **3. Recipient's Catalog No.**<br>N/A |
| **4. Title and Subtitle**<br>Hydraulic Effects of Temporary Bridge Construction Activities | | **5. Report Date** October 2020<br>**6. Performing Organization Code**<br>N/A |
| **7. Author(s)**<br>Devan Fitzpatrick, Tanner Buggs, Timothy Stephens Roderick Lammers, and Brian Bledsoe, P.E. | | **8. Performing Organization Report No.**<br>N/A |
| **9. Performing Organization Name and Address**<br>University of Georgia<br>Athens, GA 30602 | | **10. Work Unit No.**<br>N/A<br>**11. Contract or Grant No.**<br>GDOT Project Number RP17-27 |
| **12. Sponsoring Agency Name and Address**<br>Georgia Department of Transportation<br>Office of Performance-based Management and Research<br>600 West Peachtree St. NW<br>Atlanta, GA 30308 | | **13. Type of Report and Period Covered**<br>Final Report (May 2018-October 2020)<br>**14. Sponsoring Agency Code**<br>N/A |

**15. Supplementary Notes**


**16. Abstract**

Bridge construction often requires placement of temporary features such as rock jetties and cofferdams in stream and river channels during the construction process. Environmental permitting agencies seek documentation, and in some cases quantification, of the potential effects of these temporary features on instream velocities and channel bank and bed scour; however, there is no existing guidance or standard method for evaluating the potential effects of these temporary construction features on hydraulics, bank stability, and biological habitats. This research improves the Georgia Department of Transportation's ability to effectively respond to environmental permitting agency concerns about the potential geomorphic and hydraulic effects of temporary instream jetties associated with bridge construction practices. This report describes the development and application of new modeling and risk assessment tools for predicting average changes in velocity and shear stress in the contracted reach affected by a jetty using readily available information. The results can be used to determine the potential hydraulic and geomorphic effects of jetties prior to structure emplacement, and provides information about the spatial distributions of velocity and shear stress changes near jetties in areas of potential concern. This report also documents the development of a risk assessment that synthesizes 1-D and 2-D hydraulic modeling results and predictive regressions for shear stress and velocity into one comprehensive spreadsheet-based tool for predicting the potential hydraulic and geomorphic effects of jetties when more complex modeling is infeasible. This research can be applied to a large array of structures, including both temporary and semi-permanent in-stream unsubmerged structures, and advances the current set of tools available for preliminary structural design and environmental management decisions.


| | | | |
|---|---|---|---|
| **17. Key Words**<br>Temporary Construction Platforms; Jetties; Hydraulic effects; Modeling; Prediction; Velocity; Shear stress; Risk assessment | **18. Distribution Statement**<br>No restrictions. | | |
| **19. Security Classification (of this report)**<br>Unclassified | **20. Security Classification (of this page)**<br>Unclassified | **21. No. of Pages**<br>166 | **22. Price**<br>Free |

DOT Research Project RP 17-27

Final Report

# HYDRAULIC EFFECTS OF TEMPORARY BRIDGE CONSTRUCTION ACTIVITIES

Devan Fitzpatrick, Tanner Buggs, Timothy Stephens, Roderick Lammers, and Brian Bledsoe, P.E.

University of Georgia
Institute for Resilient Infrastructure Systems

Contract with

Georgia Department of Transportation

In cooperation with

U.S. Department of Transportation Federal Highway Administration

October 2020

**Notice**

This document is disseminated under the sponsorship of the U.S. Department of Transportation in the interest of information exchange. The U.S. Government assumes no liability for the use of the information contained in this document.

The U.S. Government does not endorse products or manufacturers. Trademarks or manufacturers' names appear in this report only because they are considered essential to the objective of the document.

**Quality Assurance Statement**

The Federal Highway Administration (FHWA) provides high-quality information to serve Government, industry, and the public in a manner that promotes public understanding. Standards and policies are used to ensure and maximize the quality, objectivity, utility, and integrity of its information. FHWA periodically reviews quality issues and adjusts its programs and processes to ensure continuous quality improvement.

# SI* (MODERN METRIC) CONVERSION FACTORS

## APPROXIMATE CONVERSIONS TO SI UNITS

| Symbol | When You Know | Multiply By | To Find | Symbol |
|---|---|---|---|---|
| | | **LENGTH** | | |
| in | inches | 25.4 | millimeters | mm |
| ft | feet | 0.305 | meters | m |
| yd | yards | 0.914 | meters | m |
| mi | miles | 1.61 | kilometers | km |
| | | **AREA** | | |
| $in^2$ | square inches | 645.2 | square millimeters | $mm^2$ |
| $ft^2$ | square feet | 0.093 | square meters | $m^2$ |
| $yd^2$ | square yard | 0.836 | square meters | $m^2$ |
| ac | acres | 0.405 | hectares | ha |
| $mi^2$ | square miles | 2.59 | square kilometers | $km^2$ |
| | | **VOLUME** | | |
| fl oz | fluid ounces | 29.57 | milliliters | mL |
| gal | gallons | 3.785 | liters | L |
| $ft^3$ | cubic feet | 0.028 | cubic meters | $m^3$ |
| $yd^3$ | cubic yards | 0.765 | cubic meters | $m^3$ |
| | | NOTE: volumes greater than 1000 L shall be shown in $m^3$ | | |
| | | **MASS** | | |
| oz | ounces | 28.35 | grams | g |
| lb | pounds | 0.454 | kilograms | kg |
| T | short tons (2000 lb) | 0.907 | megagrams (or "metric ton") | Mg (or "t") |
| | | **TEMPERATURE (exact degrees)** | | |
| °F | Fahrenheit | 5 (F-32)/9<br>or (F-32)/1.8 | Celsius | °C |
| | | **ILLUMINATION** | | |
| fc | foot-candles | 10.76 | lux | lx |
| fl | foot-Lamberts | 3.426 | $candela/m^2$ | $cd/m^2$ |
| | | **FORCE and PRESSURE or STRESS** | | |
| lbf | poundforce | 4.45 | newtons | N |
| $lbf/in^2$ | poundforce per square inch | 6.89 | kilopascals | kPa |

## APPROXIMATE CONVERSIONS FROM SI UNITS

| Symbol | When You Know | Multiply By | To Find | Symbol |
|---|---|---|---|---|
| | | **LENGTH** | | |
| mm | millimeters | 0.039 | inches | in |
| m | meters | 3.28 | feet | ft |
| m | meters | 1.09 | yards | yd |
| km | kilometers | 0.621 | miles | mi |
| | | **AREA** | | |
| $mm^2$ | square millimeters | 0.0016 | square inches | $in^2$ |
| $m^2$ | square meters | 10.764 | square feet | $ft^2$ |
| $m^2$ | square meters | 1.195 | square yards | $yd^2$ |
| ha | hectares | 2.47 | acres | ac |
| $km^2$ | square kilometers | 0.386 | square miles | $mi^2$ |
| | | **VOLUME** | | |
| mL | milliliters | 0.034 | fluid ounces | fl oz |
| L | liters | 0.264 | gallons | gal |
| $m^3$ | cubic meters | 35.314 | cubic feet | $ft^3$ |
| $m^3$ | cubic meters | 1.307 | cubic yards | $yd^3$ |
| | | **MASS** | | |
| g | grams | 0.035 | ounces | oz |
| kg | kilograms | 2.202 | pounds | lb |
| Mg (or "t") | megagrams (or "metric ton") | 1.103 | short tons (2000 lb) | T |
| | | **TEMPERATURE (exact degrees)** | | |
| °C | Celsius | 1.8C+32 | Fahrenheit | °F |
| | | **ILLUMINATION** | | |
| lx | lux | 0.0929 | foot-candles | fc |
| $cd/m^2$ | $candela/m^2$ | 0.2919 | foot-Lamberts | fl |
| | | **FORCE and PRESSURE or STRESS** | | |
| N | newtons | 0.225 | poundforce | lbf |
| kPa | kilopascals | 0.145 | poundforce per square inch | $lbf/in^2$ |

## TABLE OF CONTENTS

## LIST OF FIGURES

## LIST OF TABLES

## EXECUTIVE SUMMARY

Bridge construction often requires in-channel placement of temporary structures such as rock jetties and cofferdams during the construction process. Environmental permitting agencies seek documentation, and in some cases quantification, of the potential effects of these temporary features on instream velocities and channel bank and bed scour; however, there is no existing guidance or standard method for evaluating the potential effects of these temporary construction features on hydraulics, bank stability, and biological habitats. The primary objective of this research was to improve the Georgia Department of Transportation's (GDOT) ability to effectively respond to environmental permitting agency concerns about the potential geomorphic and hydraulic effects of temporary instream jetties associated with bridge construction practices. The specific research objectives and general approach for this project included the following tasks:

1. Perform a literature review
2. Survey state Departments of Transportation (DOTs) on the use and design of temporary construction jetties
3. Establish temporary instream jetty scenarios
4. Conduct hydraulic modeling ensembles
5. Develop regression equations from modeling results to describe geomorphic and hydraulic changes
6. Conduct monitoring and hydraulic modeling of field sites to validate models
7. Develop a risk assessment tool
8. Develop a hands-on workshop outlining the tool fundamentals and research findings

Specific research on temporary construction jetties is limited, but jetties are similar to other, more permanent in-stream structures, including spurs, groynes, and abutments. The literature on these structures can help identify the potential effects of temporary jetties used for bridge construction. This previous work, as well as the results of the state DOT survey, was used to inform the hydraulic modeling undertaken in this study. Models were developed for a range of conditions, including jetty length and width, channel width and slope, and discharge. Thousands of one dimensional (1-D) Hydrologic Engineering Center – River Analysis System (HEC-RAS) models were run incorporating this variability. The results from these models were then used to develop a series of simple regression equations to predict relative and absolute changes in average velocity and shear stress in the channel due to flow constriction by the jetty. Results are valid for unsubmerged structures (i.e. flow does not overtop the jetty).

Additionally, a limited set of two dimensional (2-D) HEC-RAS models were used to explore the spatial pattern of increased velocity and shear stress. The regression models and 2-D model results were incorporated into an Excel macro-based tool to aid in the assessment of the hydraulic effects of jetties. This tool also incorporates a qualitative assessment of bank erosion risk that can be used to identify potential areas of bank instability post-jetty construction. The tool and regressions in this study can be applied to both temporary in-stream jetties along with other in-stream unsubmerged vertical wall structures installed perpendicular to the bank. For example, this research may also aid DOTs in understanding potential hydraulic and geomorphic effects of cofferdams attached to the channel bank that may also be used for bridge construction. This work advances the current set of tools available for preliminary jetty design and environmental management decisions.

Primary findings of this work include:

**State DOT Survey**

1. There is no specific protocol for determining jetty height (bed to top of the structure). Some state DOTs use the 2-year flood event, others use a given height above the average discharge. The longer the structure is in place, the more important designing the structure to the accurate height is to prevent overtopping. The longer the structure is in place, the larger the probability is that a large flood event may occur.
2. Jetties increase velocity the most right before the jetty overtops.
3. Jetties are not the only bridge construction option. At 4-5 ft of water depth, there is an economic breakpoint where jetties may become more expensive to construct and it may be more feasible to use a barge. Barges can be used in channels with approximately 7 ft of water and low currents. Bridge construction access is always site-dependent.
4. Jetty use and sizes are variable. Jetties are typically used on channels up to around 656 ft (200m). The maximum jetty top width of interest are typically around 50 ft, but the most common top width is 20 ft. Jetty contraction percentages (i.e. jetty length as a percent of channel width) typically range between 10% and 50%, but can be up to 70%.

5. Field reconnaissance indicates that jetties detectably influence hydraulic patterns compared to pre-construction conditions. The magnitude and nature of this influence is largely dependent on channel contraction percentage and discharge.

6. Jetties can be accurately modeled as blocked obstructions in 1-D HEC-RAS with ineffective flow areas and coefficients of contractions and expansions mimicking bridge abutment modeling techniques.

7. Channel contraction (represented as an area ratio) is the main variable describing the increase in velocity and shear stress due to jetties. This suggests that a jetty on one side of the river versus both sides of the river taking up the same area will likely yield the same increase in velocity. However, locations of maximum shear stress and velocity and potential bank erosion risks will be different.

8. Changes in velocities determined from 1-D HEC-RAS modeling results are well represented by easy to use regressions with only a single predictor variable (channel contraction). These regression equations are valid for contraction percentages less than 50% and Froude numbers less than 0.8.

9. Analytical techniques and HEC-RAS 1-D numerical modeling regressions yield similar results when predicting changes in velocity (velocity with jetty/velocity natural conditions). Analytical techniques combine the conservation of mass equation and Manning's Equation. The resulting equations differ slightly due to differences in assumptions and the ability of HEC-RAS to include energy losses associated with contractions and expansions.

10. Regression equations to predict the absolute velocity or shear stress with a jetty in place will require one of the following variables to be known: 1) the initial value for the natural channel condition at the discharge of interest, 2) water depth at the discharge of interest, or 3) discharge of interest.

11. The maximum allowable contraction percentage of 33% permitted by the United States Army Corps of Engineers (USACE) regional permit is a defensible threshold. Relative increases in both velocity and shear stress increase significantly at contractions above this threshold. In addition, contraction percentages of 30% for all channel sizes and discharges is expected to lead to increased velocities and shear stresses on the opposite bank compared to unobstructed channel conditions. The potential for bank erosion on the opposite bank is dependent on bank stability. Keeping contraction percentages below 30% is recommended when the banks opposite of the structures are susceptible to erosion and failure.

12. Higher discharges and higher contraction percentages lead to higher maximum values of velocity and shear stress and larger downstream distances impacted by increased velocities and shear stresses. However, these 2-D results are preliminary and more research is needed in this area to better understand the effects of jetties on spatial distributions in increased velocity and shear stress.

13. Jetty top width did not appear to increase the maximum velocity and shear stress in the channel.

14. Determining the most accurate estimate of the channel contraction area ratio (the main variable used in the regression models) is essential to accurate predictions of velocity and shear stress. If the actual channel bathymetry is known, it should be used to calculate the channel contraction area ratio.

This report is organized into 6 chapters. Chapter 1 is a literature review discussing relevant information obtained from experimental and hydraulic modeling studies about potential hydraulic and geomorphic effects of temporary riprap jetties used for bridge construction. Chapter 2 outlines the use of 1-D HEC-RAS modeling and analytical techniques to predict average changes in velocity and shear stress in the contracted reach affected by jetties. This chapter includes practical regression models for predicting average changes in velocity and shear stress in the contracted reach affected by a jetty as a function of physically-based variables derived from readily available information. Results from this chapter can be used to determine the potential hydraulic and geomorphic effects of jetties prior to structure emplacement. Chapter 3 describes 2-D HEC-RAS modeling analyses and provides information about the spatial distributions of velocity and shear stress near jetties concentrating on areas of maximum values and near bank regions. This chapter builds upon the parsimonious regression models described in Chapter 2, presenting a means for spatial interpretation of results. Chapter 4 outlines an Excel macro-based tool that incorporates both the 2-D spatial interpretation results and predictive regressions for shear stress and velocity. This tool can provide valuable insights into potential hydraulic and geomorphic effects of jetties before structure emplacement when more complex modeling is infeasible. The tool also includes a qualitative assessment of bank erosion risk. Chapter 5 is an application guide outlining how to use the developed predictive regressions and the Excel tool to predict potential hydraulic and geomorphic effects of jetties. The overall findings and conclusions of this study are presented in Chapter 6.

In addition to the main chapters, this report contains three appendices. Appendix A provides additional information on regression development and statistical analysis. Appendix B provides additional insight into using the developed regressions for actual channel bathymetries compared

to rectangular channels. Appendix C provides selected questions and answers from the Qualtrics survey conducted for this research project. The Qualtrics survey was sent to all 50 state DOTs and provides valuable insights into the use of jetties across the United States. Appendix D provides a sample field data collection sheet that can be used when applying the Excel tool.

# CHAPTER 1. REVIEW OF EXISTING LITERATURE AND PROJECT BACKGROUND

## INTRODUCTION

A wide range of human activities requires the emplacement of both temporary and semi-permanent structures in streams and rivers. One use of in-stream structures includes the installation of temporary riprap jetties for bridge construction and maintenance. Though the use of in-steam river training structures is a common practice, little research has been done specifically on the use of temporary jetties for bridge construction. In-stream river training structures can be broadly classified into two categories, sills and deflectors (Radspinner, Diplas, Lightbody, & Sotiropoulos, 2010). Sills are structures that generally extend across the entire channel, whereas deflection structures protrude into the channel flow from one bank and do not reach the other side (Shields, 1983). In-stream deflection structures obstruct the channel flow, directing flow away from the adjacent bank and increasing velocities. Jetties used for bridge construction can be classified as a deflection structure and have similar hydraulic characteristics to other in-stream unsubmerged deflection structures, including spur dikes, vertical wall abutments, and groynes. This literature review includes studies conducted on the use of these structures in general due to their similarities to jetties, providing insights into potential effects of jetties on velocity and shear stress in channels. Throughout this report, the term jetty or jetties refers to all these similar unsubmerged deflection structures.

### Temporary Riprap Jetties Overview

Temporary riprap jetties are placed in river channels by state DOTs to assist in bridge construction and maintenance. These structures are typically installed to allow access to bridges

when other methods to reach the bridge are not possible. Other methods to access a bridge during construction and maintenance include direct access from the bank using a crane, floating barges, or installation of temporary work bridges. Representatives from the Georgia Department of Transportation have identified jetties as a valuable option for accessing bridge construction projects when the bridge under construction cannot be accessed using another method. To float barges, velocities must be low and typically a minimum of a 7 ft water depth is required. Additionally, the barges typically require an anchor. Barges can be anchored using "spuds" or by anchoring to the shore. A minimum of 10 ft of stable substrate is typically required to anchor barges offshore. Implementation of temporary work bridges also typically requires a minimum of 10 ft of stable substrate. If conditions are not conducive to other methods for bridge construction access, temporary riprap jetties may be installed to gain access to the bridge.

Sizing of jetties is typically highly site and project dependent. Temporary jetties are typically installed perpendicular to the channel bank but can be oriented upstream or downstream to meet project needs. Some jetties are installed with fingers oriented at different angles from the base portion of the jetty projecting into the channel. Fingers can point upstream or downstream relative to the base structure protruding into the channel flow. Jetties typically have a minimum top width (20 ft) that allows for access by construction vehicles. The height of the jetty referenced from the channel bottom to the crest of the structure is dependent on site conditions and expected flows during the lifetime of the structure.

In 2019, the Federal Highway Administration reported 617,084 bridges in the United States (U.S.), with 12,518 of those bridges in Georgia (FHWA, 2019). Thirty-seven percent of U.S.

bridges reported in 2019 need repair costing an estimated $164 billion (ARTBA, 2020). The most recent American Society of Civil Engineers (ASCE) Infrastructure Report Card from 2017 gave the U.S.'s bridge infrastructure a C+ rating, indicating the need for further improvement on bridge infrastructure (ASCE, 2017). Though the percentage of bridges in poor condition appears to be decreasing in recent years (FTA, 2019), it is estimated to take at least 50 years to complete repairs (ARTBA, 2020). Bridge construction and maintenance are on-going efforts to maintain the nations aging transportation infrastructure. Due to the large number of bridges requiring maintenance in the U.S., the implementation of jetties at certain project sites may be required.

The use of jetties to conduct bridge construction and maintenance requires ample communication between state DOTs, environmental regulatory agencies, and contractors implementing the projects (Figure 1). For bridges crossing waterways, environmental permitting agencies may seek documentation, and in some cases quantification, of the potential effects of temporary construction structures on in-stream velocities, and channel bank and bed scour. For example, the USACE regional permit for Georgia requires detailed documentation and analysis for jetties that constrict the channel by more than 25%, and prohibits any jetties that span greater than 33% of the channel width (USACE, 2018). Bridge construction projects are largely a balance between project feasibility, environmental considerations, and sociological factors. This project focuses on developing a suite of predictive regression equations to estimate changes in hydraulics around jetties that can be incorporated into a tool to inform preliminary design decisions. Having a method or tool to understand the potential hydraulic and geomorphic effects of emplacing temporary jetties in rivers under a variety of conditions can help with communication between DOTs and environmental permitting agencies for a timely and effective permitting process. The

regressions developed in this study can be utilized as an important tool during communication efforts between regulatory permitting agencies and state DOTs working to balance project feasibility and environmental considerations during bridge construction projects (Figure 1).

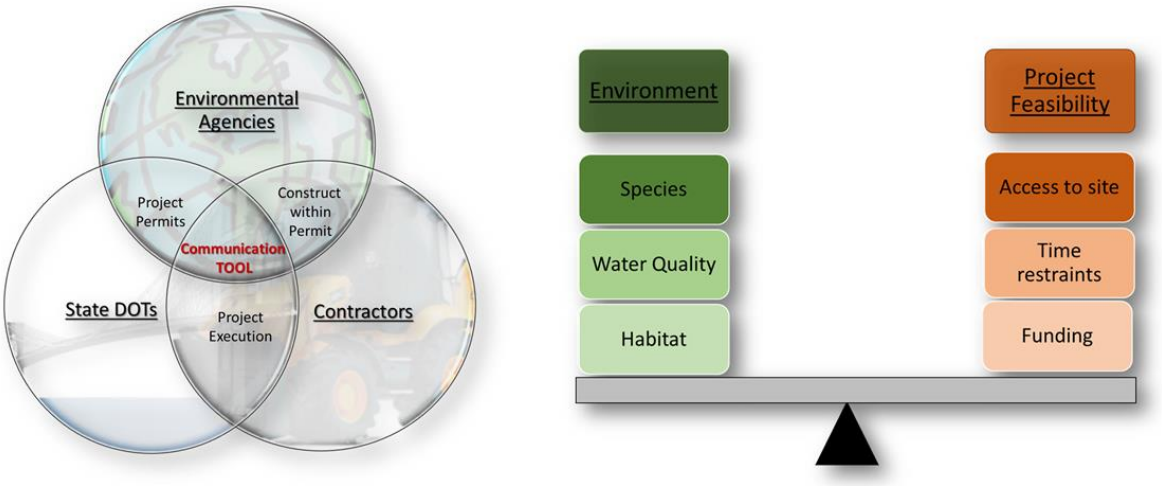


**Figure 1. Bridge construction actors and objectives. Representation of bridge construction project key actors (Venn diagram on left) and two components of bridge construction that need to be balanced for project success (on right). Key actors in bridge construction include state DOTs, environmental permitting agencies and contractors.**

### Similarities Between Jetties and Other In-stream Structures

Other in-stream structures similar to temporary riprap jetties include groynes, spur dikes, and abutments. All of these structures exhibit similar hydraulic characteristics. Structures such as groynes, and spur dikes are commonly used to stabilize channels, modify river planform, protect existing infrastructure and resources, improve channel navigation, reduce flood risks, and improve habitat quality. Jetties and the other aforementioned structures can have effects on river hydrologic and geomorphic processes (Figure 2). For example, constricting channel flow can

lead to local increases in velocity and shear stress that may result in increased bed scour and erosion on the opposite bank. Increased velocity can impede the movement of aquatic organisms, and scour can alter habitats such as mussel beds. Quantifying and predicting potential changes in hydraulics due to jetties provides valuable insight to DOTs that can be used to aid in protecting scour-prone habitats, ensuring migratory pathways for native fish species, and reducing potential bed and bank erosion. Previous research on semi-permanent structures such as spurs and groynes is extensive but lacks connection to jetties, making it previously challenging for DOTs to utilize a valuable body of literature. This literature review aimed to provide insight into the connections between jetties and other structures, identifying a large body of literature relevant to installation and design of jetties.


**Figure 2. Photos of jetties. Temporary riprap construction structures implemented for bridge construction (a) and dam removal (b). The bridge construction picture (a) was taken at the Chattooga River Georgia Department of Transportation bridge construction site.**

## HYDRAULIC EFFECTS OF JETTIES AND OTHER STRUCTURES

Jetties, like other in-stream deflection structures, extend from one bank into the main channel, constricting and redirecting the flow. They can vary in their contraction ratio, construction material, permeability, tip shape, and bank orientation (Brown, 1985), depending on the desired use. The percent of the channel flow obstructed, the deflection structure permeability, tip shape, and orientation can impact local velocities and scour patterns (Brown, 1985; Seed, 1997). The hydraulic and geomorphic changes due to emplacement of jetties may have important implications for habitat and aquatic organism passage. Understanding how different contraction percentages, permeabilities, and installation angles may impact the hydraulic and geomorphic effects of implementing jetties is important to the design and permitting process.

### Velocity and Flow Field Around Jetties and Other Structures

Implementation of a jetty or any other structure obstructs channel flow, reducing the overall flow area, *A*, for a constant discharge, *Q*. By conservation of mass (Eq. 1), it is well-known that constricting flow area for a constant discharge will cause an increase in velocity, *V*. Thus, implementation of jetties is expected to increase local velocities. The magnitude of the change in velocity, and the general flow field, has been found to depend on the physical characteristics of the structure itself.

**Eq 1.** $Q=VA$

The flow field around jetties has been found to be turbulent and three-dimensional, consisting of three general regions: the main flow zone, the mixing zone, and the return flow zone (Figure 3; Zhang & Nakagawa, 2008). Highest velocities due to jetties and other structures have been found to occur near the structure tip (Molinas, Kheireldin, & Wu, 1998; Rajaratnam & Nwachukwu, 1983). Velocities in the main flow zone are also accelerated due to the contraction. Therefore, the channel cross section constricted by a jetty is expected to have higher velocities than the natural, unobstructed condition. Eddies develop upstream and downstream of the structure due to the abrupt change in the flow area. In the return flow zone, two eddies of different sizes commonly occur with a small eddy near the structure and a larger eddy farther downstream (Zhang & Nakagawa, 2008). The reattachment point is the location downstream of the emplaced structure, where the separated flow reattaches to the channel bank (Zhang & Nakagawa, 2008).

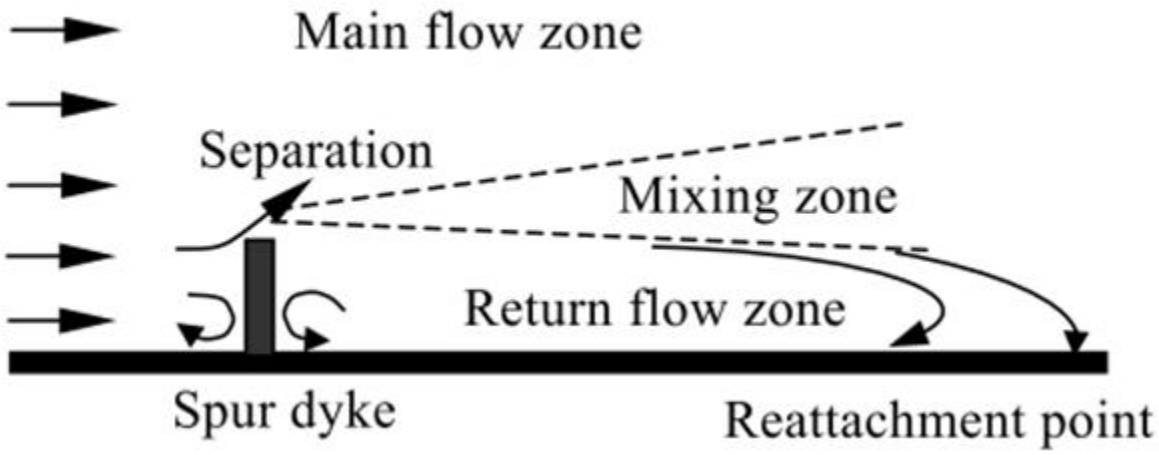


**Figure 3. Jetty hydraulics. Main flow zones near a jetty as represented by Zhang et al. 2008.**

The reattachment length has been a common phenomenon discussed in both flume and modeling studies (Karim & Ali, 1999; Oullion & Dartys, 1997; Yazdi, Sarkardeh, Azamathulla, & Ghani,

2010). The length has been found to be dependent on the length the emplaced structure projects into the main flow. However, the exact multiplier to the length of the structure has varied between studies. Oullion and Dartys (1997) reported the reattachment length for a structure perpendicular to the channel flow to be $11.5L_s$ for experimental flume results and $10.7L_s$ for a numerical modeling study, where $L_s$ is the structure protrusion length into the flow. Karim and Ali (1990) reported a reattachment length of $11L_s$ for a modeling study. The reattachment length suggests the approximate downstream length required for flow conditions to begin returning to upstream, unimpacted flow patterns, and is useful to determine potential structure impact areas. Based purely on the reattachment length, it is probable that jetties may influence the hydraulics over 11.5 times the structure length downstream of the structure tip. However, the highest velocity and shear stress are likely to be located near the jetty tip.

**Bed Scour**

Total bed scour in a riverine system is comprised of three components: general scour/bed degradation, contraction scour, and local scour (Fischenich & Landers, 1999). General scour or bed degradation removes bed material across the entire width of a channel, while contraction scour and local scour are processes that occur in certain locations. Contraction scour occurs at a channel contraction and local scour occurs where a structure obstructs flow (Fischenich & Landers, 1999). In areas impacted by jetties or other structures, all three types of bed scour occur. Scour depth at jetties and other in-stream structures depends on fluid and bed sediment characteristics, flow conditions, channel geometry, and the geometry of the emplaced structure (Zhang & Nakagawa, 2008). A horseshoe vortex forms in the scour hole upstream of the structure, and a wake vortices system forms on the downstream side of emplaced structures

(Pandey, Ahmad, & Sharma, 2018; Zhang & Nakagawa, 2008). These vortex systems are important to scour processes.

Bed scour is a patchy phenomenon and often is hard to predict. Velocity and shear stress can be used as proxies for identifying potential locations at risk for scour. Critical shear stress and permissible velocities can provide estimates for sediment entrainment near jetties. In addition to bed scour, bank scour may occur at contracted regions impacted by jetties due to increased velocities, development of eddies, and realignment of channel flows.

**Experimental Studies: Flume and Field for In-Stream Structures**

Numerous experimental and modeling studies have been conducted to evaluate mean-flow fields, local scour patterns, and turbulence characteristics around singular unsubmerged spurs, groins, and abutments. These experimental and modeling studies may have been conducted on more permanent structures, but are still mainly applicable to temporary riprap jetties. Early experimental flume studies focused on local mean-flow fields, scour depths and bed shear stress distributions (Melville, 1992; Molinas et al., 1998; Rajaratnam & Nwachukwu, 1983a, 1983b,). These early studies found increases in velocity and shear stress in the contracted regions with maximum bed shear stress occurring near the tip of the structure (Molinas et al., 1998; Rajaratnam & Nwachukwu, 1983a, 1983b).

Several studies sought to improve understanding of 2-D flow features utilizing visual observation and large scale particle velocimetry (Ettema & Muste, 2004; Koken & Constantinescu, 2008;

Yeo et al., 2005). Recent experimental studies have focused not only on mean flow fields but also on characterizing 3-D turbulence dedicated to understanding scour mechanisms or providing data for verification of numerical modeling results (Dey & Barbhuiya, 2005; Duan, 2009; Duan et al., 2009; Jeon et al., 2018; Zhang et al., 2009). Previous studies have used rectangular flumes and collected 3-D velocity data using acoustic doppler velocimeters (ADV) (Duan et al., 2009; Duan, 2009; Jeon et al., 2018). Duan et al. (2009) presented mean flow fields and 3-D hydraulic characteristics in a stable flatbed, while Duan (2009) presented hydraulic characteristics for both a scoured bed and a smooth channel bed. Jeon et al. (2018) evaluated 3-D flow characteristics for two different discharges in the vicinity of jetties for a stable bed and provided detailed 3-D ADV data. Experimental flume studies have evaluated the effects of structure length, shape, permeability, and orientation angle on hydraulic characteristics. However, flume studies are generally limited in the number of scenarios that can be evaluated, often necessitating hydraulic model simulation to further understand outcomes of interacting variables across variable site conditions.

**Hydraulic Modeling Studies around In-Stream Structures**

Due to the 3-D nature of flow fields in contracted reaches impacted by jetties and other structures, numerical modeling studies typically are two- or three-dimensional. Studies utilizing 2-D depth-averaged models have computed velocity (Molls, Hanif Chaudhry, & Wasey Khan, 1995) and, in some cases, bed shear stress distributions in contracted reaches (Ali, Hasan, & Haque, 2017; Tingsanchali & Maheswaran, 1990). Three-dimensional hydraulic models have been conducted to further evaluate mean-flow fields and bed shear stresses (Zhang and Nakagawa, 2008; Oullion & Dartys, 1997), determine effects of permeability and contraction

percentages on tip velocities (Ho, Yeo, Coonrod, & Ahn, 2007), evaluate impacts of orientation angle on flow fields (Koken, 2011; Yazdi et al., 2010), and provide detailed insight into turbulence characteristics and scour mechanisms (Koken, 2011; Koken & Constantinescu, 2008; Li, Lang, & Ning, 2013; Zhang, Nakagawa, Kawaike, & Baba Yasuyuki, 2009). Some studies have utilized commercially available software, including Flow-3D (Ho et al., 2007; Li et al., 2013) and Fluent (Karim & Ali, 1999; Yazdi et al., 2010) that could be used for modeling jetties by DOTs. Multi-dimensional hydraulic modeling is becoming more common in practice; however, 2-D and 3-D modeling techniques can be costly and time consuming, limiting their use by practitioners. Development of regressions to predict changes in hydraulics around jetties can limit the need for more complex modeling by DOTs when evaluating different jetty construction options.

## DESIGN GUIDELINES AND PREDICTIVE RELATIONSHIPS FOR IN-STREAM STRUCTURES

The extensive research conducted on and widespread application of semi-permanent structures such as groynes and spurs has led to the establishment of design guidelines (Brown, 1985; Lagasse et al., 2009a) and regression equations to predict maximum velocities (Seed, 1997; Yeo, Kang, & Kim, 2005). These design guidelines and regression equations for maximum velocities, though developed for more permanent structures, are also expected to be useful for jetties. The design guidelines and predictive relationships revealed during this literature review may be helpful for structural design and predicting maximum velocities; however, they do not address the cross section-averaged changes in hydraulics that may be useful to address permitting and regulatory concerns such as for fish passage and physical habitat. This study developed

regressions for cross section averaged changes in velocity to aide DOTs in predicting changes in cross section averaged (mean) values without the need for extensive hydraulic modeling. The regressions developed in this study can be used alongside existing guidelines and predictions for maximum velocities outlined by previous researchers. Some of the most relevant literature on design guidelines for more permanent structures that will still be useful for the design of jetties is discussed below. The literature outlined served as good potential references for DOT engineers and biologists working to design and limit potential impacts of jetties.

Brown (1985) provided general recommendations for the application and design of spur-like structures, addressing permeability, structure length, the spacing between multiple structures for bank protection, structure orientation angle relative to the bank, structure height, structure geometry, and maintaining structure contact with the channel bed and bank. This early report outlines recommendations for spur design largely based on bank protection efforts and provides initial insight into potential velocity and scour effects due to structure emplacement. However, this report lacks the development of equations that can be applied to quantify potential changes in velocity or shear stress for a range of structure types and contractions.

Seed (1997) used results from a validated 2-D rectangular model to predict relative changes in velocities due to groyne fields considering structure length, the spacing between multiple structures for bank protection, structure orientation angle relative to the bank, and the taper of the groyne. The study focused on predicting three velocities: the maximum depth-averaged velocity in the main channel between groynes, the near-bed velocity near the groyne tip, and the near-bed velocity at the toe of the riverbank. This study is useful for groyne fields and predicting

maximum bed velocities; however, it lacks predictive relationships for cross section-averaged changes in velocity and does not attempt to predict shear stress. Yeo et al. (2005) developed relationships to predict depth-averaged velocity at the tip of a single groyne using results from flume studies, expanding upon results by (Seed 1997).

The Federal Highways Administration has synthesized bridge scour and stream stability countermeasures in a series of reports (Lagasse et al., 2009b). Volume 2 of this report specifically addresses design guidelines for spur dike structures. This study focuses on the use of spurs for bank protection and improving flow alignment under bridges. The report provides general guidelines to select spur type, permeability, spur orientation angle relative to the bank, and riprap sizing. Similar to the peer-reviewed literature, this report also lacks quantitative predictions for changes in velocity and shear stress.

Molinas et al. (1998) developed regressions to predict the total bed shear stress near abutments based on experimental data for three different contraction percentages (10%, 20%, and 30%). Total bed shear stress was calculated as the sum of shear stress due to the contraction and shear stress due to the emplaced structure. These equations for bed shear stress require the Froude number, making shear stress challenging to predict without having conducted hydraulic modeling or knowing the depth of water at the structure. Regressions developed in this report aim to limit the need for a Froude number for ease of application by DOTs.

## SUMMARY OF JETTY EFFECTS ON VELOCITIES AND SHEAR STRESS

Numerous jetty characteristics, including structure length, permeability, geometry, and installation angle relative to the bank, have been found to impact velocities and shear stress in regions contracted by jetties. Table 1 summarizes general conclusions about jetty characteristic effects on velocities and bed shear stresses, assuming constant channel size and discharge.

**Table 1. Jetty hydraulic effects. Jetty effects on velocities and bed shear stress in river channels.**

| Characteristic | Shear Stress | Velocity | Study Examples |
|---|---|---|---|
| **Length** | Direct relationship | Direct relationship | Molinas et al., 1998<br>Yazdi et al., 2010 |
| **Permeability** | Inverse relationship with shear and tip depth. Scour occurs at all openings in permeable jetties | Inverse relationship | Yeo et al., 2005<br>Ho et al., 2007<br>Zhang & Nakagawa, 2008 |
| **Installation Angle** | Structures at 90° to flow have the highest shear stresses compared to structures orientated upstream or downstream | Structures at 90° have the highest velocities | Yazdi et al., 2010<br>Melville, 1992 |

# CHAPTER 2. DEVELOPMENT OF PREDICTIVE REGRESSION MODELS TO ESTIMATE SHEAR STRESS AND VELOCITY IN REGIONS CONTRACTED BY JETTIES

The overall goal of this chapter is to develop parsimonious models to predict changes in mean velocity and bed shear stress due to the emplacement of temporary riprap jetties, which will aide Georgia Department of Transportation (GDOT) in preliminary structure design, environmental management, and regulatory decision making. This research aims to develop straightforward and efficient tools that can be applied to jetties for planning, preliminary design, and decision making when more complex modeling is infeasible. Modeling can be costly and time consuming, limiting the ability of DOTs to predict potential effects of temporary jetties on local mean velocity and shear stress for a range of channel sizes, contractions, and flow conditions. The predictive regressions developed in this chapter only require a few physically-based predictor variables derived from readily available information for ease of application. Readily available information refers to measurements that can be easily obtained during field site visits or from readily available software and data sets such as Geographic Information System (GIS) and stream gauges.

The specific objectives of this chapter are:

1. Evaluate the use of 1-D analysis using the widely available Hydrologic Engineering Center - River Analysis System (HEC-RAS) to predict mean changes in velocity and shear stress in regions contracted by jetties by comparing model predictions with

previous experimental studies. This objective ensures HEC-RAS can accurately model changes in hydraulics around temporary jetties.

2. Systematically develop and execute >50,000 hydraulic model simulations that adhere to geomorphic scaling properties to represent a wide range of realistic channel sizes, geomorphic settings, channel roughness characteristics, contraction percentages, and discharges. Developing a large dataset of potential construction scenarios utilizing jetties for bridge construction ensures that developed models can be used for a large variety of situations GDOT may encounter when utilizing jetties.
3. Use results from 1-D hydraulic model simulations in combination with analytical techniques to develop practical regression relationships for predicting mean changes in velocity and shear stress at the contracted river cross section as a function of physical variables that can be derived from readily available information.
4. Perform field measurements of velocity changes at jetties at an active bridge construction site and combine these observations with existing flume studies to test the new predictive relationships. This objective ensures that the developed regression models are accurate.

## METHODS

A combination of analytical approaches, 1-D hydraulic modeling and regression analysis were used to assess the effects of jetties on mean hydraulics (Figure 4). An analytical approach informed independent variable selection for regression models. One-dimensional hydraulic modeling was performed in HEC-RAS to develop an extensive data set spanning a wide range of channel conditions and geometries to develop predictive regressions for altered shear stress and

velocity in jetty contraction regions. Field and flume data were used to assess the performance of the developed regression models.

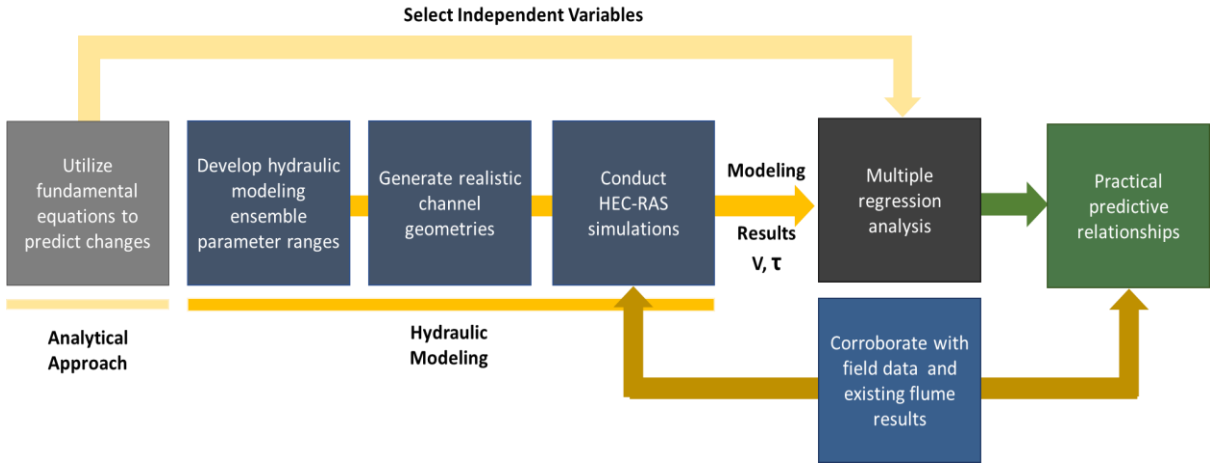


**Figure 4. Study methodology. Overview of the study methodology that includes an analytical approach, hydraulic modeling, multiple regression analysis, and corroboration of modeling results and predictive regression equations using existing flume studies and collected field data.**

## Analytical Approach

An analytical approach based on conservation of mass and the Manning equation was used to characterize hydraulic changes around jetties in rectangular channels and to identify potential independent variables for predictive regression models (Figure 4). Continuity under steady flow requires that cross-sectional area, $A$, discharge, $Q$, and velocity, $V$ are related according to Eq. 2. To determine the relative change in mean $V$ due to structure emplacement, Eq. 3 can be rearranged to solve for the ratio of the velocity with the structure in place, $V_s$, to the initial velocity, $V_i$ (Eq. 4). Relative changes in $V$ become a simple function of unobstructed flow area, $A_i$, and flow area with the structure in place, $A_s$.

**Eq 2.** $Q = VA$

**Eq 3.** $V_i A_i = V_s A_s$

**Eq 4.** $A_i / A_s = V_s / V_i$

When predicting $V_s$, Eq. 4 can be rearranged given that $V_i$ for a given $Q$ is known (Eq. 5). In practice, the $V_i$ for a given $Q$ can be obtained through direct measurement, hydraulic modeling, or through estimation using the Manning equation. Here we use the Manning equation to develop Eq. 6, where $R$, $S$, $n$ and $\emptyset$ are the hydraulic radius, bed slope, Manning's roughness and a units conversion factor (1.49 for English, and 1 for SI), respectively (Chow, 1959), recognizing that hydraulic modeling and field measurements are often infeasible. This is especially true when conducting large numbers of studies at different sites across multiple discharges, which may be common during the initial phases of bridge construction projects. The flow area with the structure in place, $A_s$, can be re-written as $A_i$ subtracted from the structure area, $A_{st}$.

**Eq 5.** $V_s = V_i * [A_i / A_s]$

**Eq 6.** $V_s = \left[\left(\frac{\emptyset}{n}\right) * R^{\frac{2}{3}} * S^{\frac{1}{2}}\right] * [A_i / (A_i - A_{st})]$

The second term of Eq. 2 is the ratio of the unobstructed channel area to the flow area with the structure in place. Since the unobstructed channel area is the flow area with the structure in place added to the structure area, the second term of Eq. 6 can be re-written as the structure area divided by the flow area with the structure in place, $A_{st}$, plus one (Eq. 7). The structure area divided by the flow area with the structure in place (*aaratio*) has been identified as a critical empirical variable by other studies to predict tip velocities (Seed, 1997; Yeo *et al.*, 2005), maximum depth-averaged channel velocities and near bank bed velocities around jetties (Seed,

1997). To complete the analytical solution, the $R$ can be replaced with initial water depth, $D_{i,}$ assuming a large width to depth ratio (Eq. 8). The structure and flow areas can be expanded into their core variable forms (Eq. 8), where $W_c$ and $L_s$ are the channel unobstructed width and the length of the structure projecting into the channel flow.

$$\textbf{Eq 7. } V_s = \left[\left(\frac{\emptyset}{n}\right) * R^{\frac{2}{3}} * S^{\frac{1}{2}}\right] * \left[\left(\frac{A_{st}}{A_i - A_{st}}\right) + 1\right]$$

$$\textbf{Eq 8. } V_s = \left[\left(\frac{\emptyset}{n}\right) * D_i^{\frac{2}{3}} * S^{\frac{1}{2}}\right] * \left[\left(\frac{(L_s * D_s)}{(W_c * D_i) - (L_s * D_s)}\right) + 1\right]$$

Noting that shear stress $(\tau)$ is proportional to $V^2$, it follows that parameters identified by the analytical solution for $V$ should also serve as useful predictive variables for $\tau$. To use the analytical solution directly to determine $V_{s,}$ the depth of water interacting with the structure, $D_{s,}$ and water depth before structure emplacement, $D_{i,}$ must be known. The use of the analytical solution is limited; determining $D_s$ and $D_i$ requires field measurements, hydraulic modeling, or introduction of additional equations. However, under conditions where the flow is not choked, these depths are assumed to be relatively similar, resulting in the *aaratio* being largely dependent on the contracted width (Eq. 9). Here we focus on developing an *aaratio* for rectangular channels; however, this ratio can be defined for other simplified geometries or calculated directly if the bathymetry of a channel and the dimensions of an obstruction are known.

$$\textbf{Eq 9. } V_s = \left[\left(\frac{\emptyset}{n}\right) * D_i^{\frac{2}{3}} * S^{\frac{1}{2}}\right] * \left[\left(\frac{(L_s)}{(W_c) - (L_s)}\right) + 1\right]$$

## Hydraulic Modeling

Hydraulic modeling was conducted using the United States Army Corps of Engineers (USACE) 1-D Hydrologic Engineering Center River Analysis System (HEC-RAS) Version 5.0.3 (Brunner, 2016a). Hydraulic modeling was performed as a complement to the analytical solution because HEC-RAS includes eddy losses in the form of contraction and expansion coefficients and ineffective flow areas (Brunner, 2016b) that can occur downstream and upstream of jetties. Although previous studies have shown that the flow field around jetties is complex in nature, 1-D modeling in HEC-RAS was chosen to allow thousands of model simulations representing a full array of geomorphic settings and jetty contractions to be performed. Running the full array of conditions in 2-D is largely infeasible given the significantly greater time and computational demands associated with running 50,000 simulations in 2-D. Additionally, accurate calibration of some 2-D modeling coefficients for a large array of conditions is impractical, leading to potential increased errors. HEC-RAS has been used extensively to model bridge hydraulics and abutments. Hydraulic characteristics around spurs and groynes are similar to abutments (Molinas *et al.*, 1998; Zhang and Nakagawa, 2008), suggesting 1-D HEC-RAS models can estimate mean velocities around jetties with reasonable accuracy. Additionally, HEC-RAS can be controlled autonomously through Visual Basic for Applications (VBA) utilizing the HECRAS Controller (Goodell, 2014), allowing large numbers of model simulations to be completed in batch mode.

For this study, we compared 1-D HEC-RAS model results to two previously conducted flume studies (Duan *et al.*, 2009; Jeon *et al.*, 2018) to confirm the capability of 1-D HEC-RAS to accurately determine mean velocities around jetties before additional modeling was performed in batch mode. Jeon et al. (2018) flume data from supplemental materials and Duan et al. (2009)

relative changes in mean velocity data due to an in-stream structure were used to corroborate the HEC-RAS model prediction capabilities around jetties. To develop a large data set for developing predictive regressions, we performed 50,000 hydraulic modeling simulations by automating 1-D HEC-RAS using VBA, where hydraulic modeling ensembles were systematically developed to represent a range of rectangular channel geometries, contraction percentages, roughness scenarios, and discharges.

### *Determination of Hydraulic Modeling Ensemble Parameter Ranges*

Before conducting hydraulic modeling to determine potential changes in velocity and shear stress due to temporary jetties, a range of construction feature scenarios needed to be determined. Different scenarios include ranges of jetty geometries, channel geometries, and jetty placement/orientation within the channel. Parameter ranges for hydraulic modeling were defined using plausible ranges of channel geometries suitable for the emplacement of temporary riprap jetties and typical jetty sizes. Such structures tend to be implemented on wide, relatively shallow rivers where access from the bank using a crane and floating barge are infeasible.

Channel geometric characteristics of interest for HEC-RAS modeling included average channel depth, top width, and bed slope. Jetty characteristics included length, installation angle, width, and the percent of the channel constricted (contraction %). Ranges of plausible channel and structure characteristics were defined using plans for seven Georgia Department of Transportation (GDOT) bridge construction projects that implemented temporary riprap construction platforms (

Table 2) and survey data received from 26 additional state DOTs. Survey results were used to supplement information provided by GDOT to garner insights about temporary structure implementation across the US, including the structure and channel characteristics (Appendix C). Survey results indicated a contraction % range of 10% -70% with a typical maximum of 50%. Synthesizing results from the survey and example projects, we (research team) developed realistic model ensemble ranges for channel geometries and contraction percentages (Table 3). All model simulations were conducted with structures placed perpendicular to the flow and banks.

**Table 2. Example projects. Channel and temporary structure characteristics of example projects with temporary structures.**

| **Channel characteristics of example projects with temporary structures** | | | |
|---|---|---|---|
| **Parameter** | **Symbol** | **Max** | **Min** |
| Bed Slope | $S$ | 0.1% | 0.03% |
| Channel Width (ft) | $W_c$ | 332 | 133 |
| Channel Depth(ft) | $D_c$ | 22.5 | 10 |
| **Temporary structure characteristics based on state DOT construction projects** | | | |
| **Parameter** | **Symbol** | **Max** | **Min** |
| Platform Width (ft) | $W_s$ | 139 | 24 |
| Platform Length (ft) | $L_s$ | 104 | 69 |
| Percent Contraction | $NA$ | 67% | 31% |
| Angle from Bank | $\angle$ | 130° | 90° |
| Time in the water (months) | $t$ | 24 | 1 |

**Table 3. Summary of model values. Summary of model ensemble ranges, parameter ranges and features.**

| **Model Ensemble Ranges** | | | |
|---|---|---|---|
| **Parameter** | **Symbol** | **Max** | **Min** |
| **Bed Slope** | $S$ | 2.00% | 0.001% |
| **Channel Width (ft)** | $W_c$ | 664 | 33 |
| **Channel Depth (ft)** | $D_c$ | 46 | 3 |
| **Percent Contraction** | *NA* | 80% | 10% |
| **Angle from Bank** | $\angle$ | 90° | 90° |
| **Model Parameter Ranges** | | | |
| **Parameter** | **Description** | **Range** | **Modeling Values** |
| **Contraction Percentage** | Percentage of channel width the jetty constricts | 0%-80% | 0%, 10%,20%,30%, 33%, 40%, 50%, 60%, 70%, 80% |
| **Manning's *n*** | Representation of channel roughness | 0.02-0.04 | 0.02, 0.025, 0.03, 0.035, 0.04 |
| **Discharge, *Q*** | Volume of water in channel | $0.1*Q_b$ - $Q_b$ | $0.1Q_b$, $0.2Q_b$, $0.3Q_b$, $0.4Q_b$, $0.5Q_b$, $0.6Q_b$, $0.7Q_b$, $0.8Q_b$, $0.9Q_b$, $Q_b$ |
| **Model Features** | | | |
| **Specification** | **Description** | **Value** | **Notes** |
| **Ineffective Flow Areas** | Areas with minimal downstream flow contribution | 1:1 or 2:1 | 1:1 upstream of structure<br>2:1 downstream of structure |

| | | | |
|---|---|---|---|
| **Contraction coefficients** | Account for energy losses due to expansion of flow | 0.1 or 0.3 | 0.1 for cross section unaffected by structure<br>0.3 for cross sections affected by structure |
| **Expansion coefficients** | Account for energy losses due to contraction of flow | 0.3 or 0.5 | 0.3 for cross section unaffected by structure<br>0.5 for cross sections affected by structure |
| **Downstream Boundary Condition** | Downstream boundary condition was set at normal depth | NA | Set to bed slope |
| **Cross Sections** | The user defined sections used to represent channel bathymetry | 82 | Spacing of cross sections was decreased in the vicinity of the jetty |

***Generation of Channel Geometries***

Rectangular channel geometries that adhere to geomorphic scaling properties were developed using downstream hydraulic geometry relationships (Parker *et al.*, 2007) and *R* scripts to automate the development of realistic combinations of bed slope, width and depth based on vector inputs of bankfull discharge ($Q_b$). The resulting channel geometries were filtered to include only geometries within the defined modeling ensemble ranges (Table 3) with some exceptions for depth, due to the desire to include geometries developed at smaller discharges. One-hundred channel geometries were randomly selected for 1-D modeling from the remaining 200 geometries. Width to depth ratios and dimensionless specific stream powers (Church, 2006) for selected channels were realistic and ranged between 17 - 35 and 0.03 - 0.2, respectively. Initially, channel geometries were developed for both sand and gravel bed rivers to represent a large variety of possible river geometry scenarios. Sand and gravel bed rivers have different

characteristics and hydraulic geometries and can be represented using separate dimensionless hydraulic geometry equations. However, it was determined that regressions appeared to be similar for both sand and gravel geometries early on in the study, so only geometries developed using hydraulic geometry equations for gravel (Parker *et al.*, 2007) were used.

### *Modeling Procedure*

One-dimensional hydraulic modeling in HEC-RAS was automated with VBA and the HEC-RAS Controller (Goodell, 2014). Visual Basics for Applications is the code utilized to run Excel. The developed VBA code consists of one main module that runs HEC-RAS, records results, and calls four-sub-scripts that alter channel geometry, contraction percentage, Manning *n* values, and the steady flow file containing scaled discharges and a normal depth downstream boundary condition (Figure 5). Jetties were modeled as blocked obstructions. For each new structure contraction percentage, the code automatically adjusts the length of ineffective flow areas and the number of cross sections with increased contraction and expansion coefficients. Ineffective flow areas and contraction and expansion coefficients were set based on standard guidelines for abutments (Table 3, Brunner, 2016a). Jetties can also be modeled in HEC-RAS by changing the channel geometry to represent a jetty shape projecting into the channel flow resulting in similar results as modeling jetties as blocked obstructions. However, we found modeling jetties as blocked obstructions was  simpler and more efficient.

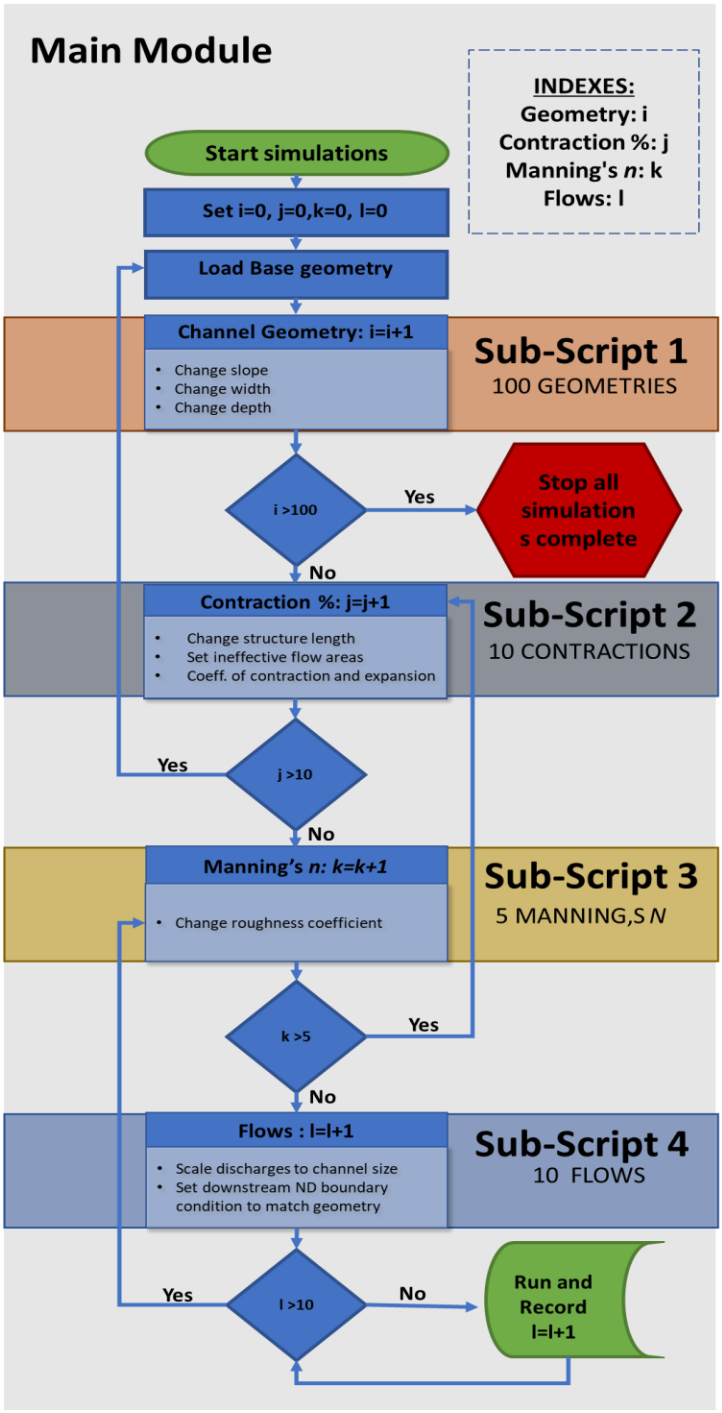


**Figure 5. Code process diagram. Flow diagram of the VBA code that includes a main module that runs HEC-RAS, records results and calls sub-modules that alter the channel geometry, contraction percentage, Manning *n* values, and the steady flow file.**

Channel geometries were created by altering individual pairs of station and elevation data via the VBA code, which reads input data defining a channel width, depth, and slope from the set of 100 realistic channel geometries. The length of the model (0.5 miles), and the number and spacing of cross sections remained constant for all simulations. For a given geometry, the code: 1) set the length of an emplaced structure based on a contraction percentage, 2) set a Manning *n* value, 3) ran the simulation for 10 scaled discharges, 4) recorded velocities, water depths, and shear stresses for each discharge at all cross sections, and 5) continued steps 1-6 for all possible combinations of parameters (Table 3). Fifty thousand HEC-RAS model simulations were conducted using 100 channel geometries, 50 combinations of contraction percentages and Manning *n* values, across 10 discharges scaled to channel size as a percentage of the bankfull discharge utilized to generate the channel geometry (Table 3). Only model simulations where the jetty did not overtop were retained for the regression analysis.

**Regression Analysis**

Multiple regression analysis (MRA) was used to derive predictive regressions to determine relative changes and absolute values of velocity, $V_s$, and shear stress, $\tau_s$, due to the emplacement of jetties in simulated river channels. The analysis was conducted in the statistical programs *R* Version 3.5.1 and JMP Pro 14.1 (R Core Team, 2019; SAS Institute Inc., 2018). Evaluation of regression options focused on the development of easily applied relationships requiring physically-based predictor variables derived from readily available information (Table 4). The Froude number (*Fr*) in the contracted region influenced by jetties may be challenging for a user to estimate since $D_s$ must be known; several alternative representations of the *Fr* were tested in this analysis (Table 4). Determining the depth of water with the structure in place before the

structure is installed is impossible without hydraulic modeling. To limit the need for hydraulic modeling we focused on developing regressions that did not require the depth of water at the structure to be known.

We initially concentrated on predicting relative changes in $V$ and $\tau$ calculated as the value with the structure in place divided by the initial value without the structure in place (0% contraction) at the cross section with the emplaced jetty. The regressions developed for relative changes were expanded to predict $V_s$ and $\tau_s$ in the contracted region impacted by a jetty by multiplying by the initial value without the jetty in place. This approach is conducive to practical applications, providing the option to utilize a known $V_i$ or $\tau_i$, or allowing for estimation of initial values. Final selected models for predicting relative changes in $V$ were corroborated using existing flume data and results from the field study.

**Table 4. Independent variables used in regression analyses.**

| **Independent Variables** | | | |
|---|---|---|---|
| **Independent Variable** | **Description** | **Equation** | **Basis for Inclusion** |
| $\boldsymbol{D_i}$ | Initial water depth, before structure emplacement | NA | Analytical solution |
| $\boldsymbol{D_s}$ | Water depth at structure tip | NA | Analytical solution |
| **aaratio*** | Area ratio: structure area/flow area | $\frac{(L_s * D_s)}{(W_c * D_i) - (L_s * D_s)}$ | Analytical solution |

| | | | |
|---|---|---|---|
| **Contraction percentage** | Structure length/ channel width | $\left(\frac{L_s}{W_c}\right) * 100$ | Constricted flow area |
| **$L_S$** | Jetty length into stream | NA | Analytical solution |
| **n*** | Manning's roughness | NA | Analytical solution |
| **1.49/n** | Inverse of Manning's Roughness | NA | Analytical solution |
| **Q*** | Discharge | NA | Forcing variable |
| **R** | Hydraulic radius | Area/ Wetter perimeter | Analytical solution |
| **S*** | Bed Slope | NA | Analytical solution |
| **$W_c$*** | Channel Width | NA | Analytical solution |
| **$W_c$ / $D_c$*** | Width to depth ratio of channel | $\frac{W_c}{D_c}$ | Geomorphology |
| **$W_{cadj}$ / $D_c$** | Width to depth ratio adjusted for constriction | $\frac{W_c - L_s}{D_c}$ | Geomorphology |
| **xs*** | Number of cross sections (*xs*) with ineffective areas | NA | Potential modeling effect |
| **Alternative Representations of *Fr*** | | | |
| **Approach *Fr* _ND** | Approach Froude # with Normal Depth (*ND*) replacing flow depth | $\frac{Q}{(W_c) * ND^{3/2} * g^{1/2}}$ | Obtaining flow depth may be infeasible |
| ***Fr* _hydraulic geometry at structure** | *Fr* with depth replaced with $Q^{0.4}$ based on at a station hydraulic geometry | $\frac{Q^{0.4}}{(W_c - L_s) * g^{1/2}}$ | Flow depth at the structure may be less obtainable than an estimate of *Q* |
| **Fr #_ND at structure** | Froude # with Normal Depth replacing flow depth | $\frac{Q}{(W_c - L_s) * ND^{3/2} * g^{1/2}}$ | Obtaining flow depth may be infeasible |
| **$s/n^2$** | Proportionality derived from Darcy-Weisbach and Manning relations | $\frac{S}{n^2}$ | Influences flow behavior |

### *Relative Changes in Velocity and Shear Stress Regressions*

We strove to develop parsimonious regression models for predicting relative changes in $V$ and $\tau$ resulting from temporary riprap jetties. Variables with collinearity issues with the *aaratio* (Pearson *r* values over 0.6) were eliminated from best subsets analysis first because previous studies have shown that the *aaratio* is an essential variable for accurately predicting changes in $V$ due to emplacement of other jetties (Seed, 1997; Yeo *et al.*, 2005). We reduced the variable pool to eight by further examining collinearity among the remaining independent variables. The remaining predictor variables (Table 4) were employed in the 'leaps' package in R to perform an exhaustive search for the best subset of predictor variables (Lumley, 2020). The regsubsets() function was used to identify the best linear model for a given number of predictor variables. Linear models were evaluated based on their complexity, adjusted $R^2$ ($adjR^2$) values, and overall model accuracy based on root-mean-square error (RMSE). Sensitivity to the input independent variables was evaluated throughout the model selection process by exchanging selected input variables with other similar variables that were originally excluded due to collinearity.

In addition to linear equations, power functions using the best predictors of relative change in $V$ were developed using both parametric and non-parametric approaches. Quadratic equations were also evaluated for $\tau$ since $\tau \propto V^2$. All regressions were developed using a randomly selected training data set consisting of 80% of the available data from the HEC-RAS simulations. The remaining 20% was utilized for cross-validation to ensure models were not over-fit and to test overall regression performance.

Since $adjR^2$ values cannot be used to compare linear and non-linear regressions, models were selected based on RMSE. Model accuracy and bias in predicting relative changes in $V$ at all contraction percentages were also considered and evaluated in cross-validation using percent error between predicted and actual values from HEC-RAS simulations for each contraction %. Percent errors were evaluated using a One-way ANOVA to test for significant differences between mean percent errors by contraction % groups ($p$-value=0.05). The interquartile ranges (IQR) and the One-way ANOVA results of the percent errors were used to assess model accuracy and bias at all contraction percentages and provide insight into the residual variability of regression predictions.

Contraction percentages over 50% had significantly larger errors for all candidate models and were removed from analysis to improve accuracy, as temporary jetties exceeding 50% are rarely encountered in construction practice. Froude numbers in the contracted cross section were limited to <0.8 to ensure models were developed for subcritical flow conditions.

***Absolute Velocities and Shear Stress Regressions***

Absolute $V$ and $\tau$ regressions were developed using the top predictive model for relative change in $V$ and $\tau$ based on cross-validation. Relative changes were then multiplied by various estimates of initial values without the jetty in place. One set of regressions to predict $V_s$ and $\tau_s$ used initial values estimated using either the Manning equation or the shear stress equation, respectively. These equations require known values of $R$ and, therefore, $D_i$. They also represent estimates that

could be obtained from hydraulic models such as HEC-RAS. Additional regressions were tested where water depth was estimated using variables that may be more easily obtained (*Q*, *S*, *n*, etc.).

Three models for predicting $V_s$ were tested. The first two models expanded upon the regression developed for relative changes in *V*. The first model calculated the $V_i$ using the Manning equation assuming the $D_i$ is known, and the second model replaced depth in the Manning equation with a proxy for depth based on at-a-station hydraulic geometry (Knighton, 1998; $D \alpha Q^{0.4}$). The third model mimicked the analytical solution (Eq. 8), developing a power function to predict $V_s$ using the Manning equation to calculate the $V_i$. However, *R* was replaced by depth assuming wide geometry and $\frac{Q}{W_C}$ was used as a proxy for depth (Eq. 9). Two models for predicting $\tau_s$ were tested. The first model utilized $\tau_i$ obtained from the shear stress equation with a known *R*. The second model used substituted $D_i$ for *R* and estimated $D_i$ using a proxy for depth derived from the Manning equation ( $D_i = \left[\frac{(Q * n)}{(W_C * S^{0.5} * \emptyset}\right]^{3/5}$ ).

The prediction accuracy of the regressions was quantified as percent errors of absolute values of velocity and shear stress. The regression models for relative changes in velocity and shear stress were fit on a subset of data from the HEC-RAS modeling results. The remaining HEC-RAS data were then used to test the ability of these models to predict absolute values of shear stress and velocity post-jetty installation. The goal of predicting absolute values was to determine usable regressions for preliminary analysis of emplacing jetties and to understand the regression limitations, especially when estimating depths. Other methods to predict $V_s$ and $\tau_s$ likely exist with other variations of depth approximations.

**Eq 3.9.** $V_s = X * \left[\left(\frac{\emptyset}{n}\right)^a * Q^b * W_c^{\ C} * S^d\right] * [aaratio + 1]^e$

where *a*, *b*, *c*, *d*, *e* are fitted exponents and *X* is a fitted coefficient.

**Field Work**

Field work for this project aimed to estimate changes in mean *V* magnitudes in the contracted region of an installed jetty compared to unobstructed channel conditions to test the regression models. Field work was conducted near Lyerly, Georgia, at a bridge replacement project (PI No. 0003081 Chattooga County) on the Chattooga River that implemented temporary riprap jetties. All site visits were organized through the project manager Robert Bell. Field visits consisted of measuring velocity profiles for 5 cross sections and taking turbidity measurements, and drone videos if time allowed. Throughout the entirety of this research project, the project team conducted five site visits. Velocity and turbidity measurements were taken during four of the site visits, and drone videos were captured for three of the site visits.

Velocity measurements were taken using a Teledyne StreamPro Acoustic Doppler Current Profiler (ADCP) set up on a tethered pully system (Figure 6c) for two different structure configurations (Table 5). The first temporary access structure configuration consisted of one jetty extending into the channel from the left bank (looking downstream). The second configuration consisted of two jetties, one on each bank (Figure 6b). The jetties impacted the channel width at cross sections 2 and 3 (Figure 6a). Stationary moving bed tests were conducted at each cross section for a minimum of five minutes to ensure measurement accuracy (Mueller and Wagner,

2009). No moving beds were detected. A minimum of four transects were completed at each cross section to provide an average *Q* value. Additional transects were collected if one *Q* varied by > 5% from the mean of all the discharges (Mueller and Wagner, 2009). Transects with discharges varying over 10% of the average *Q* for all transects at a given cross were removed during data analysis.

Between site Visits 3 and 4, discharges varied greatly, a large tree washed into the study site, and bridge pier locations and shape varied due to ongoing construction. Due to the differences in relative magnitudes of discharges and the cross section changes, we grouped site Visits 1 and 2 and site Visits 3 and 4 for analysis of relative changes in *V*. Field data collection was largely limited by changing site conditions due to the active construction; for example, channel contraction percentages may have been impacted by a change in pier shape and size not solely by the jetty itself.

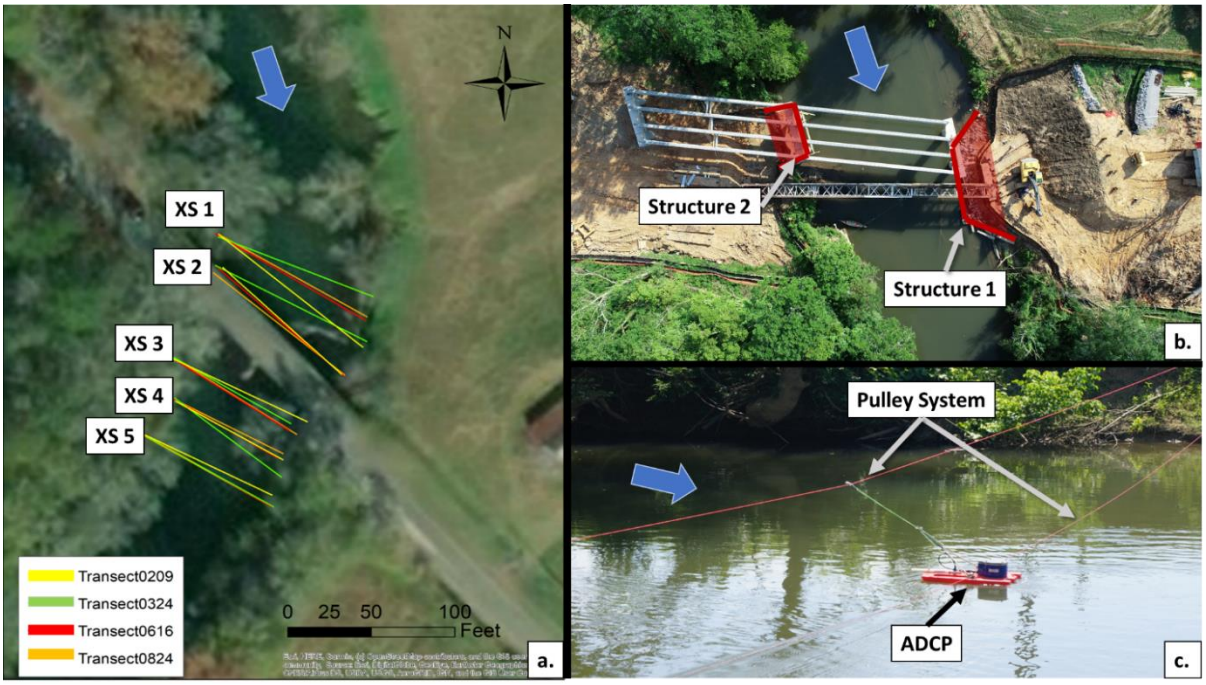


**Figure 6. Field methods. Field methods overview where blue arrows represent flow direction. Location of cross sections for all site visits (a). Locations of cross sections on the left bank varied between site visits based on flow heights and changes in bank safety. Temporary riprap structure placement for 6/16/2019 (b). ADCP pulley system set up for one cross section (c).**

**Table 5. Collected field data at Lyerly, GA bridge replacement site.**

| Visit # | Field Visit Type | Avg. Measured Discharge for All XS (cfs) | % Contraction from Temporary Structure |
|---|---|---|---|
| **1** | Pre- bridge construction | 367 | 0% |
| **2** | Structure configuration 1 | 558 | XS 2=16% |
| | | | XS 3=18% |
| **3** | Structure configuration 2 | 199 | XS 2= 11% |
| | | | XS 3= 21% |
| **4** | Post-bridge construction | 159 | 0% |

## RESULTS

Practical relationships for predicting mean relative changes and absolute values of $V$ and $\tau$ resulting from the emplacement of jetties in rectangular channels are presented in Table 6. Relative changes in mean $V$ and $\tau$ determined from 1-D HEC-RAS modeling results were well represented by easily applied regressions developed with one variable, for contraction percentages $\leq$ 50% and $Fr$ <0.8. Regression analysis results indicated the main variable affecting change in $V$ and $\tau$ between an unaltered channel and a channel with a jetty was a contraction area ratio (*aaratio*). Percent errors between flume studies and regression models of relative change in $V$ ranged from -9% - 17%. Absolute velocity and shear stress in the contracted region impacted by jetties can be estimated by rearranging the relative regression models, multiplying by an initial value. Initial values can be known values from field data or hydraulic modeling studies or can be estimated. Models of $V_s$ and $\tau_s$ that require input estimates of velocity and shear stress in the absence of jetties resulted in median absolute prediction errors of 1-5% with errors in the 90$^{th}$ and 10$^{th}$ percentiles <15% for $\tau_s$ and <10% for $V_s$.

**Table 6. Regression models. Models for predicting relative changes and absolute values of velocity and shear stress resulting from jetties.**

| Model Type | Model Form | Model |
|---|---|---|
| **Relative Change in Velocity *** | Linear | $\frac{V_s}{V_i} = 1.0377 * (aaratio) + 1.0017$ |
| **Absolute Velocity:** Velocity at jetty | Power Function | $V_s = 0.8 * \left[\left(\frac{1.49}{n}\right)^{0.7} * S^{0.348} * \mathrm{W}_c{}^{-0.4} * Q^{0.412}\right] * \left[((aaratio) + 1)^{1.097}\right]$ |
| **Absolute Velocity:** Velocity at jetty | Linear: Manning's Eq. predict $V_i$ | $V_s$=$[1.0377 * (aaratio) + 1.0017\ ]$*$\left[\left(\frac{\emptyset}{n}\right) * R^{\frac{2}{3}} * S^{\frac{1}{2}}\right]$ |
| **Relative Change in Shear Stress*** | Quadratic | $\frac{\tau_s}{\tau_i} = 1.066 * (aaratio)^2 + 2.13 * (aaratio)$+0.987 |
| **Absolute Shear Stress** | Quadratic: Manning's estimated $D_i$ | $\tau_s = [1.066 * (aaratio)^2 + 2.13 * (aaratio) + 0.987] * \gamma * \frac{(Q * n)}{(\mathrm{W}_c * S^{0.5} * \emptyset)}^{3/5} * S$ |
| ***aaratio****** | | **Full form**: $\frac{(L_s * D_s)}{(\mathrm{W}_c * D_i) - (L_s * D_s)}$ **Simplified form**: $\frac{(\mathrm{L}_s)}{(\mathrm{W}_c) - (L_s)}$ |

**The relative change equations can be rearranged to solve for absolute values if initial values without a structure are known from field data or modeling studies.*

*** Absolute models provide a means of calculating mean values at a structure without the need for depth data.*

****aaratio can be estimated assuming initial depths and depths with the structure in place are similar, resulting in a ratio of the structure length to the flow area*

## 1-D HEC-RAS Models of Previous Flume Studies

Differences in velocities at jetty contracted regions between previous physical modeling studies and HEC-RAS simulations ranged from -5.2% - 17%. Differences in predicted upstream mean velocities ranged from -2.4% - 1. 5% (Appendix A, Table 10). HEC-RAS predicted values were generally more accurate for the Jeon et al. (2018) flume experiments compared to the Duan et al. (2009) flume experiment. The HEC-RAS simulations appeared to adequately predict velocity in contracted regions impacted by jetties modeled as obstructions with ineffective flow areas and coefficients of contractions mimicking abutment modeling techniques. Therefore, this technique should provide adequate results for the development of predictive relationships for *V*.

## Predictive Models for Velocity

### *Effects of Jetties on Relative Velocities*

The *aaratio* was the best predictor of relative changes in *V*, explaining >99% of variability in the linear models (Appendix A, Table 11). This result agrees well with the analytical solution and linear models suggested by Seed et al. (1997) and Yeo et al. (2005) for other in-stream structures. A linear model with *aaratio* as the only variable has a RMSE of 0.027. Relative changes always exceeded unity, and for contraction percentages ranging from 10-50% the linear model with *aaratio* only predicted relative changes in *V* from 1.12 - 2.03 with mean errors of 1.3 - 2.4%. The linear *aaratio* model underpredicted *V* for larger *Fr* and overpredicted for smaller *Fr* (Appendix A, Figure 39). Addition of the *Fr*, the second-best predictor variable, to the linear solution improved the RMSE to 0.0205 ($adjR^2$ = 0.995). Addition of the *Fr* provided the largest change in $adjR^2$ compared to addition of other independent variables (Appendix A, Figure 38b).

A linear model containing all 8 independent variables slightly improved the RMSE to 0.0154 ($adjR^2$ = 0.997; Appendix A, Figure 38, Table 11).

Cross validation of the linear *aaratio* model indicated systematic overprediction errors that increased with contraction percentage (Figure 7a). The model, including *aaratio* and *Fr*, slightly underpredicted relative change in *V* (Figure 7b). This model had larger interquartile ranges (IQRs) for 10% and 20% contractions compared to the univariate model; however, IQRs were smaller for all other contraction percentages when *Fr* was included. The univariate model with *aaratio* was biased in mean prediction errors across contraction percentages ($p$<0.001); however, the mean percent prediction errors between contraction percentages were not statistically different for the two variable linear model including *Fr* ($p$=0.055).

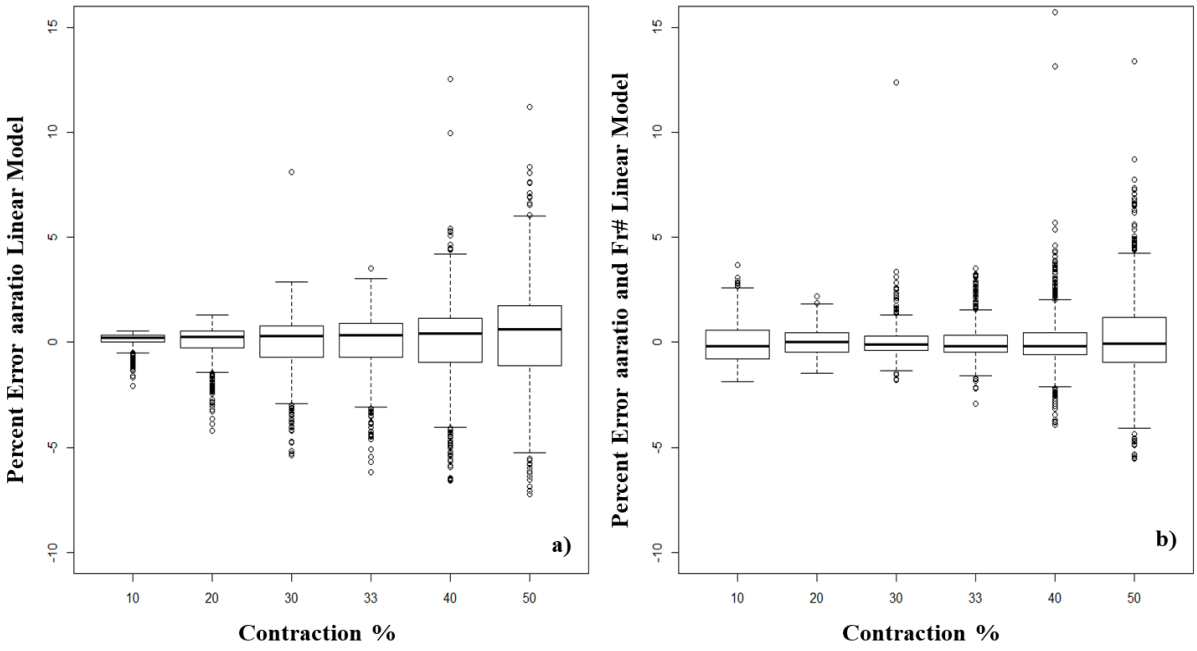


**Figure 7. Cross validation. Cross-validation results for (a) univariate model based on *aaratio*, and (b) a two variable linear model containing *aaratio* and *Fr*.**

Easily applied representations of the *Fr* were tested in linear regressions because predicting *Fr* at the contraction can be challenging. Including alternative representations of *Fr* derived from at-a-station hydraulic geometry and the Darcy-Weisbach equation improved the RMSE from 0.0273 for the *aaratio* model to 0.0217 and 0.0221, respectively (Appendix A Table 11). Though the RMSE was slightly smaller for the hydraulic geometry representation of *Fr*, the residuals for the Darcy-Weisbach were less biased. Power functions using *aaratio* and *Fr* were also tested but did not improve model accuracy.

Adding additional variables, including the *Fr*, did marginally improve overall model accuracy (max RMSE decrease of 0.0119); however, the univariate *aaratio* model (Eq. 10) was taken to be

the best model to predict relative changes in *V* due to its parsimony, and the exclusion of the need to estimate *Fr* which could introduce extraneous error and complexity.

**Eq 10.** $V_s/V_i$=1.0377*$(aaratio)$+1.0017

The univariate *aaratio* model was physically intuitive and agreed well with data from previous experimental studies and the field measurements (Figure 8). The *aaratio* model predicted lower relative changes in *V* compared to the Yeo et al. (2005) and Seed et al. (1997) models for predicting *V* increases at the tip of a jetty at 60% depth and the maximum depth averaged main channel *V*, respectively. Differences between flume studies (Duan *et al.*, 2009; Jeon *et al.*, 2018; Molinas *et al.*, 1998) and the *aaratio* model from this study ranged from - 9% - 17%. The *aaratio* model most accurately predicted relative *V* from Molinas et al. (1998), followed by Jeon et al. (2018). The *aaratio* model over predicted relative *V* for two field data points and the Duan et al. (2009) study.

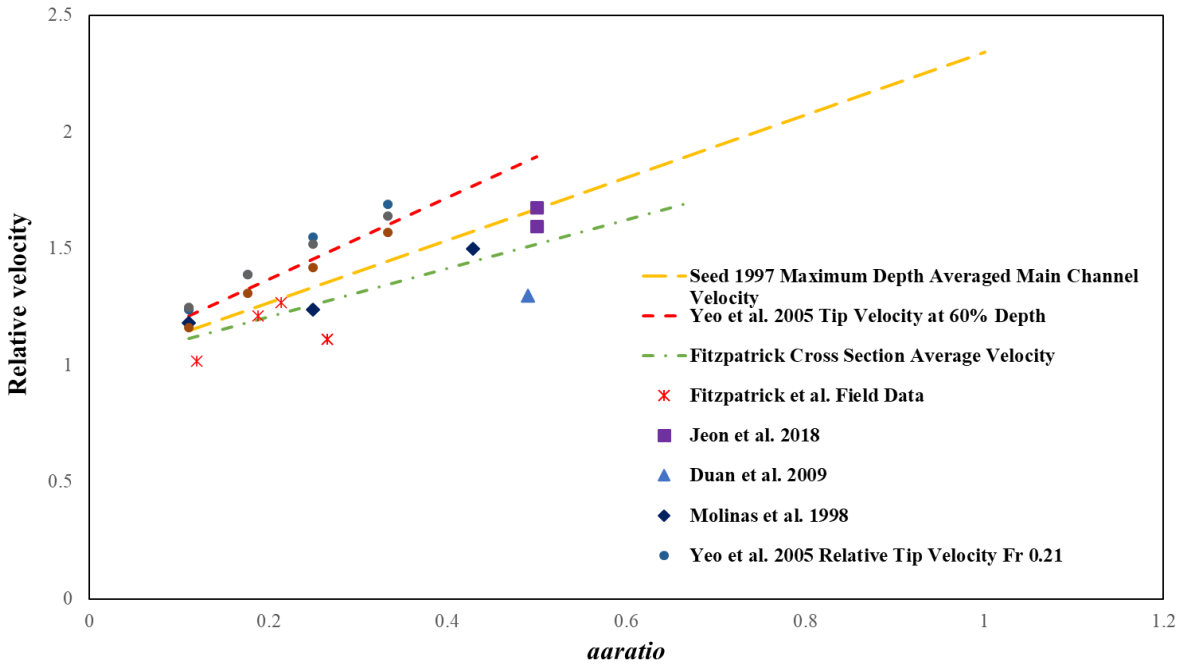


**Figure 8. Regression validation. Comparison of jetty effects on velocity based on a univariate *aaratio* model developed in this study versus previous experiments and field data collected for this study.**

### *Jetty Effects on Absolute Velocities in the Contracted Region*

Both the model using the Manning equation to predict initial values of $V$ with a known $R$ (Eq. 11) and the power function model using $\frac{Q}{W_c}$ as a proxy for relative depth (Eq. 12) reasonably predicted the $V_s$ in the region contracted by jetties (Figure 9). Cross validation indicated that the model using the Manning equation with a known $R$ to predict $V_s$ generally over predicted $V_s$ whereas the power function generally underpredicted $V_s$ (Figure 9a). Prediction accuracies of linear versus power function models varied among contraction ratios, with the IQR of errors increasing for higher contraction percentages for the linear model but decreasing for the power function. Mean errors between contraction percentages were statistically different for both the linear model ($p<0.001$) and the power function ($p<0.001$). Both models were biased, with more

accurate and less variable predictions for higher or lower contraction percentages when predicting $V_s$. However, both models are still valuable options to use to predict $V_s$ with 90$^{th}$ and 10$^{th}$ percentile absolute values of error <10%. Equation 11 was developed using English units resulting in units of ft/s. Equation 12 is dimensionally homogeneous and can be used with English or SI units resulting in $V_s$ in ft/s or m/s, respectively.

**Eq. 11** $$V_s = 0.8 * \left[\left(\frac{1.49}{n}\right)^{0.7} * S^{0.348} * W_C{}^{-0.4} * Q^{0.412}\right] * \left[((aaratio) + 1)^{1.097}\right]$$

**Eq. 12** $$V_s = [1.0377 * (aaratio) + 1.0017\ ] * \left[\left(\frac{\emptyset}{n}\right) * R^{\frac{2}{3}} * S^{\frac{1}{2}}\right]$$

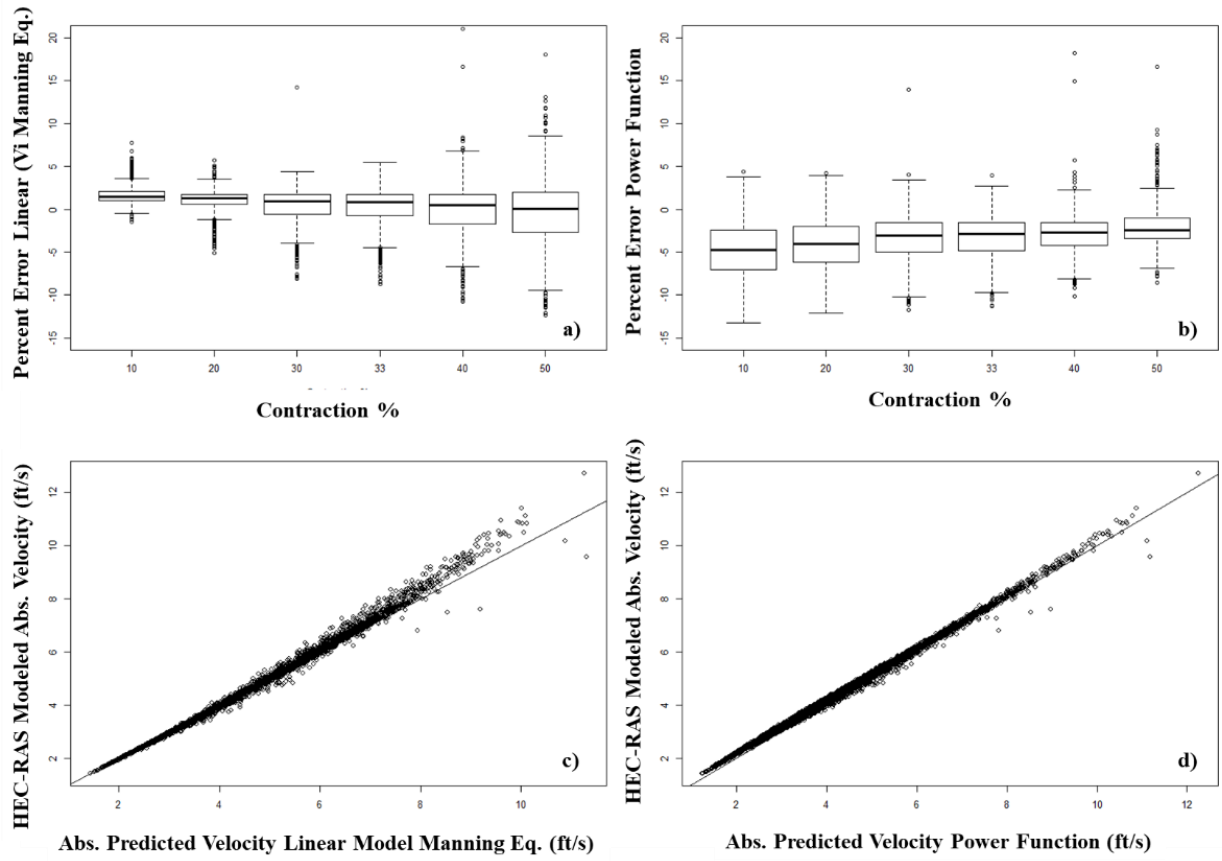


**Figure 9. Regression performance. Percent errors in prediction of $V_s$ using (a) the linear model utilizing the Manning equation with a known $R$ to predict $V_i$, and (b) the power**

**function model. The linear model tends to underpredict $V_s$ in a contracted region impacted by a jetty (c), and the power function tends to overpredict the $V_s$ (d).**

## Predictive Models for Shear Stress

### *Effects of Jetties on Relative Change in Shear Stress*

The univariate *aaratio* quadratic model was the best predictor of relative changes in $\tau$ (RMSE = 0.117; Appendix A, Table 12). A univariate *aaratio* linear model also reasonably predicted relative changes in $\tau$ ($R^2$ = 0.975, RMSE = 0.15; Appendix A, Table 12), however was biased in its prediction errors across contraction percentages. Addition of the *Fr,* the second-best predictor variable, to the linear solution resulted in an $adjR^2$ and RMSE of 0.988 and 0.104, respectively.

Cross validation revealed that the median errors in relative $\tau$ change for the linear univariate model were highly variable across contraction percentages (underprediction for the 10% and 50% contraction percentages versus overprediction for all other contractions, Figure 10a). The quadratic model slightly overpredicted the median IQR of errors, increasing with contraction percentages (Figure 10b). Differences in mean errors between contraction ratios were significant for the linear univariate model ($p$<0.001), but not for the quadratic model ($p$=0.3955).

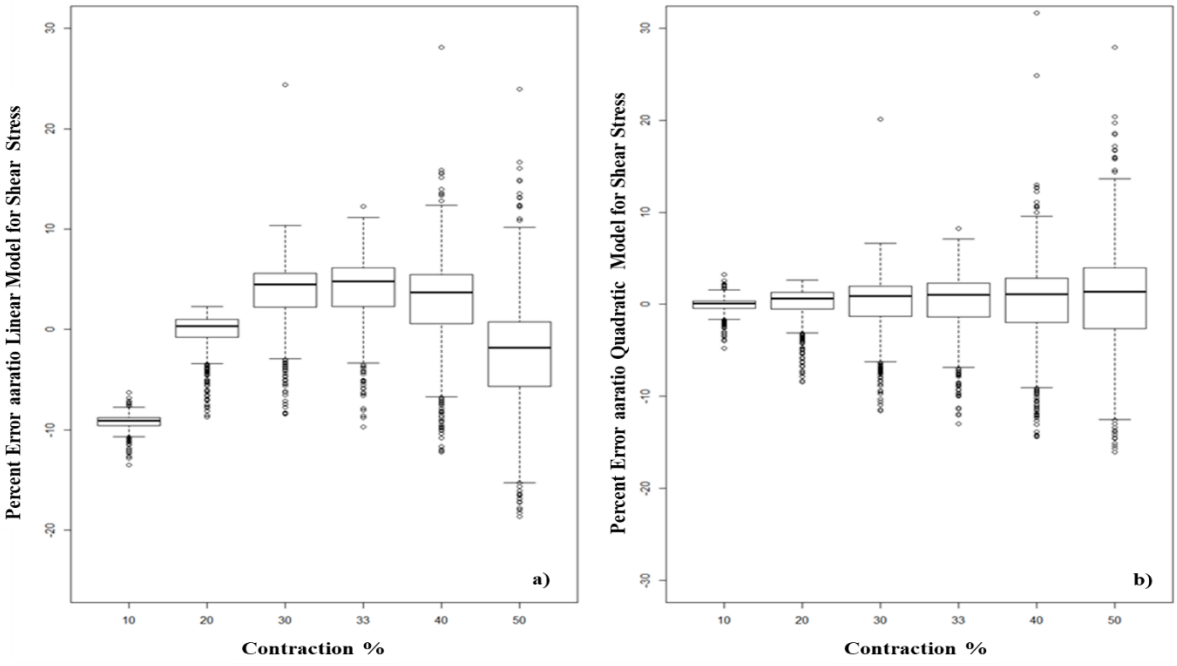


**Figure 10. Cross validation. Cross-validation results for a (a) linear and (b) quadratic univariate model for predicting relative changes in shear stress based on *aaratio*.**

The univariate quadratic model based on *aaratio* (Eq. 13) was selected based on parsimony, and the exclusion of the need to estimate *Fr*, which introduces complexity and the potential for error propagation, and unbiased errors across contraction percentages. However, the variability in prediction errors increases with increasing contraction percentages.

$$\textbf{Eq. 13}\ \frac{\tau_s}{\tau_i} = 1.066 * (aaratio)^2 + 2.13 * (aaratio) + 0.987$$

***Jetty Effects on Absolute Shear Stresses in the Contracted Region***

Both the model using (Eq. 14), a known *R*, and the model using the Manning equation with $R = D_i$ (Eq. 15) reasonably predicted the $\tau_s$ in the jetty contraction region. Both models overpredicted

$\tau_s$ with median errors consistently positive (Figure 11). Error IQRs increased with contraction ratio and were smaller for the model using the Manning approach compared to the model with a known *R* except at 10% contraction. Median errors increased with contraction ratio for the model utilizing the Manning approach, but decreased and approached zero for the model using a known *R*. Mean errors were significantly different between contraction percentages for the model with a known *R* ($p$<0.001) but were not for the model using a depth estimate ($p$=0.3955). Variability in $\tau_s$ prediction errors increased with contraction ratio. Both models were found to be valuable options for predicting $\tau_s$ with 90$^{th}$ and 10$^{th}$ percentile absolute values of error not exceeding 15%. Equations 14 and 15 are dimensionally homogeneous and can be used with English or SI units resulting in $\tau_s$ in lb/ft$^2$ or Pascals, respectively.

**Eq. 14** $\tau_s = [1.066 * (aaratio)^2 + 2.13 * (aaratio) + 0.987] * \gamma * R * S$

**Eq. 15** $\tau_s = [1.066 * (aaratio)^2 + 2.13 * (aaratio) + 0.987] * \gamma * (\frac{(Q*n)}{(W_C*S^{0.5}*\emptyset)})^{3/5} * S$

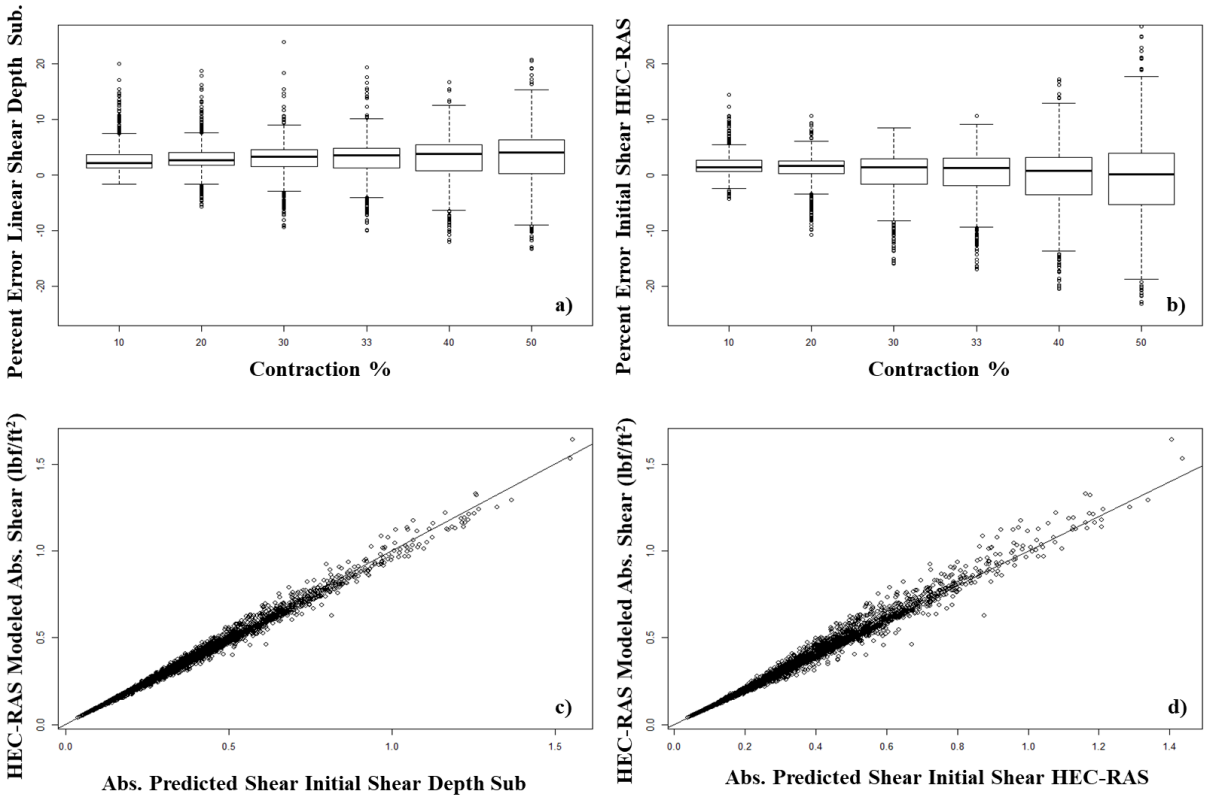


**Figure 11. Regression performance. Percent errors in prediction of $\tau_s$ using the model replacing $R$ in the shear stress equation with $D_i$ and estimating $D_i$ using the Manning equation to predict $\tau_i$ (a,c) and the model utilizing the shear stress equation with a known $R$ to predict $\tau_i$ (b,d). Both models on average over predict $\tau_s$ with median percent errors consistently above zero.**

## DISCUSSION OF FINDINGS

We found that 1-D HEC-RAS simulations adequately predicted mean velocity in contracted regions affected by perpendicular jetties. Jetties were modeled as blocked obstructions with ineffective flow areas and coefficients of contractions mimicking abutment modeling techniques. Comparisons with previous experimental studies were limited to small scale rectangular flumes with contraction percentages of 33%. Given the paucity of detailed field observations around jetties and other in-stream structures, additional studies across diverse contraction percentages

may prove valuable for further testing of 1-D model fidelity to actual jetty effects. The HEC-RAS simulations for 33% contractions appeared to adequately predict velocity in contracted regions. Therefore, this technique should provide adequate results for the development of predictive relationships for *V*.

Practical relationships for predicting mean relative changes and absolute values of *V* and $\tau$ due to the emplacement of jetties in rectangular channels were developed (Table 6). These models can be used for diverse applications, including structure design to reduce potential bed and bank erosion, as a communication tool about potential effects of emplacement of jetties, and for identification of mobile bed material grain sizes due to changes in hydraulics. Models developed here were based on rectangular channels and vertical-wall rectangular structures constructed perpendicular to the flow. Application of these models to actual channel bathymetries may yield higher percent errors if careful consideration is not taken when estimating depth or calculating *aaratios.* Appendix B of this report provides additional insight into using developed equations for actual channel bathymetries.

Relative changes in mean *V* and $\tau$ estimated by HEC-RAS simulations were found to be well represented by easily applied regressions based on *aaratio*, and in some instances *Fr*. These results were consistent with models previously developed by Seed et al. (1997) and Yeo et al. (2005) who also identified *aaratio* as the primary variable controlling relative changes in *V*. The selected model for predicting relative changes in *V* agreed well with data from previous experimental studies and field work conducted during this study at a jetty (Figure 8). As

expected, the developed model predicted lower relative changes in mean *V* at a cross section compared to Yeo et al. (2005) and Seed et al. (1997) models because their models predict *V* changes at the tip of an emplaced structure. Velocities at the tip of a jetty are expected to be higher than cross section averaged velocities that were estimated in this study.

The relative *V* model developed in this study corresponds most closely with the data from Molinas et al. (1998). They presented relative velocities for different contractions as the maximum depth averaged velocities in the contracted region divided by the upstream *V* around abutments. Because they presented maximum depth averaged velocities in the contracted region, we expected to slightly underpredict relative velocities presented by this study. The model from the present study slightly underpredicted velocities for two out of three of the contractions examined by Molinas et al. (1998). The Jeon et al. (2018) dataset provided detailed data that we would expect to best represent 1-D HEC-RAS velocities since 1-D HEC-RAS predicts cross section depth averaged downstream components of *V*. The model underpredicted the relative mean streamwise components of *V* in the contracted region of a spur dike for two different discharges using the Jeon et al. (2018) dataset. The percent difference between the model and the Jeon et al. (2018) data set was relatively small, being $\leq$ 9%. The model over predicted relative velocities for the Duan et al. (2009) study which presented relative *V* as the mean streamwise component of *V* at the contracted section divided by the approaching upstream *V*. The relative change in *V* regression appears physically reasonable with respect to other developed equations for maximum relative velocities (Seed, 1997; Yeo *et al.*, 2005) and how it is bracketed by the best available flume data. Percent errors between all flume studies (Duan *et al.*, 2009; Jeon *et al.*, 2018; Molinas *et al.*, 1998) indicated the model did not over predict or under predict consistently

for a range of contraction percentages and discharges, suggesting the model is valuable in predicting relative changes in velocities around jetties and other structures that may constrict channel flow such as a cofferdam.

The regression model for predicting relative change in *V* was applied to field data collected in this study. This model overpredicted change in *V* for two observed data points and underpredicted relative *V* for the remaining two data points. The underpredicted relative velocities had higher observed discharges than the two data points where velocity was overpredicted. It is possible that the differences between the two sets of field days may be partially attributed to differences in ADCP accuracy at different flow conditions. During low flow conditions, it was challenging to keep the ADCP boat speed below half the water speed. During high flow conditions, the ADCP tended to get caught in eddies and not maintain an orientation perpendicular to the flow. Field data collected during this study may have been impacted by changing channel bathymetries and bed structures (logs) due to large flows between sampling events. Contractions may have been somewhat altered by ongoing construction, such as changes in bridge pier shape and locations that could have affected results.

The selected model to predict relative changes in $\tau$ was found to be best represented by a quadratic equation with the *aaratio* as the only variable. This result makes physical sense because $\tau \propto V^2$. The shear stress models were not corroborated with flume or field data. Other studies have presented predictive models to quantify $\tau$ amplification in contracted regions impacted by in-stream structures similar to jetties (Molinas et al., 1998), while others have

developed predictive relationships for scour depths and patterns (eg. Pandey et al., 2018; Zhang & Nakagawa, 2008). However, these models typically require a form of *Fr* and flow depth, which may not be readily obtainable. Scour is a patchy phenomenon and difficult to predict (Haschenburger, 1999). Nevertheless, easily-applied models to predict relative changes in *V* and $\tau$ should prove useful in certain situations to estimate potential scour impacts due to various jetty contraction percentages.

Models for relative changes in both *V* and $\tau$ are non-linear with respect to contraction percentage (Figure 12). This is important because current USACE regional permits prohibit the use of temporary jetties that span greater than 33% of the channel width (shown as a vertical line in Figure 12). The regressions produced here support such a maximum allowable contraction percentage as the rate of increase in both *V* and $\tau$ (especially $\tau$) increase substantially above this threshold. Limiting jetties to less than 33% contraction percentage will keep increases in shear stress and velocity below 2.5 and 1.5, respectively (assuming rectangular channel geometry).

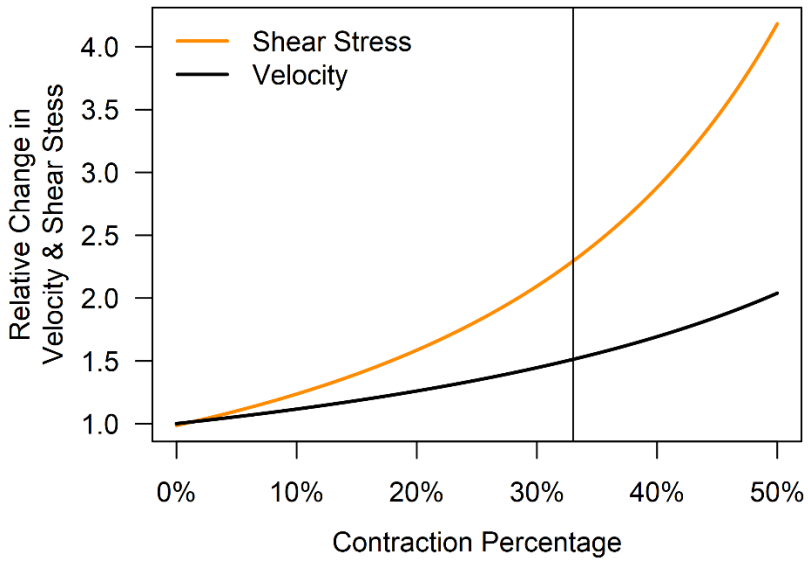


**Figure 12. Contraction percentage effects. Relative changes in velocity and shear stress versus jetty contraction percentage based on the developed regression equations. Based on rectangular channel geometry. Values will differ for more complex channels.**

Absolute $V$ and $\tau$ models were developed by expanding on relative regression models, with the goal of outlining several easily applied physically-based regressions and providing insight into those regression limitations, especially when estimating depths. Depth, either with or without a structure in the channel, can be a limiting factor impacting the ability of DOTs to predict velocities in channels using simply the Manning or shear stress equation if modeling and field data are not available. Absolute $V$ and $\tau$ models were presented here with the opportunity to develop predictions based on estimates for depth or based on known values of depth and hydraulic radius. Relative change models can be used to predict absolute values by multiplying by the initial value. This may reduce error in predictions if measured or modeled initial values are known for the discharge of interest.

Regression models for $V_s$ and $\tau_s$ have reasonable accuracy with median absolute prediction errors of 1 - 5% with errors in the 90$^{th}$ and 10$^{th}$ percentiles <15% for $\tau_s$ and <10% for $V_s$. These models along with the relative regression models can be used as tools for communication between DOTs and environmental permitting agencies and to better understand the potential hydraulic effects of constructing jetties in river channels. Using the developed models can save time and money by reducing the need for hydraulic modeling. The models can be used to simplify the assessment of potential hydraulic and geomorphic effects of the emplacement of jetties under numerous conditions.

Regression analysis indicated that *Fr* may improve model predictions for both *V* and $\tau$. This finding aligns with previous studies where *Fr* plays an important role in models predicting scour depths (eg. Pandey et al., 2018; Zhang & Nakagawa, 2008) and shear stresses around other in-stream structures (Molinas *et al.*, 1998). Froude number has also been identified as a key factor in flume studies evaluating relative *V* changes near structures (Yeo *et al.*, 2005). Though the addition of *Fr* was found to increase model accuracy, we excluded *Fr* based on this project's goal of developing easily-applied, parsimonious models to predict *V* and $\tau$ changes. Alternative approximations of *Fr* were examined and were found to also increase model accuracy, albeit at the cost of model complexity and potential error propagation via *Fr* estimation.

## CHAPTER SUMMARY

In this chapter, we outlined how we developed practical, physically-based relationships to predict mean relative changes and absolute values of $V$ and $\tau$ due to the emplacement of jetties for bridge construction access. Relative changes in mean $V$ and $\tau$ estimated with >50,000 HEC-RAS model simulations were well represented by easily applied regressions developed with one variable representing contraction area ratio, with applicability to contraction percentages ≤50% and Froude numbers <0.8. All chosen models were cross validated and had reasonable accuracy and should prove to be useful for estimating changes in velocity and shear stress at jetties implemented for bridge construction access. Percent errors between flume studies and regression models of relative change in $V$ ranged from -9% - 17%. Models of $V_s$ and $\tau_s$ that require input estimates of velocity and shear stress in the absence of jetties resulted in median absolute prediction errors of 1-5% with errors in the 90$^{th}$ and 10$^{th}$ percentiles <15% for $\tau_s$ and <10% for $V_s$. Addition of $Fr$ to models with only the area ratio was found to improve model accuracy for both $V$ and $\tau$ predictions. However, determination of the $Fr$ without hydraulic modeling or field work can be challenging, limiting the use of models containing the $Fr$. Froude number approximations using hydraulic geometry and flow resistance equations were found to also improve model accuracy. These approximations were still excluded from the final model suggestions due to the need for further study on potential errors due to approximation and added model complexity with a limited increase in accuracy.

Regression equations to predict $V_s$ or $\tau_s$ with a jetty in place require knowledge of the initial values without the jetty in place. Velocity or shear stress for the natural channel condition at the

discharge of interest may be determined using hydraulic modeling, field measurements, or can be estimated using the Manning or shear stress equations requiring a known hydraulic radius and, therefore, water depth. If available, stage-discharge relationships or hydraulic geometry can be used to determine approximate flow depth for discharges of interest and used to predict initial values. The suite of models presented in this report include models to estimate initial values with known *R* and depth or estimated values for depth using easily obtainable variables.

This chapter outlined the analytical approach defining the importance of the area ratio in predicting changes in velocity due to the emplacement of jetties. We found that one-dimensional HEC-RAS adequately predicts velocities in contracted regions impacted by jetties modeled as obstructions with ineffective flow areas and coefficients of contractions and expansions mimicking abutment modeling techniques. Automation of HEC-RAS using VBA and the HECRAS Controller provides valuable opportunities to conduct hydraulic modeling for a range of channel geometries and conditions. This technique may be useful for other potential GDOT research projects.

The relationships developed in this chapter were designed to be user-friendly and provide estimates of mean changes in hydraulics due to the emplacement of temporary riprap jetties that can be used as a planning and communication tool. Accurate prediction of $V_i$, and $\tau_i$, and the *aaratio* is vital as the quality of available input data determines model accuracy. Further information on how to apply the predictive regressions developed in this chapter to bridge construction projects using jetties can be found in Chapter 5.

# CHAPTER 3. EFFECTS OF JETTIES ON SPATIAL PATTERNS OF VELOCITY AND SHEAR STRESS

The goal of this chapter is to evaluate altered spatial distributions of $V$ and $\tau$ in river reaches containing jetties and discuss how the spatial distributions are affected by changes in discharge, channel geometry, and jetty characteristics. This chapter builds upon Chapter 2 providing a means to identify potential locations within a river channel at higher risk for bank and bed erosion due to the emplacement of temporary jetties. Chapter 2 developed a set of predictive equations to provide quantitative estimates of relative and absolute cross section averaged velocities and shear stresses. This chapter provides insight into where maximum velocities and shear stresses may occur.

The specific objectives are to:

1. develop a set of 2-D HEC-RAS simulations that describe the spatial distributions of $V$ and $\tau$ in a river reach containing a jetty for a range of channel dimensions and contraction percentages with emphasis on locations of maxima and near bank regions; and
2. describe how the modeling results can be used with predictive relationships for $V$ and $\tau$ (Chapter 2) to identify potential locations at the highest risk for increased bed and bank erosion due to structure emplacement.

## METHODS

Two-dimensional hydraulic modeling was conducted using the United States Army Corps of Engineers (USACE) Hydrologic Engineering Center River Analysis System (HEC-RAS)

Version 5.0.7 (Brunner, 2016a). A total of 42 HEC-RAS models were created representing three channel widths, seven structure contraction percentages, and two streamwise structure widths (20ft and 50ft). Streamwise structure width is the top width of the jetty where machinery would drive on to access the bridge during construction. The length of the model (0.5 miles) and Manning roughness value (0.035) remained constant for all simulations. The three channel sizes were selected to represent a narrow, medium, and wide channel to evaluate the effect of channel width on erosion potential on the bank opposite the emplaced structure, with emphasis on the moderate and narrow widths. The narrow and wide channels were selected from the 100 channel geometries developed in Chapter 2. The jetty was unsubmerged (i.e. did not overtop) for all modeled scenarios).

Straight, rectangular channel geometries that adhere to the geomorphic scaling properties of natural channels were developed in Chapter 2 using dimensionless downstream hydraulic geometry relationships (Parker *et al.*, 2007). The medium channel was developed based on average channel dimensions for the Chattooga River near Lyerly, GA, where field work was conducted at a bridge construction site utilizing jetties. The narrow, medium and wide channels had widths of 60.4 ft, 114.03 ft and 519.17 ft, respectively. The analysis focused on the narrow and medium channel widths due to the limited use of jetties in very wide channels. Each channel geometry was run for six structure lengths and two structure widths with contraction percentages of 0%, 10%, 20%, 30%, 33%, 40% and 50%. The simulations with a 0% contraction (no structure) served as a baseline for $V$ and $\tau$ in the channel under unobstructed conditions. All model ensembles were conducted for three discharges scaled to channel size (Table 7).

Mesh sizes were decreased within the jetty contraction zone to improve computation accuracy in the focal area of interest (Table 7, Figure 13). HEC-RAS has the capability to run 2-D computations using either the Saint-Venant (Full Momentum Method) or Diffusion Wave Equations. The Full Momentum Method was chosen for its superior representation of changes in forces resulting from abrupt contractions such as jetties, and the inclusion of an additional turbulence term (Brunner, 2016b). Computation intervals and mesh sizes were set to keep Courant numbers below two for model stability and accuracy; Courant numbers as high as three can still produce accurate results for the Full Momentum Method (Brunner, 2016a).

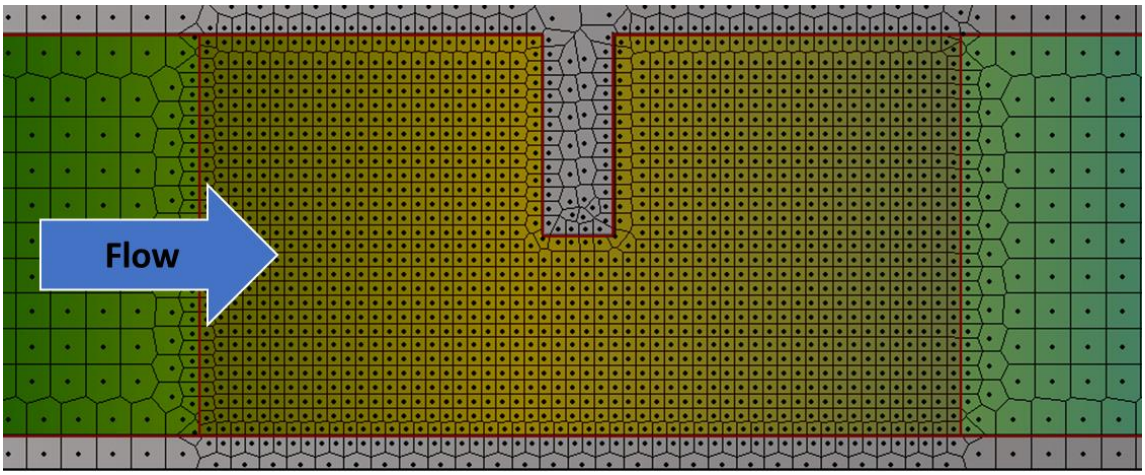


**Figure 13. 2-D model schematic. Representative mesh used in the 2-D HEC-RAS simulations (medium channel width and a 50% contraction) with increased resolution in the vicinity of the structure.**

**Table 7. 2-D model parameters.**

**Summary of 2-D model inputs and parameters used in the 42 HEC-RAS simulations.**

| Relative Size | Channel Width (ft) | Channel Depth (ft) | Slope | *Q* (cfs) | Mesh Size (ft) | Detailed Mesh at Jetty (ft) | Length of Detailed Mesh Up and Downstream |
|---|---|---|---|---|---|---|---|
| **Narrow** | 60.4 | 2.86 | 0.0059 | 10, 100, & 300 | 30 x 30 | 12 x 12 | 100 ft |
| **Medium** | 114.03 | 13.07 | 0.0018 | 100, 1000, 3000 | 10 x 10 | 4 x 4 | 100 ft |
| **Wide** | 519.17 | 19.43 | 0.0018 | 333, 3333, 33333 | 6 x 6 | 2.4 x 2.4 | 100 ft |

Eddy viscosity coefficients used to provide turbulence closure were calibrated using the Jeon et al. (2018) Case 1 flume data from their supplemental materials. Given this study's focus on regions of amplified erosion potential, the eddy viscosity coefficient was calibrated using the reattachment length and locations of relatively large increases in velocity as opposed to velocity values and water surface elevations. Based on this calibration, eddy viscosity coefficients were held constant at 0.25 for all model simulations. This value is typical for straight channels with smooth surfaces and on the upper limits of the "little transverse mixing" intensity range suggested in the HEC-RAS 2-D manual (Brunner, 2016b). Abrupt contractions likely lead to increased transverse mixing; however, a value of 0.25 appears reasonable being on the upper end of the straight channel range and is a precautionary approach that brackets higher estimates of *V* and erosion potential. A sensitivity analysis on eddy viscosity indicated smaller eddy viscosity

coefficients lead to larger $V$ and flow reattachment lengths and thus larger areas of amplified $V$ and $\tau$. Modeled mean $V$ at the structure tip in Jeon et al. (2018) Case 1 was underestimated by 0.16 ft/s, a difference that may be partially attributable to grid resolution and scale effects in simulating the 2.95 ft wide flume.

All models were assessed for changes in spatial distributions of $V$ and $\tau$ relative to the unobstructed channel condition. Regions with relative changes in $V$ and $\tau$ of 1.1, 1.3, 1.5 and 2.0 times the unobstructed channel condition were compared across discharges, contraction percentages, obstruction widths and channel sizes to draw conclusions about the general effects of jetties in diverse river settings. The analysis concentrated on areas of maxima and near bank regions to identify locations in the reach with the highest potential risk for increased bed scour and bank erosion.

The 2D hydraulic modeling results were also used to develop regression equations to determine the spatial distribution of increased velocity due to jetties. Specifically, we were interested in quantifying three metrics: 1) how far downstream the higher velocity region extended, 2) whether or not higher velocities reached the bank opposite the jetty, and 3) the length of the "recirculation zone" downstream of the jetty where velocity and bank erosion risk are expected to be low.

## TWO-DIMENSIONAL MODELING RESULTS

Hydraulic modeling results indicated that higher discharges and higher contraction percentages lead to larger maximum values of absolute $V$ and $\tau$, as well as longer downstream distances with $V$ and $\tau$ exceeding unobstructed channel conditions by more than 10% (Figure 14 a and b). These changes in the length of downstream effects did not increase linearly with structure length (Figure 14 c and d). For all channel widths, contraction percentages and discharge combinations explored increases in $V$ of 1.1, 1.3, 1.5 and 2.0 times the unobstructed channel condition extended a maximum length of approximately $9L_S$, $5L_S$, $3.5L_S$ and $1.8L_S$, respectively, from the downstream edge of the structure, where $L_S$ is the structure protrusion length into the channel. Higher discharge and larger contraction percentages led to longer distances downstream impacted by increased $V$ and $\tau$. Channels with a 50% contraction had velocities up to 1.9, 2.1 and 2.5 times the unobstructed channel $V$ for the narrow, medium, and wide channel, respectively. Shear stresses were up to 3.2, 4.6 and 4.4 times the unobstructed channel shear stress ($\tau_i$) for the narrow, medium, and wide channel. Contractions above 30% increased $V$ on the opposite bank by 1.1 - 1.3 times the unobstructed channel condition for all channel sizes and modeled discharges. Increases in structure streamwise width did not systematically increase the length downstream of the impacted regions as no consistent relationship was observed between structure streamwise width and increases in $V$ and $\tau$. General observed trends for changes in discharge, contraction percentage and structure widths were consistent across the three channel widths. At relatively higher discharges and higher contraction percentages, some flow conditions became supercritical in the contracted regions.

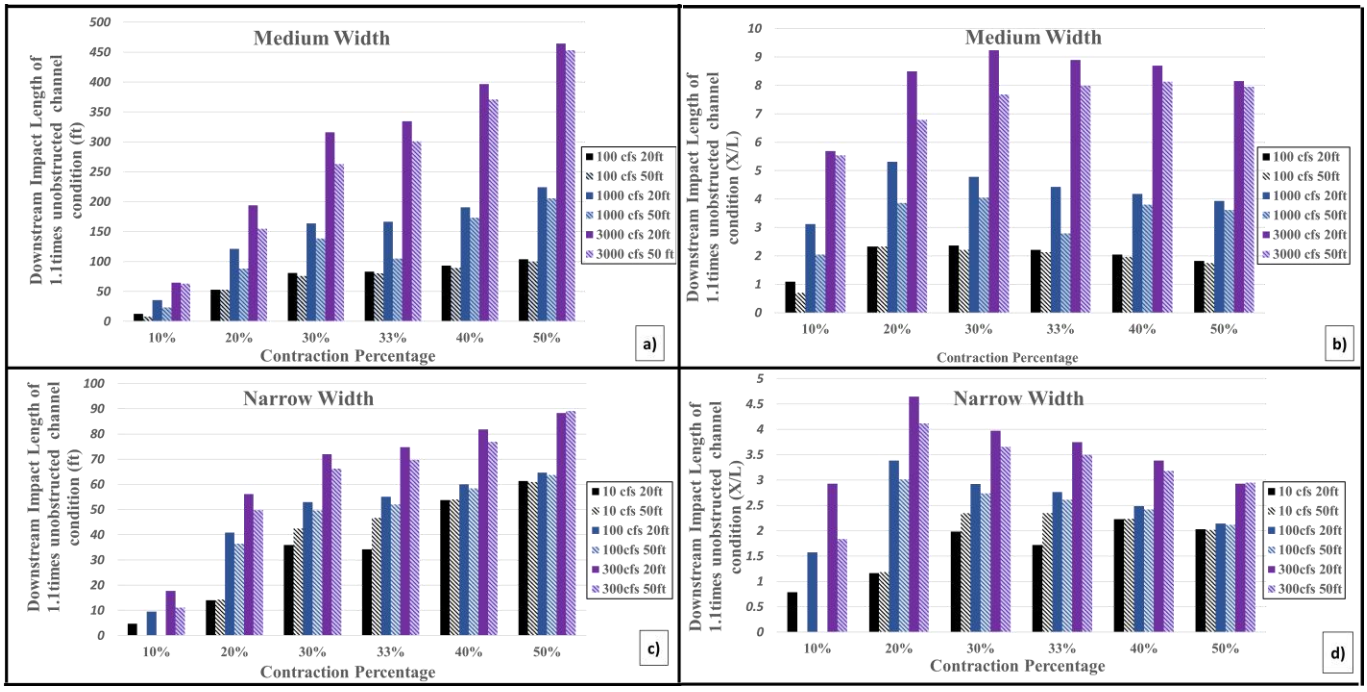


**Figure 14. 2-D model results summary. Downstream length of area with >10% increase in unobstructed channel velocity for a range of discharges and contraction percentages for medium and narrow width channels represented as a distance (a,b) and as a ratio of structure length (c,d).**

### Effect of Discharge

Increasing relative discharge generally led to an increase in the length of channel with $V$ and $\tau$ at least 1.1 times higher than the initial unobstructed channel condition for a constant channel width, structure width, and contraction percentage (Figure 15). Increases in discharge also generally led to an increase in downstream recirculation length. Increasing the discharge while holding contraction percentage constant increased the absolute maximum $V$ and $\tau$ for all channel sizes. The location of the maximum was pushed downstream farther away from the structure tip for larger discharges; for smaller discharges, the maximum $V$ and $\tau$ occurred directly at the structure tip. Due to the increase in impacted streamwise length, larger discharges led to larger

areas on the opposite bank impacted by increased $V$ and $\tau$. Regions with relative $\tau$ of 1.1, 1.3, 1.5 and 2.0 times the unobstructed channel condition were larger than relative $V$ regions generally extending farther downstream and across the channel. Areas directly behind the jetty had low $V$ and $\tau$ with minimal risk for bank erosion and bed scour. The areas directly behind the jetty may not have a high risk for bank and bed erosion but may be prone to sediment deposition. If sensitive habitats that are prone to smothering exist behind the location where a jetty may be implemented, careful consideration of potential effects to that habitat should be considered.

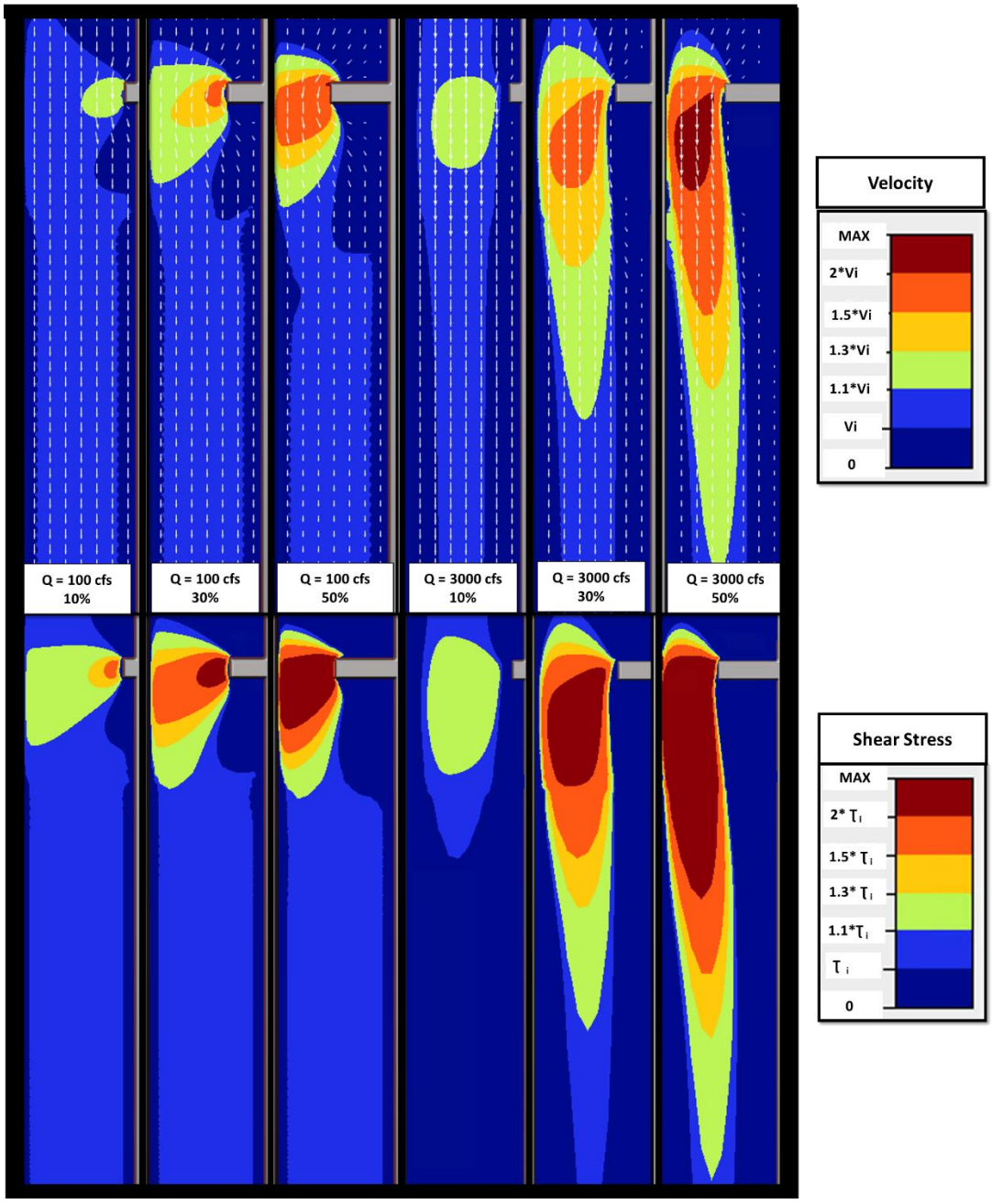


**Figure 15. 2-D graphical results variable discharge. Relative shear stress and velocity regions for low and high discharge in the medium sized channel for three contraction percentages. An increase in discharge leads to longer impacted regions downstream and higher maximum values for all contraction percentages.**

**Effect of contraction percentage**

Increasing the percent contraction while holding other parameters constant generally led to an increase in streamwise length of channel with amplified $V$ and $\tau$ (Figure 16). Additionally, $V$ and $\tau$ maxima increased, consistent with previous experimental and modeling studies examining a narrower range of conditions (Molinas *et al.*, 1998; Seed, 1997; Yeo *et al.*, 2005). Maximum depth averaged $V$ in the narrow and medium channel widths at a 10% contraction ranged from 1.1 - 1.3 times the initial velocity ($V_i$) for all discharges. Maximum depth averaged $V$ in the narrow and medium channel widths at a 50% contraction were higher relative to the 10% contraction and ranged from 1.7 - 2.2 times the $V_i$. Maximum depth averaged $\tau$ in the narrow and medium channel widths at a 10% contraction ranged from 1.2 - 1.6 times the initial shear stress ($\tau_i$) for all discharges. Maximum depth averaged $\tau$ in the narrow and medium channel widths at a 50% contraction were higher relative to the 10% contraction and ranged from 2.4 - 4.6 times the $\tau_i$.

Higher contractions pushed the region of increased $V$ and $\tau$ towards the opposite bank, increasing potential risk for bank erosion. Even for relatively large rivers, contractions of 30% can lead to increases of at least 1.1 times the $V_i$ on the opposite bank and 1.5 times the $\tau_i$**.** For 50% contractions, results indicated that velocities at least 30% larger than the unobstructed condition reach the opposite bank for all discharges and channel sizes. For contraction percentages over 30%, careful attention should be paid to the bank opposite of the installed jetty. If the bank opposite of the jetty appears to be unstable and prone to failure, jetty lengths should be minimized to be below a 30% contraction to limit potential bank failure.

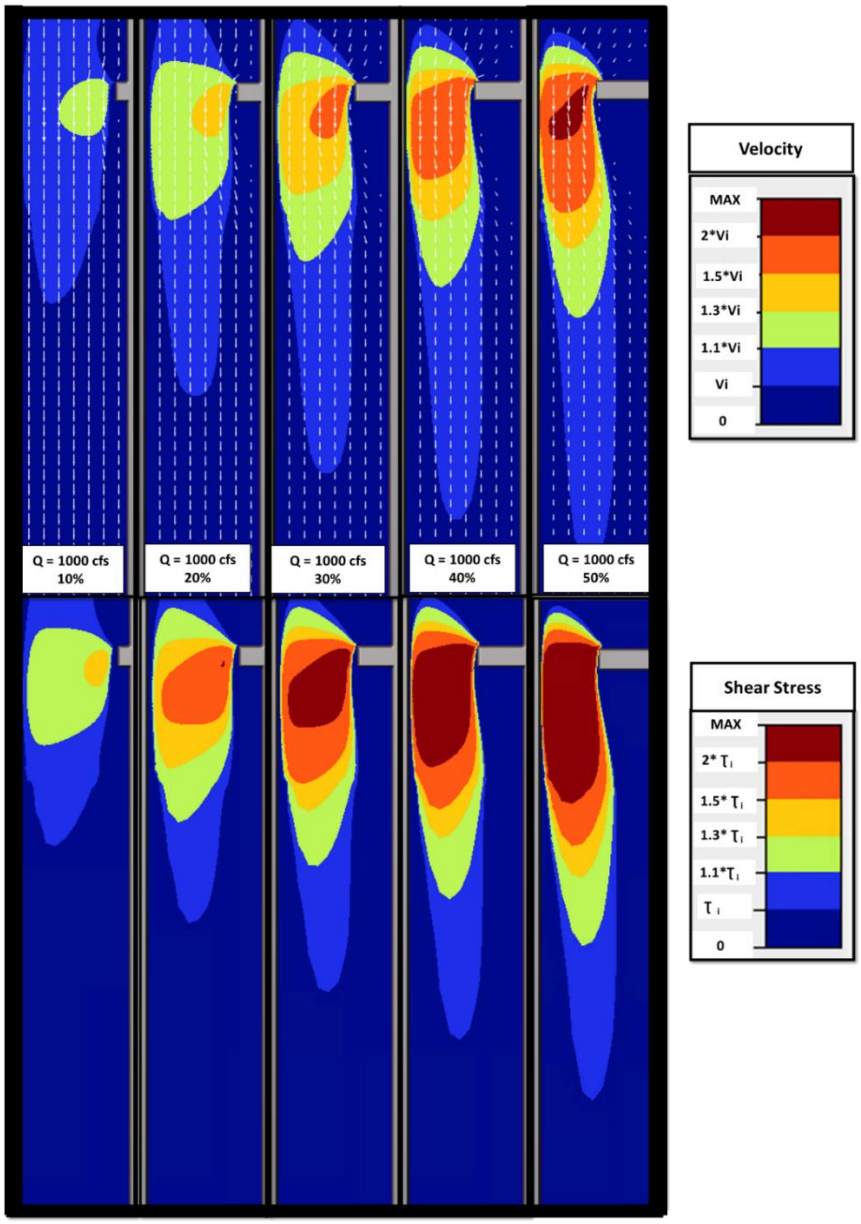


**Figure 16. 2-D graphical results variable contraction. Relative shear stress and velocity regions for a range of contraction percentages in the medium channel width. An increase in contraction percentage leads to longer impacted regions downstream and higher maximum values.**

**Effect of structure width**

Increasing the streamwise structure width did not appear to substantially increase the length of regions with amplified $V$ and $\tau$ (Figure 14; Figure 17). No consistent relationship was observed between the streamwise length required to return to unobstructed channel conditions and structure streamwise width.

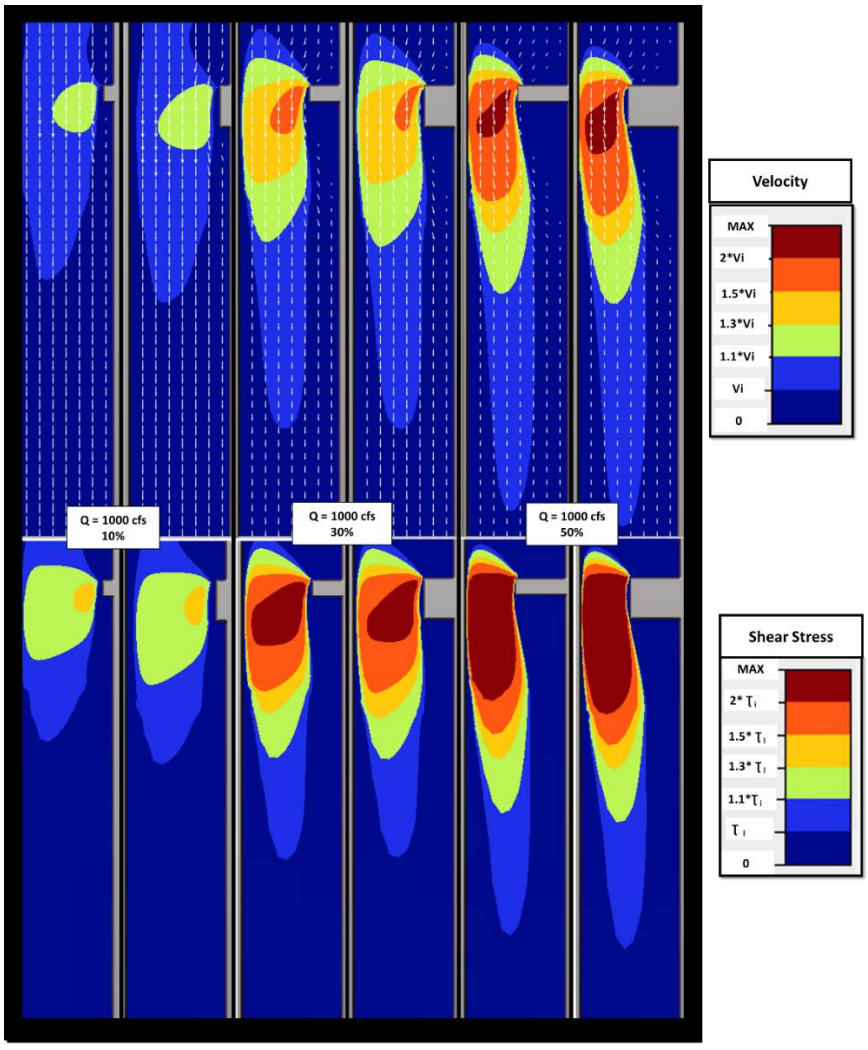


**Figure 17. 2-D graphical results variable jetty width. Relative shear stress and velocity regions for two different structure widths (20ft and 50ft) at a range of contraction percentages for the medium channel width. An increase in structure width leads to longer downstream regions with amplified velocities and shear stresses.**

**Comparison of results to predictive relationships**

Maximum relative changes in *V* (the ratio between the maximum velocity with the structure in place and the unobstructed channel condition) for the medium and narrow channels were plotted for simulations with subcritical flow and compared to predictive relationships from Chapter 2 of this report and previous studies (Seed, 1997; Yeo et al., 2005) using an area ratio (*aaratio*) as the independent variable (Figure 18). Seed (1997) predicted the maximum-depth averaged *V* in the main channel between groynes, and Yeo et al. (2005) developed relationships to predict depth averaged *V* at the tip of a single groyne using results from conducted flume studies. Cross section average *V* was predicted using 1-D hydraulic modeling in HEC-RAS (Chapter 2). HEC-RAS 2-D predictions of maximum *V* using a constant eddy viscosity coefficient in jetty contractions varied substantially for a given *aaratio* (Figure 18). Most of the HEC-RAS 2-D predictions for maximum velocity plotted above the relationship presented in Chapter 2 for cross section average *V* as expected.

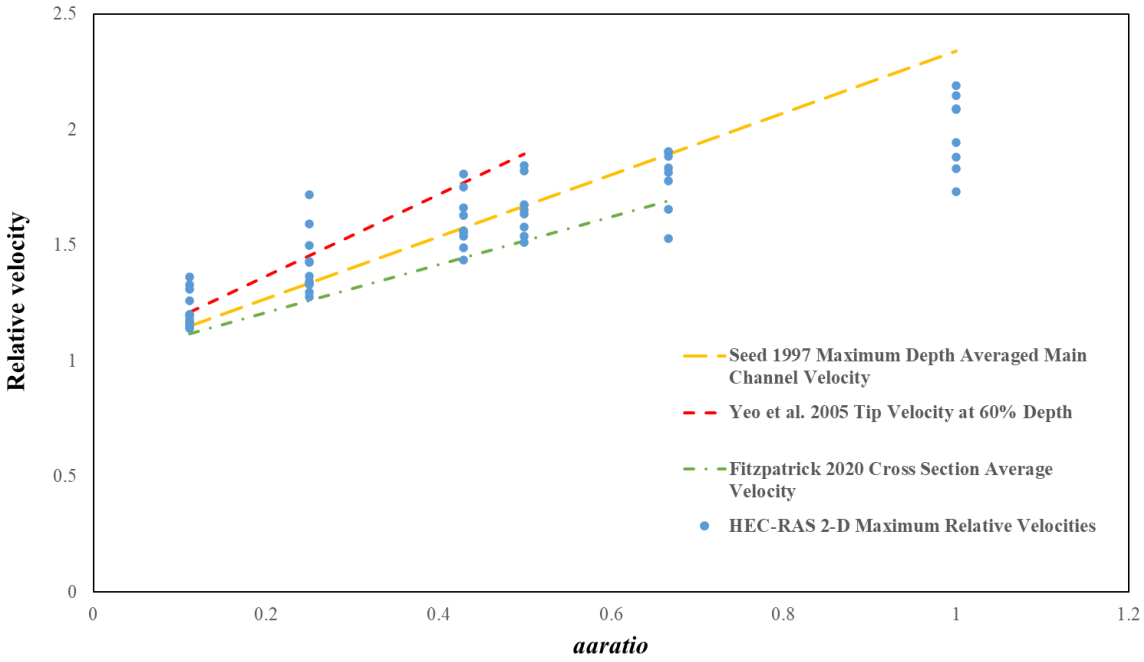


**Figure 18. 2-D results and regression predictions. HEC-RAS 2-D maximum velocities for medium and narrow channel widths compared to three predictive models of relative changes in velocity due to emplaced jetties.**

### Regression equations to predict locations of elevated velocity

Regression equations were developed to quantify three metrics: 1) how far downstream the higher velocity region extended, 2) whether or not higher velocities reached the bank opposite the jetty, and 3) the length of the "recirculation zone" downstream of the jetty where velocity and bank erosion risk are expected to be low.

For the distance downstream, a power function was found to fit the data best. The distance downstream with a specified elevated velocity can be predicted by the following equation:

**Eq. 16** $distance\ DS = 0.49 * \left(\frac{Q}{w-Ls}\right)^{0.34} * \left(\frac{Ls}{w} * 100\right)^{0.69} * w^{0.61} * \left(\frac{V_s}{V_i}\right)^{-3.1}$

The first term is unit discharge ($Q$ is total discharge in ft$^3$/s, which is divided by the flow width in feet), $Ls$ is the jetty length (ft), $w$ is the channel width (ft), $V_s/V_i$ is the relative increase in velocity.

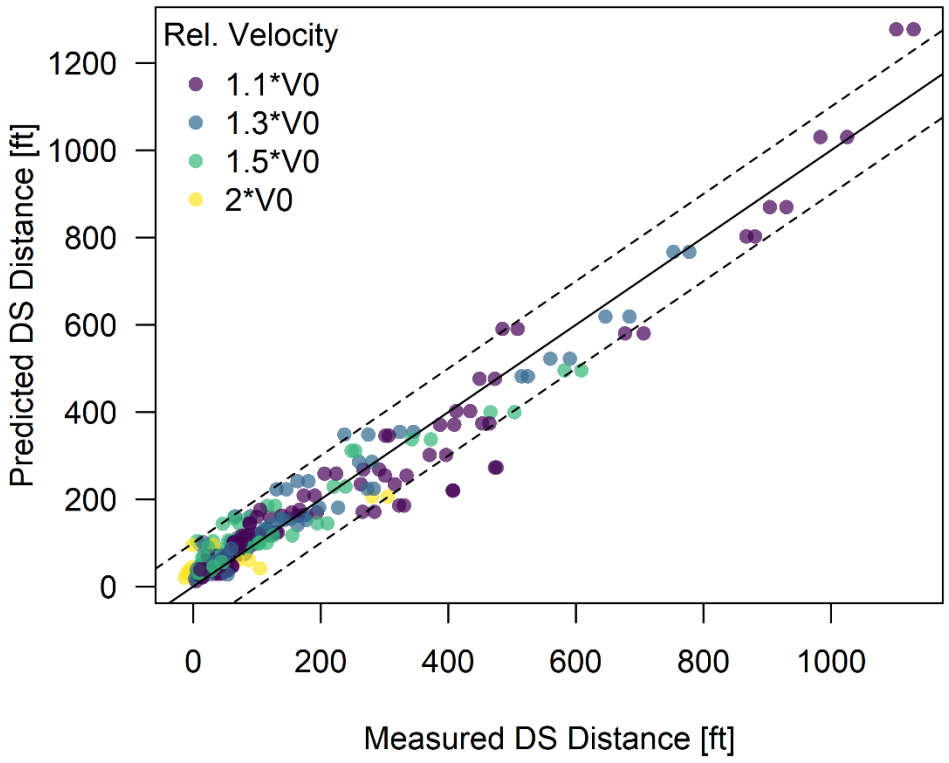


**Figure 19. Predicted downstream distances. Predicted versus measured distance downstream of different relative velocities. Dashed lines show ±100 ft, an estimate of the 95% prediction interval.**

Logistic regression was used to predict the probability that elevated velocity regions reached the bank opposite the jetty. Logistic regression predicts the probability that a binary event occurs

(e.g. a high velocity either reaches the opposite bank or it does not). The following equation was found to best predict this probability:

**Eq. 17** $\ln\left(\frac{p}{1-p}\right) = 20.3 + 0.05\left(\frac{Q}{w-Ls}\right) + 0.4\left(\frac{Ls}{w} * 100\right) - 26.8\left(\frac{V_s}{V_i}\right)$

Where $p$ is the probability of the higher velocity region reaching the opposite bank. The table below shows the performance of the logistic regression. It correctly predicts whether the region reaches the opposite bank 91% of the time. In 5% of cases, it produces a false negative. In 4% of cases, it produces a false positive.

**Table 8. Performance of logistic regression.**

| | | Reaches Opposite Bank - Predicted | |
|---|---|---|---|
| | | No | Yes |
| Reaches Opposite Bank - Observed | No | 43% | 4% |
| | Yes | 5% | 48% |

The final regression used a power function to predict the length of the "recirculation zone" downstream of the jetty. This is an area where the flow is directly disrupted by the jetty and we expect low velocity and, therefore, low bank erosion risk. Essentially, the jetty is protecting a section of the bank immediately downstream from erosion.

**Eq. 18** $recirculation\ length = 8.5 * \left(\frac{Q}{w-Ls}\right)^{0.75} * Ls^{1.55} * w^{-1.27}$

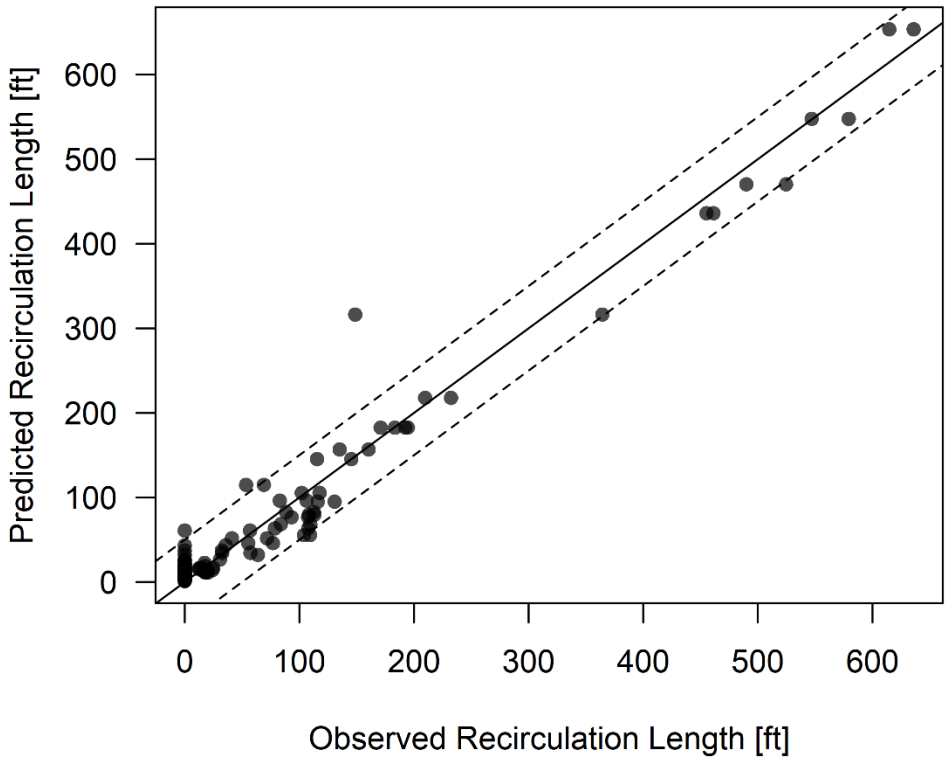


**Figure 20. Predicted recirculation lengths. Predicted versus observed recirculation length. Dashed lines show ±50 ft, an estimate of the 95% prediction interval.**

These three regression equations are useful for providing estimates of the spatial extent of altered velocity due to jetties. However, the values calculated by these equations contain a high degree of uncertainty and should only be used in determining relative locations of high velocity regions. For example, Eq. 16. may predict that an area with twice the initial velocity may extend 200 feet downstream of the jetty. The true value could actually be anywhere from 100-300 feet downstream. Care should be taken when applying these equations to real jetty structures.

## DISCUSSION OF FINDINGS

This study found that increases in contraction percentage and discharge led to larger maximum values of absolute $V$ and $\tau$ in addition to longer downstream distances with increased $V$ and $\tau$ relative to unobstructed channel conditions. To minimize the risk of potential bed scour and erosion on the opposite bank, contraction designs should be informed by these results with careful consideration of the potential for large runoff events during the expected lifetime of the structure. The risk of erosion on the opposite bank will depend on bank characteristics such as bank angle, presence of vegetation and material cohesion. For temporary structures such as bridge construction access platforms, in-water working windows may serve as a valuable time frame reference for determining the probability of larger storm events. At relatively high discharges and contraction percentages, some hydraulic model simulations became supercritical in the contracted regions. Supercritical flow conditions may lead to hydraulic jumps and high velocities that may impede the movement of aquatic organisms.

Two-dimensional modeling results indicated that higher contractions push the increased $V$ and $\tau$ regions towards the opposite bank, potentially increasing the risk of bank erosion. Contractions of 30% can lead to 10% increases in $V$ and 50% increases in $\tau$ on the opposite bank. Previous guidance on installing spurs in narrow river channels, which are similar to jetties (<250ft wide) suggest flow constriction may cause erosion on the bank opposite of the jetty but, in some cases, may be purposely used to shift the channel location (Lagasse *et al.*, 2009). For temporary structures such as jetties, the stability and erodibility of the opposite bank should be carefully evaluated to determine the potential risk for contraction percentages ≥30%. Modeling results also

indicated that the length downstream impacted by velocities of at least 1.1 times the $V_i$ was not linearly related to structure length. Longer structures contributed to relatively smaller changes in distance impacted downstream compared to shorter structures.

Calibration of the eddy viscosity coefficient for a range of channel contraction percentages and discharges was limited by a paucity of large-scale field data available in the literature. The eddy viscosity coefficient was calibrated using the Jeon et al. (2018) flume study; however, HEC-RAS 2-D modeling of small scales flumes proved challenging due to the need for small mesh sizes and time steps to produce stable and accurate simulations. The eddy viscosity coefficient in this study was held at a constant value for all model simulations, while in reality this value likely increases with increasing contraction percentage and may change with discharge. Though this study held the eddy viscosity coefficient constant, general trends observed in changes in spatial locations of increased relative $V$ and $\tau$ were consistent with previous studies (e.g. Jeon et al., 2018), indicating that these results can provide useful insights to jetty effects on spatial patterns of $V$ and $\tau$.

Comparison of maximum relative changes in $V$ to predictive relationships from previous studies and Chapter 2 using an area ratio predictor variable (*aaratio*) showed that the 2-D HEC-RAS predictions varied for a given *aaratio* but, generally fell within the range of relationships suggested by Seed (1997) and Yeo et al. (2005). The variability in 2-D HEC-RAS predictions from the regressions may be due in part to the lack of calibration of the eddy viscosity coefficients for increasing contraction percentages and discharges. Future studies are

recommended to evaluate the effect of contraction percentage and discharge on the eddy viscosity coefficient and improve model accuracy. Such data would be particularly useful to DOTs modeling bridge abutments in 2-D HEC-RAS; however, such a study would require detailed field data or large-scale flume studies.

This study focused on rectangular channel geometries and vertical-wall jetties installed perpendicular to the bank. Many studies have been conducted on rectangular channels and some have evaluated changes in installation angle and structure shape (Melville, 1992; Yazdi *et al.*, 2010). However, studies on irregular and complex channel bathymetries are rare. Future research should evaluate the effects of compound channels, and other realistic channel bathymetries on flow fields in contracted regions. Results from this study are expected to be representative of general trends, even for actual river channels. However, more complex channel geometries are expected to exhibit some variance from these results.

## CHAPTER SUMMARY

Two-dimensional hydraulic modeling results indicated that higher discharges and contraction percentages led to larger maximum values of $V$ and $\tau$ thereby increasing the risk of potential bank erosion and bed scour. Maximum depth averaged $V$ in the narrow and medium channel widths at a 10% contraction ranged from 1.1 - 1.3 times the $V_i$ for all discharges. Maximum depth averaged $V$ in the narrow and medium channel widths at a 50% contraction were higher relative to the 10% contraction and ranged from 1.7 - 2.2 times the $V_i$. Maximum depth averaged $\tau$ in the narrow and medium channel widths at a 10% contraction ranged from 1.2 - 1.6 times the

$\tau_i$ for all discharges. Maximum depth averaged $\tau$ in the narrow and medium channel widths at a 50% contraction were higher relative to the 10% contraction and ranged from 2.4 - 4.6 times the $\tau_i$.

Increasing discharge and contraction percentage led to an increase in streamwise length of channel impacted by *V* and $\tau$ at least 10% higher than the initial unobstructed channel condition. Longer jetties and higher discharges, therefore, increase the area at higher risk for potential bed and bank erosion. Increasing channel contraction percentage pushed increased *V* and $\tau$ regions closer to the opposite bank. Results indicated contraction percentages over 30% may lead to increases in *V* and $\tau$ on the opposite bank regardless of channel size. Contractions above 30% increased *V* on the opposite bank by 1.1 - 1.3 times the unobstructed channel condition for all channel sizes and modeled discharges. Relative changes in $\tau$ compared to unobstructed channel conditions were approximately 46% larger on average than relative changes in *V*.

These 2-D modeling results are preliminary and cover a much smaller range of scenarios than were included in the development of the 1-D regression models. Still, findings from this study can be used with predictive relationships (Chapter 2) to develop straightforward and efficient tools that can be applied to jetties for planning, preliminary design, and decision making. Chapter 4 of this report discusses the development of an Excel-based tool that combines qualitative predictions from Chapter 2 with spatial results from this chapter. The Excel-based tool integrates the 2-D spatial patterns in hydraulics revealed in this chapter with the predictive models for *V* and $\tau$ (Chapter 2) into a unified framework that was developed to provide valuable

insights into potential hydraulic and geomorphic effects of jetties before structure emplacement when more complex modeling is infeasible.

# CHAPTER 4. EXCEL BASED MACRO TOOL DEVELOPMENT

A spreadsheet tool was developed in an Excel macro-based workbook to help the Georgia Department of Transportation respond to environmental permitting concerns about potential hydraulic and geomorphic effects of temporary jetties used for bridge construction. The tool combines the predictive regressions for estimating cross section averaged absolute and relative changes in velocity and shear stress from Chapter 2 with spatial results from Chapter 3. Additionally, a module allows the user to estimate the relative risk of bank erosion.

## EXCEL BASED MACRO TOOL OVERVIEW

The Excel-based management tool integrates the 2-D spatial patterns in hydraulics from Chapter 3 with the predictive models for $V$ and $\tau$ from Chapter 2 into a unified framework that can provide valuable insights into potential hydraulic and geomorphic effects of jetties before structure emplacement when more complex modeling is infeasible. The tool aims to combine results and recommendations from this study into a user-friendly format for ease of application for state DOTs as they plan and design jetties for bridge construction. To improve usability, the Excel-based tool contains a set of Visual Basic for Applications macros to automate user tasks or calculations.

The tool contains two main modules: the jetty hydraulics module and the bank erosion risk module. The jetty hydraulics module uses predictive regressions from this study to provide estimates of mean relative and absolute changes in velocity and shear stress and provide

estimates of maximum tip velocities using regressions developed by Yeo et al. (2005). The second module helps identify bank erosion risk potential in a qualitative sense: high risk, medium risk, low risk.

## JETTY HYDRAULICS MODULE DEVELOPMENT

The jetty hydraulics module predicts mean and relative changes in $V$ and $\tau$ based on inputs of structure length, channel dimensions, discharge, Manning $n$, and bed slope using the equations developed in Chapter 2. Relative changes in mean velocity and shear stress may be useful for DOTs for comparison of increases in velocities and shear stresses between multiple potential jetty configurations for a given project, and as a communication tool. Absolute velocity and shear stress magnitudes are predicted based on estimates of $V_i$ based on field or modeling data and equations developed in Chapter 2. Absolute mean velocity and shear stress can help DOTs estimate the risk of bed scour and provide insights into whether the installed jetty will hinder the aquatic organism passage. This module also estimates maximum mobile bed grain size based on the calculated mean absolute shear stress.

Although this study did not develop predictive regressions for maximum velocity, we included maximum velocity predictions into the main module based on regressions developed by Yeo et. al (2005). The Yeo et al. (2005) equation predicts depth averaged velocities at the jetty tip. Based on the literature review, there does not appear to be an easily applied regression to predict maximum shear stress in a river channel due to jetty emplacement. Therefore, the tool currently does not have the capacity to predict maximum shear stress due to jetty emplacement. Previous

research has developed equations to predict scour depths (eg. Pandey et al., 2018; Zhang & Nakagawa, 2008) and shear stresses around other structures similar to jetties (Molinas *et al.*, 1998); however, these typically require a form of Froude number and flow depth which may not be readily obtainable.

Finally, the jetty hydraulics module also contains data on spatial distributions of increased velocities and shear stress from the 2-dimensional hydraulic modeling (Chapter 3). The regression equations developed in Chapter 3 are included to predict 1) how far downstream the elevated velocity regions extended, 2) whether or not elevated velocities reached the bank opposite the jetty, and 3) the length of the "recirculation zone" downstream of the jetty where velocity and bank erosion risk are expected to be low.

## BANK EROSION RISK MODULE DEVELOPMENT

In addition to the main module, the tool contains a bank erosion risk module focused on identifying locations susceptible to bank erosion. The bank erosion risk module will largely serve as a risk assessment tool. The main purpose of this module is to help identify bank erosion risk potential qualitatively due to jetty emplacement: high risk, medium risk, low risk.

The bank erosion module was developed to aid GDOT inspectors determine the level of bank erosion risk associated with bridge installation projects with in-stream jetties. The goal was to provide a robust but easy to use tool to determine whether stream banks were at high, medium,

or low risk of erosion following jetty installation. The bank erosion module was developed based on review of the published literature and professional experience. This tool was designed to be applied to multiple locations surrounding the bridge and jetty (e.g. upstream and downstream, on both the left and right banks). Different bank locations may have different erosion potential and should be evaluated separately. However, the assessment of bank erosion risk uses estimates of velocity at the bank opposite the jetty. This is therefore a worst-case scenario for bank erosion and these predictions may not be directly applicable to other bank locations. This module consists of a series of questions to be answered by the user, as well as some quantitative data (e.g. bank height and angle for cohesive/consolidation material). The basis of the bank erosion risk tool is summarized below and in a simple flow chart (Figure 23) and a figure/table (Figure 22; Table 9).

**Flow Chart Overview**

If there is evidence of recent erosion (e.g. bare bank face from recent scour or collapsed soil blocks from bank failure), then this bank is at high risk of erosion. A jetty installed on one or both banks will likely prevent erosion of streambanks immediately downstream by diverting potentially erosive flows away from those banks into the center of the channel. Streambanks within a certain distance downstream of the jetty will likely be protected from erosion in this fashion, and are therefore at low risk of bank erosion. The distance downstream that is protected by the in-stream structure can vary significantly, and is estimated based on the power function for recirculation length described in Ch. 3. If the bank is not currently eroding and will not be protected by the installation of the jetty, a more detailed risk assessment is warranted. This assessment is based primarily on the bank material, bank toe (base of the bank) material, bank

geometry (height and angle), and vegetation. This assessment is drawn largely from the work of Bledsoe et al., (2012). Each of these variables is described in more detail below:

- Bank material: Banks consisting of cohesive, consolidated material (e.g. clay and silt) are generally more resistant to bank erosion than unconsolidated, granular material (e.g. sand and gravel) (Simon et al., 2000; Thorne, 1982). Examples of bank consolidation can be found in Figure 21.

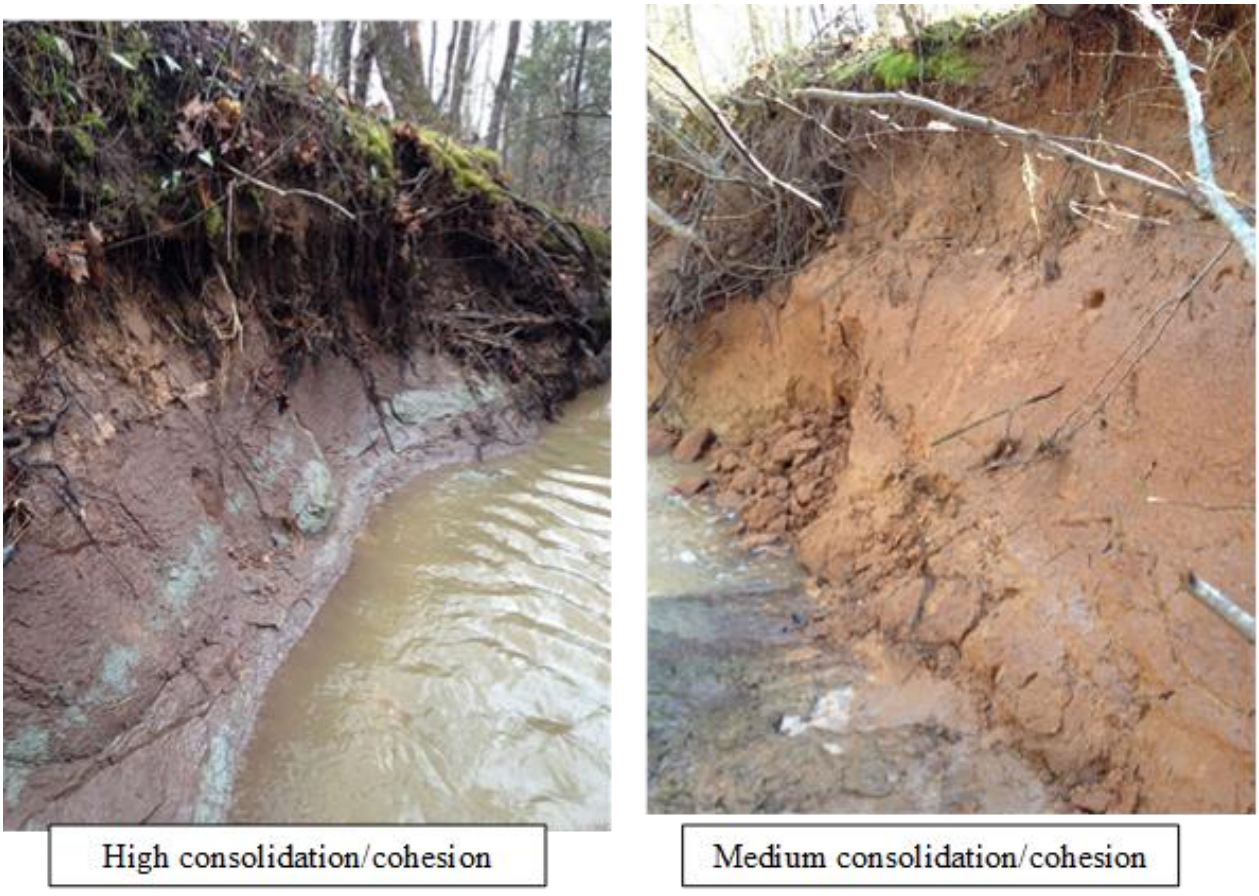


**Figure 21. Bank photos. Examples of high and medium consolidation for river banks.**

- Bank toe material: The toe of the bank (e.g., the base where the normal low water level is located) is critical for the stability of the whole streambank (Thorne, 1982). Erosion of this toe can create an undercut bank, leading to failure of the whole streambank. On the other hand, a toe that is resistant to erosion can prove remarkably adept at keeping the entire streambank in place.

- Bank geometry: The angle and height of the bank strongly control bank stability, with shallow, short banks more stable and less prone to erosion than steep, tall banks. This is also dependent on bank material. Tall, steep banks may be stable if they are made of a cohesive material. These interacting effects were accounted for in this analysis. Figure 22 and Table 9 show stability curves for streambanks of different materials. These data can be used to estimate the "critical" bank height for stability, based on bank angle and soil type. If the measured bank height is higher than this critical height, the bank is likely unstable[1].

[1] These curves were calculated using the Culmann relationship for critical bank height (Bledsoe et al., 2012; Terzaghi, 1943): $H_c = \frac{4c' \sin \propto \cos \phi'}{\gamma(1-\cos(\alpha-\phi'))}$, where $H_c$ is the critical bank height (m), $c'$ is the effective soil cohesion (kPa), $\phi'$ is the soil friction angle (degrees), $\gamma$ is the unit weight of the soil (kN/m$^3$), and $\alpha$ is the bank angle (degrees). For this analysis, typical values of $\phi'$ (20°) and $\gamma$ (kN/m3) were used along with representative values of $c'$ for low (1 kPa), medium (2.5 kPa), and highly consolidated/cohesive material (5 kPa) (Simon et al., 2011).

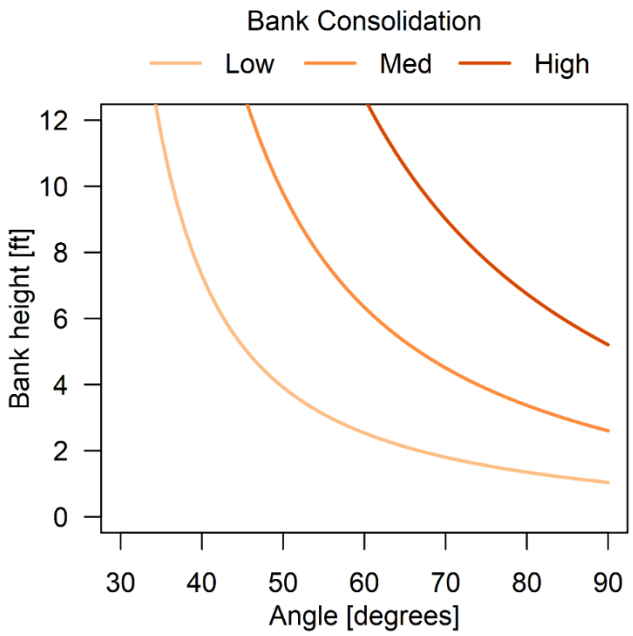


**Figure 22. Bank stability curves. Critical bank height curves for various bank soil consolidation and angles. Data are provided in tabular format below.**

**Table 9. Bank stability table. Critical bank height curves for various bank soil consolidation and angles.**

| Angle (degrees) | Critical Bank Height (ft) | | |
|---|---|---|---|
| | Low Consolidation | Med Consolidation | High Consolidation |
| 30 | 22.5 | 56.4 | 112.7 |
| 35 | 11.5 | 28.8 | 57.6 |
| 40 | 7.3 | 18.3 | 36.5 |
| 45 | 5.2 | 12.9 | 25.8 |
| 50 | 3.9 | 9.8 | 19.6 |

| | | | |
|---|---|---|---|
| 55 | 3.1 | 7.8 | 15.5 |
| 60 | 2.5 | 6.3 | 12.7 |
| 65 | 2.1 | 5.3 | 10.6 |
| 70 | 1.8 | 4.5 | 9.0 |
| 75 | 1.6 | 3.9 | 7.8 |
| 80 | 1.3 | 3.4 | 6.7 |
| 85 | 1.2 | 3.0 | 5.9 |
| 90 | 1.0 | 2.6 | 5.2 |

- Vegetation: Vegetation (either naturally occurring or intentionally planted) can increase bank resistance to erosion both by increasing roughness near the bank and strengthening bank soil with roots (Pollen-Bankhead and Simon, 2010). Vegetation on the face of the bank is especially important.

These variables are incorporated into the flowchart below. Users follow the flowchart, answering the relevant questions to determine the risk category of the analyzed bank (low, medium, or high). The near-bank velocity (with the jetty in place) is estimated from the hydraulics portion of the tool. The relative velocity increase that has a 50% chance of reaching the opposite bank is estimated from Eq. 17 (using p = 0.5). This relative velocity is then multiplied by the pre-jetty in-channel velocity to estimate the near-bank velocity opposite the jetty. For all banks, the maximum permissible velocity of the bank material ($v_c$) is estimated based on Fischenich

(2001). If the calculated velocity ($v$) is higher than this value, erosion is likely to occur. To account for uncertainty in these calculations and provide some factor of safety, the following categories were used: $v < 0.9v_c$ = low risk; $0.9v_c \leq v \leq 1.5v_c$ = medium risk; and $v > 1.5v_c$ = high risk. For consolidated banks only, the risk of bank erosion by mass failure/collapse is also assessed using the critical bank heights and angles shown in Figure 22/Table 9. Similar categories of risk are assessed by comparing bank height to the critical bank height for stability. For these consolidated banks, the total erosion risk is the higher of either risk from collapse or excess shear stress (e.g. if $v > 1.5v_c$ and $H < 0.9H_c$, the bank is at high risk of erosion). These risk categories can be used to determine whether any additional mitigation measures are necessary:

- **Low Risk:** No bank erosion mitigation measures are required.
- **Medium Risk:** We suggest continued monitoring of these streambanks during the course of the construction project. Stabilization measures may be required if excess erosion is observed.
- **High Risk:** We recommend stabilizing streambanks in the high risk category to mitigate potential damaging effects. The severity of the bank erosion threat depends on the proximity to infrastructure or private land that must be protected.

## CHAPTER SUMMARY

The Excel-based management tool described in this chapter can be applied to gain insights into potential hydraulic and geomorphic effects of in-stream temporary riprap jetties for bridge construction before jetties are emplaced in the channel. This will allow GDOT to communicate

efficiently and effectively with environmental permitting agencies about potential implications of jetty emplacement in river channels. This Chapter described the two main modules included in the tool and how they were developed. Chapter 5 is an application guide describing how to use the tool and the individual equations developed in Chapter 2.

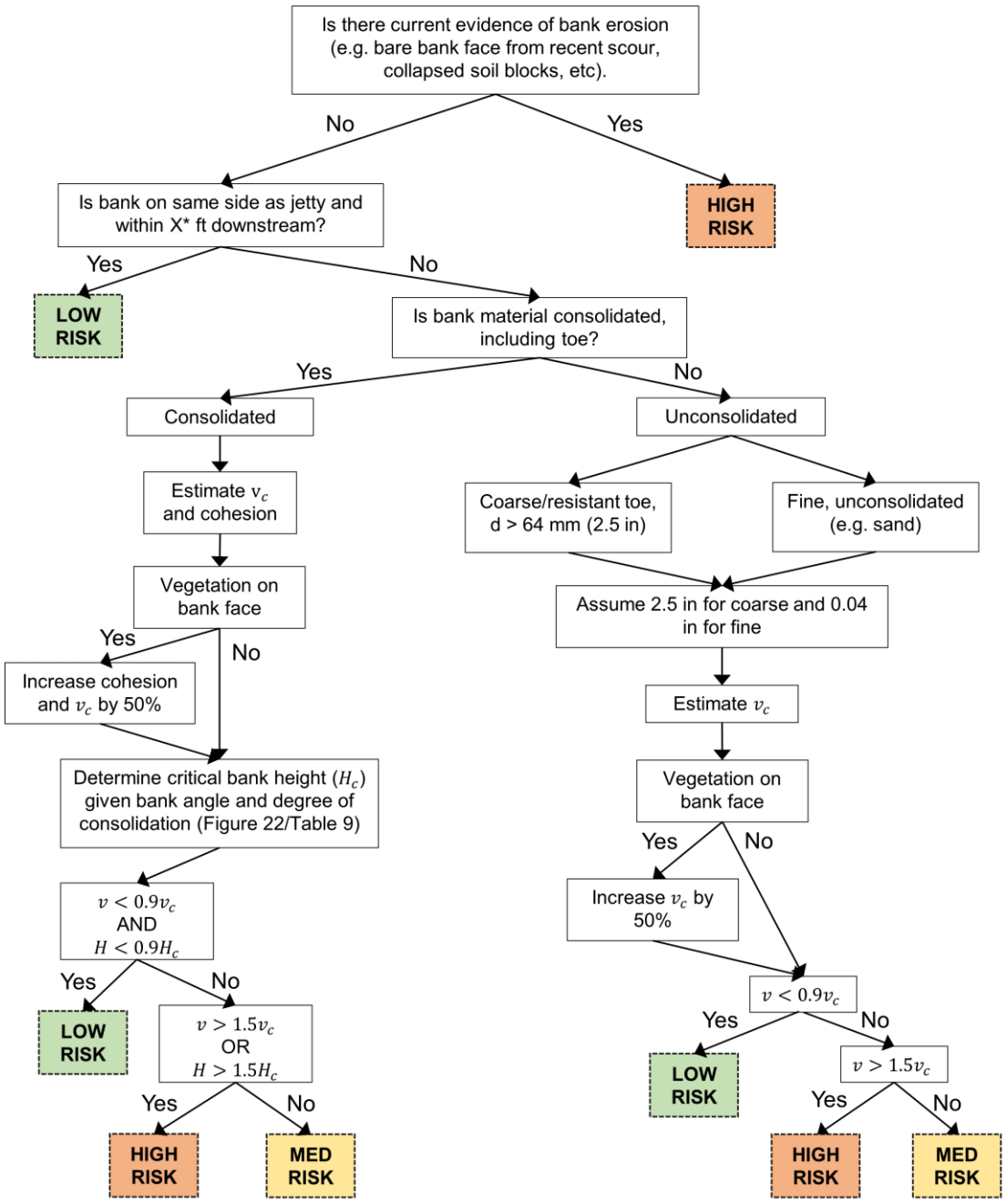


**Figure 23. Bank erosion risk flow chart. Flow chart used in the Excel tool to determine bank erosion risk in a qualitative sense. *Distance downstream where the bank is protected by the jetty is estimate from Eq. 18.**

# CHAPTER 5. APPLICATIONS GUIDE

This chapter serves as an applications guide for the developed regressions and the Excel-based management tool. This Chapter is a step by step guide to implementing the developed regressions and Excel-based management tool to determine potential hydraulic and geomorphic effects of jetties before they are installed in river channels. The developed regressions can be applied on their own or can be applied using the Excel-based management tool. Both applying the regressions and using the Excel-based tool will require collection of some data.

## DATA COLLECTION FOR HYDRAULICS TOOL AND ASSESSING BANK EROSION RISK

The first step to applying the velocity and shear stress regressions or the Excel-based macro tool is to collect the following data. An example field data collection form is provided in Appendix D.

1. **Jetty length:** Length of the jetty projecting into the main channel flow. This should be measured from where the jetty touches the bank to the tip of the jetty in the flow.
    a. The jetty length can be based off of a preliminary design or measured if the jetty is already installed.
    b. In the field, length can be measured using a total station, or measuring tape.

2. **Channel width:** Width of the channel at the structure installation height at the location where the jetty will be installed. This should be measured from the channel bank, where the structure will be installed to the channel bank on the opposite side.
    a. Channel width can be measured in the field using a total station or measuring tape.
    b. Channel width can also be measured from the office using GIS data or google earth if field data is not available.
3. **Bed Slope:** The slope of the channel bed in the region where the jetty will be installed.
    a. Bed slope can be estimated by collecting two data points, one upstream of the jetty location and one downstream of the jetty location. The bed elevations should be subtracted from one another and divided by the distance between the two points.
    b. Bed elevation and the distance between the two points can be measured in the field using a total station.
    c. If field data is not available, bed slope can be calculated using bathymetry data, or ArcGIS data assuming water surface slope approximates bed slope.
4. **Manning Roughness Coefficient:** The roughness of the channel based on grain size, bed forms vegetation and channel morphology.
    a. Manning roughness can be estimated based on grain size, channel morphology and the presence of vegetation, and bedforms using professional judgment or Manning roughness estimation equations.

b. In the field, practitioners should document the relative amount of vegetation, the average grain size and if bedforms are present to help justify the selection of a given Manning roughness value. Pictures may also prove to be useful to collect in the field.

5. **Discharge of interest:** The discharge that is expected to be flowing through the cross section with the emplaced jetty throughout the lifetime of the structure. For conservative estimates of absolute mean velocities and shear stresses and maximum velocities the highest expected discharge during the lifetime of the jetty should be used. However, the regression equations assume (1) the discharge is wholly contained within the channel (no overbank flow) and (2) the jetty does not overtop. Therefore, this discharge should be the largest expected discharge that will not go overbank and not overtop the jetty.

To improve prediction accuracy, the following data should be obtained if available:

1. **Actual Channel Bathymetry:** Actual channel bathymetry or the channel shape can be used to provide more accurate estimates of the *aaratio* then just knowing the channel width itself.

    a. Actual channel bathymetry can be obtained using a collection of total station data points, using green lidar data, or from acoustic doppler current profilers with bottom tracking capabilities.

2. **Cross section average velocity or shear stress without the jetty:** The cross section average velocity or shear stress without the jetty in place can be used along with the relative change in velocity regressions to predict absolute velocities by multiplying by the unobstructed channel condition.

    a. Cross section average velocities or shear stresses can be obtained using collected field data at the discharge of interest when the jetty was NOT in the river channel.

    b. Cross section average velocity or shear stress can be obtained from existing hydraulic models of the anticipated bridge construction site if they are available for the discharge of interest. Hydraulic models can be from HEC-RAS, SRH-2D or any other hydraulic modeling software.

3. **Average cross section water depth without the jetty:** The depth of water at the cross section where the jetty will be installed without the jetty in place for the discharge of interest. This value can be used to estimate initial velocity or shear stress using the Manning Equation and the shear stress equation, respectively, if the initial values are not known from field measurement or hydraulic models.

    a. Water depth can be measured in the field using a total station, or a measuring stick.

    b. Water depth for the discharge of interest may also be obtainable through stage discharge relationships from USGS gauges if field data is not available.

Furthermore, the following data are required to use the tool to assess bank erosion risk. Different locations along the channel may have different levels of bank erosion risk. Therefore, multiple bank locations should be assessed separately, with data collected for each. Downstream impacts of jetties can vary, but may extend up to 10 times the jetty length downstream. Note that the estimated velocity used to assess bank erosion risk is estimated for the bank opposite the jetty. This should be considered a maximum near-bank velocity in the reach and may not be applicable to all assessed banks.

1. **Presence and description of vegetation on bank face:** Vegetation on the face of the bank can help reduce erosion in two ways. First, roots can increase the strength and stability of the bank material. Second, vegetation increases roughness and prevents the detachment of bank material by flowing water. The tool uses a binary assessment of bank vegetation (e.g. present or not).

2. **Bank material:** Bank material is classified as consolidated/cohesive or unconsolidated. Consolidated material includes silt and clay. Unconsolidated material includes sand and gravel/cobble.

    a. **Unconsolidated banks:** For unconsolidated banks, the tool will assume a grain size of the bank material based on a user input of “coarse” (e.g. cobble and larger) or “fine” (e.g. sand and gravel).

    b. **Consolidated banks:** Consolidated banks can be classified into “low”, “medium”, and “high” consolidation. Photos are provided in Chapter 4 to help

determine the relative consolidation of each bank. A bank height and angle are required for consolidated banks. Bank height can be measured using a tape or survey equipment. The simplest method is to lay a tape from the base of the bank to the top (measuring the length of the bank slope). This can then be converted to a vertical height based on the measured bank angle. Bank angle can be measured in the field using a construction angle finder (e.g.: https://www.grainger.com/product/JOHNSON-Protractor-Angle-Finder-6A511). Alternatively, the horizontal and vertical dimensions of the bank can be measured and used to calculated the bank angle.

## MEAN VELOCITY AND SHEAR STRESS REGRESSIONS

This report outlined five predictive regressions to estimate changes in mean velocity and shear stress. Mean velocity and shear stress refer to the cross section depth averaged velocity and shear stress values. The guidelines in this section can be used to predict changes in velocity and shear stress due to jetty implementation without using the Excel-based management tool. Note the Excel-based management tool also implements these equations and can be used to automate calculations. The first step to implementing any of the predictive regressions is to calculate the *aaratio*.

### Calculating the *aaratio*

The first step to implementing any of the predictive regressions is to calculate the *aaratio*. The *aaratio* is simply the area of the jetty (grey area in cross section view of Figure 24) divided by the remaining flow area with the structure in place (blue area in cross section view of Figure 24).

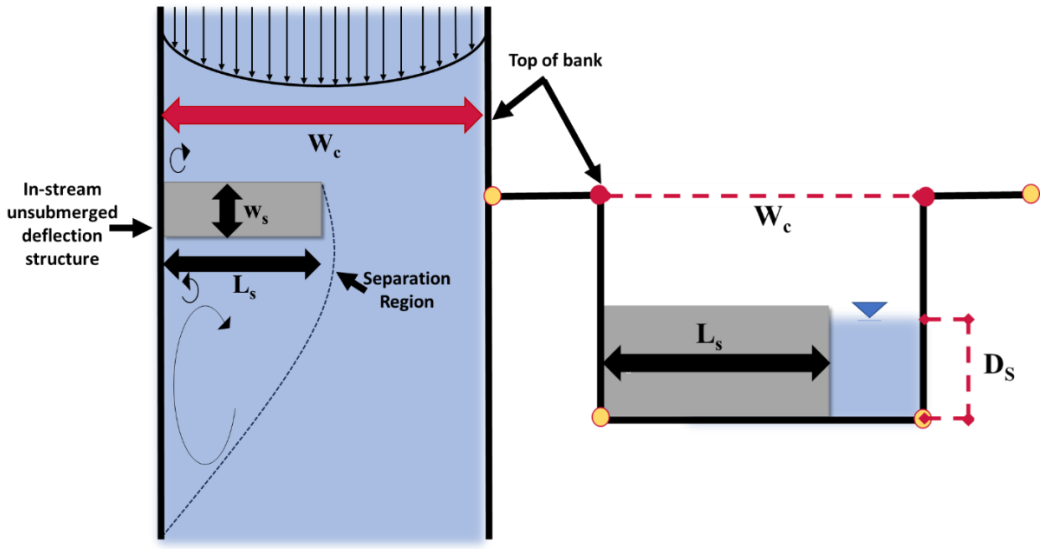


**Figure 24. Conceptual figure of jetty and channel. Profile and plan view of typical jetty where $W_c$, $L_s$, and $D_s$ are the channel width, structure length, and height of the structure in contact with water, respectively. The grey area in the cross section view represents the jetty area, the remaining blue area is the flow area with the jetty in place.**

The aaratio should be calculated with the best available data to ensure model prediction accuracy. If the channel bathymetry is known, the aaratio should be calculated using the channel bathymetry. If the channel bathymetry is not known, the aaratio can be estimated assuming a rectangular channel geometry.

**Known bathymetry**: To estimate the *aaratio* if the channel bathymetry is known, both the jetty area and the flow area with the structure in place need to be calculated. Equation 19 should be applied if the actual channel bathymetry is known. The jetty area can be calculated as the jetty length, $L_s$, multiplied by the depth of water in the channel for the discharge of interest, assuming a rectangular jetty geometry. The remaining flow area can be calculated as the initial flow area without the structure in place subtracted from the jetty area. The initial flow area without the

structure in place can be calculated using the actual channel bathymetry by using a trapezoidal approximation.

**Eq. 19.** $aaratio = \frac{jetty\ \ area}{remaining\ \ \ flow\ \ area\ \ with\ structure\ \ \ in\ place}$

**Unknown Bathymetry:** To estimate the *aaratio* if the channel bathymetry is unknown, the *aaratio* can be calculated assuming a rectangular channel geometry. This method increases the error of model prediction for non-rectangular channels. If channel bathymetry is unknown, the Excel tool applies a factor of safety of 1.2 to velocity predictions and 1.4 for shear stress predictions to be conservative. If the actual channel bathymetry is unknown, the *aaratio* can be estimated using Equation 20.

**Eq. 20.** $aaratio = \frac{jetty\ \ length}{channel\ \ width - jetty\ \ length} = \frac{(L_s)}{(W_c) - (L_s)}$

## Velocity Estimates

### *Estimating Relative Changes in Velocity*

Relative changes in velocity due to implementing a temporary in-stream jetty are calculated as the velocity with the jetty in place divided by the velocity without the structure in place. Multiplying the ratio described above by 100% gives a percent change between the unobstructed channel condition and the velocity with the jetty in place. Relative changes in velocity may be useful for comparing differences between installing different jetty lengths and for communication with environmental permitting agencies.

To calculate the relative change in velocity Equation 21 should be used with the calculated *aaratio*.

**Eq. 21.** $\frac{V_s}{V_i} = 1.0377 * (aaratio) + 1.0017$

***Estimating Absolute Velocity***

This report outlines two predictive regressions that can be used to estimate absolute mean velocity in the river channel with the jetty in place. Being able to predict the mean absolute velocity is important for understanding the potential implications of jetty installation on aquatic organism passage. It is important to note that the mean absolute velocities estimated using the following methodologies are depth averaged and cross section averaged. Some velocities within the channel may be larger or smaller than the cross section averaged values.

When estimating absolute velocities, the best available data should be used. To calculate absolute velocity, we recommend a hierarchical approach based on which pieces of data are available and trusted. If the initial velocity in the channel without the structure in place for the discharge of interest is known, then that initial velocity should be used. If the initial velocity is not known, then the initial velocity can be estimated using the Manning Equation and the depth of water without the structure in place for the discharge of interest. Finally, if the initial velocity is not known and cannot be estimated using the Manning Equation with a known water depth, then the absolute velocity can be estimated using the power function developed in this report for limited data situations.

If the initial velocity in the channel without the structure in place for the discharge of interest is known, then that initial velocity should be used using Equation 22. This equation is the relative change in velocity equation rearranged to solve for the absolute velocity when the jetty is in the channel. If the initial velocity is not known, then the initial velocity can be estimated using the Manning Equation if the depth of water without the structure in place is known for the discharge of interest using Equation 23. When using Equation 23, hydraulic radius, *R*, can be replaced with depth if the width to depth ratio of the channel is large. Both equations 22 and 23 can be used with SI or English units.

**Eq 22**. $V_s$=$[1.0377 * (aaratio) + 1.0017\ ]$*$Vi$

**Eq. 23.** $V_s$=$[1.0377 * (aaratio) + 1.0017\ ]$*$\left[\left(\frac{\emptyset}{n}\right) * R^{\frac{2}{3}} * S^{\frac{1}{2}}\right]$

If the initial velocity is not known and cannot be estimated using the Manning Equation with a known depth of water, then the absolute velocity can be estimated using the power function (Eq. 24). Equation 24 was developed to be used with English units.

**Eq. 24.** $V_s = 0.8 * \left[\left(\frac{1.49}{n}\right)^{0.7} * S^{0.348} * \mathrm{W_c}^{-0.4} * Q^{0.412}\right] * \left[\left((aaratio) + 1\right)^{1.097}\right]$

**Shear Stress Estimates**

***Estimating Relative Changes in Shear Stress***

Relative changes in shear stress due to implementing a temporary in-stream jetty are calculated as the shear stress with the jetty in place divided by the shear stress without the structure in place. Multiplying the ratio described above by 100% gives a percent change between the unobstructed channel condition and the shear stress with the jetty in place. Relative changes in

shear stress may be useful for comparing differences between installing different jetty lengths and for communication with environmental permitting agencies.

To calculate the relative change in shear stress Equation 25 should be used with the calculated *aaratio*.

**Eq. 25** $$\frac{\tau_s}{\tau_i} = 1.066 * (aaratio)^2 + 2.13 * (aaratio) + 0.987$$

***Estimating Absolute Shear Stress***

Similarly, to absolute velocity predictions, this report outlines two predictive regressions that can be used to estimate absolute mean shear stress in the river channel with the jetty in place. Being able to predict the mean absolute shear stress is important for understanding the potential implications of jetty installation on scour potential and identifying the maximum mobile grain size. The maximum mobile grain size is the largest grain size that would be expected to move based on the cross section averaged shear stress value. Again, it is important to note that the mean absolute shear stress values estimated using the following methodologies are depth averaged and cross section averaged. Some shear stresses within the channel may be larger or smaller than the cross section averaged values. The shear stress models developed have larger errors then the absolute velocity models described above.

When estimating absolute shear stress, the best available data should be used. To calculate absolute shear stress, we recommend a hierarchical approach based on which pieces of data are

available and trusted. If the initial shear stress in the channel without the structure in place for the discharge of interest is known, then that initial shear stress should be used if it is believed to be accurate. If the initial shear stress is not known, then the initial shear stress can be estimated using the shear stress equation (Eq. 26) if the depth of water without the structure in place is known for the discharge of interest. Finally, if the initial shear stress is not known and cannot be estimated using the shear stress equation with a known depth of water, then the initial shear stress can be estimated using a depth estimate derived from the Manning Equation. Equation 5.8 can be used with SI or English units.

**Eq. 26.** $\tau_i = \gamma * R * S$

If the initial shear stress in the channel without the structure in place for the discharge of interest is known, then that initial shear stress can be used directly to calculate the post-jetty shear stress (Equation 27). This equation is the relative change in shear stress equation rearranged to solve for the absolute shear stress when the jetty is in the channel. If the initial shear stress is not known, then the initial shear stress can be estimated using the shear stress equation (Equation 26) if the depth of water without the structure in place is known for the discharge of interest using Equation 27. Equation 27 can be used with either SI or English units.

**Eq. 27.** $\tau_s = (1.066 * (aaratio)^2 + 2.13 * (aaratio) + 0.987) * \tau_i$

If the initial shear stress is not known and cannot be estimated using the shear stress equation with a known depth of water, then the initial shear stress can be estimated using a depth estimate derived from the Manning Equation using Equation 28. Equation 28 was developed to be used with SI or English units.

$$\textbf{Eq. 28. } \tau_s = [1.066 * (aaratio)^2 + 2.13 * (aaratio) + 0.987] * \gamma * \frac{(Q*n)}{(W_c * S^{0.5} * \emptyset)}^{3/5} * S$$

## EXCEL BASED TOOL APPLICATIONS GUIDE

### Jetty Hydraulics

The regression equations discussed above are implemented in an Excel workbook to aid calculation. The tool takes several user inputs and then calculates relative and absolute increases in velocity and shear stress due to jetty installation. This guide walks through the application of this tool with a simple example.

The main page is shown below:

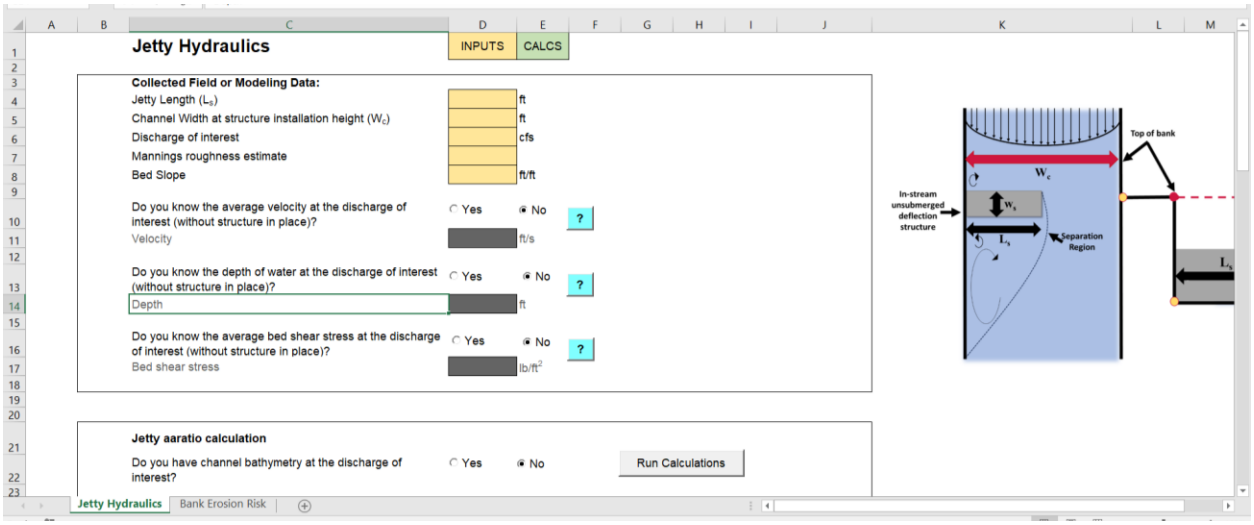


**Figure 25. Excel tool main page. Main page of the "Jetty Hydraulics" part of the Excel tool.**

The “Jetty Hydraulics” tab is where most of the data are inputted and where results are shown. All cells requiring user inputs are shaded yellow. Required inputs are: (1) Jetty length (ft), (2) channel width (ft), (3) discharge of interest ($ft^3/s$), (4) Manning roughness coefficient, and (5) bed slope (ft/ft). Optional inputs include average velocity (ft/s), depth (ft), and bed shear stress ($lb/ft^2$) in the channel at the discharge of interest before jetty installation. If these values are not provided, they are estimated using the Manning and shear stress equations (see description above for more details). An additional optional input is channel bathymetry data. If these data are available, they should be entered to allow the tool to more accurately calculate the *aaratio* parameter, or ratio of jetty area and channel flow area. As an initial example, we will assume only the required inputs are available. Once those inputs are entered (and “no” selected for bathymetry data), the user can click the “Run Calculations” button:

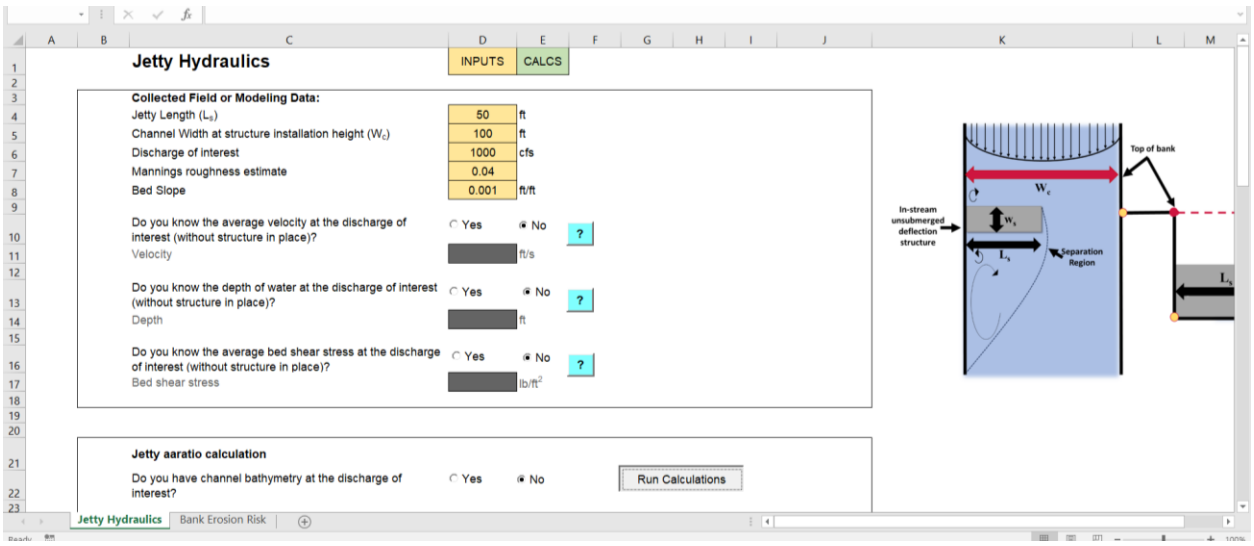


**Figure 26. Example tool application 1. Required inputs added to appropriate cells.**

Scrolling down shows the calculated results for different sections (green cells):

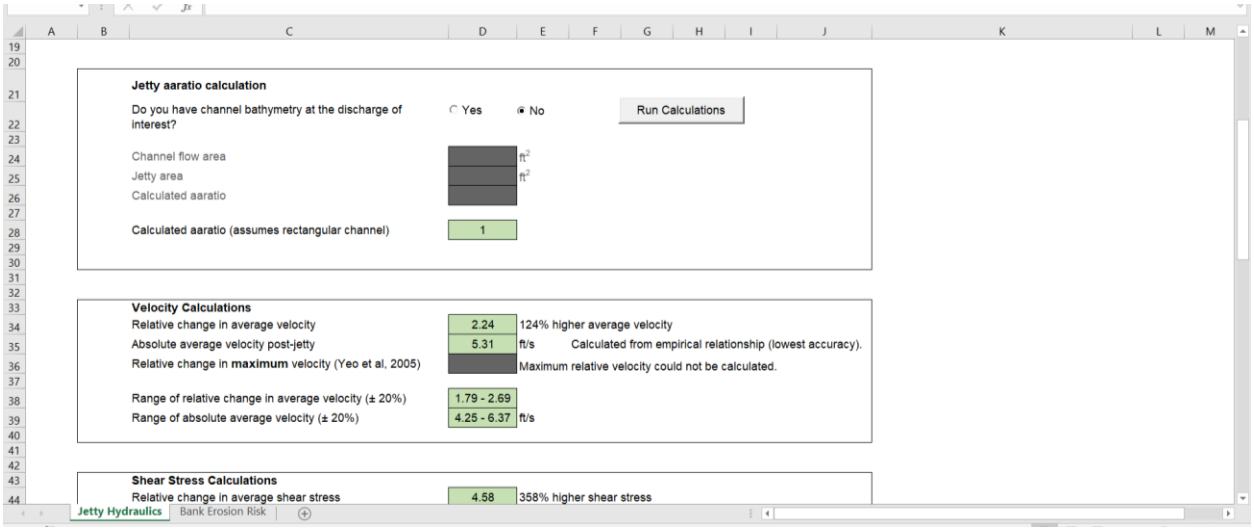


**Figure 27. Example tool application 2. Aaratio and velocity calculation results.**

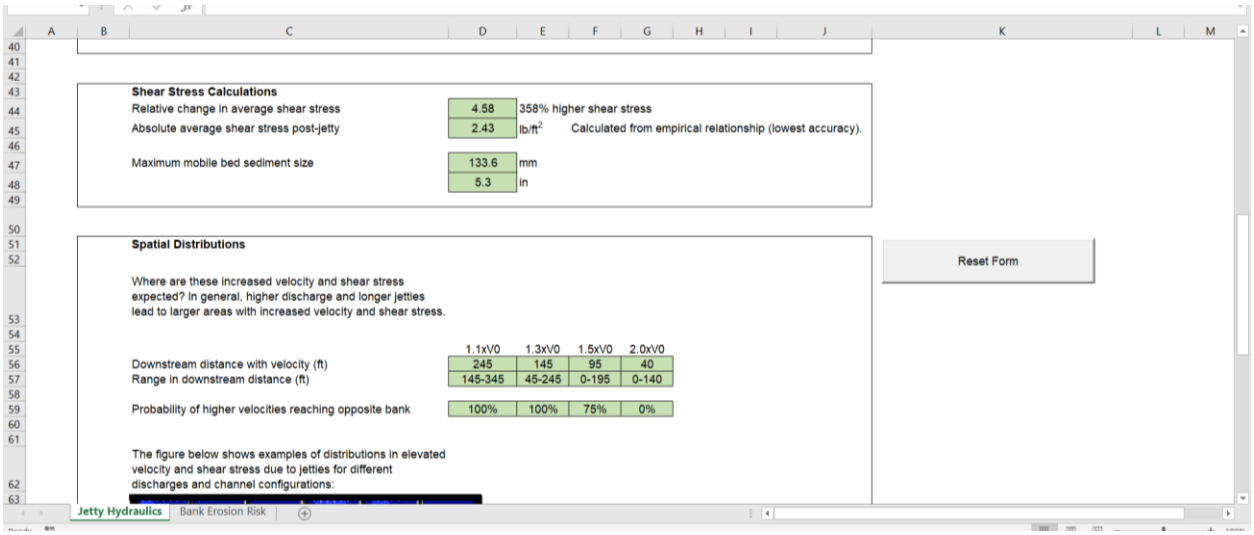


**Figure 28. Example tool application 3. Shear stress and spatial distribution calculation results.**

In this example, the *aaratio* is calculated as 1. The regression equations described above are then applied to estimate a relative change in the average velocity of 2.24 and the average shear stress of 4.58. Since the tool assumed a rectangular channel geometry to calculate *aaratio*, a safety

factor of 1.2 (for velocity) and 1.4 (for shear stress) were applied. If channel bathymetry is provided, no safety factor is used. Absolute values of velocity and shear stress are also shown, along with the method used to calculate them (e.g. empirical equation or using supplied velocity/shear stress values). If possible, the relative change in maximum velocity (from Yeo et al. 2005) is also shown. This value is only calculated if the *aaratio* is between 0.02 and 0.35. Under the shear stress section, the maximum mobile grain size for the calculated shear stress is also shown (in both mm and in). This is based on an estimated critical shear stress for mobilization from Fischenich (2001).

Finally, under the Spatial Distributions section, there are estimates of the distance downstream with 1.1x, 1.3x, 1.5x, and 2x the initial velocity. These values (and ranges) are calculated based on the regression equations discussed in Ch. 3. Additionally, the results of the logistic regression equation from Ch. 3 are shown as the probability that these higher velocities reach the bank opposite the jetty. Figure 15 from Ch. 3 is included in the tool and shows representative spatial distributions of elevated velocity and shear stress under different jetty lengths and discharges. This figure is shown only as an example, and does not correspond to calculated values for the user's specific case.

Supplying pre-jetty average velocity (or depth) and shear stress allows for more accurate calculation of the post-jetty velocity and shear stress. If those data are available, simply select the "Yes" checkbox and the appropriate cell will be highlighted yellow. Enter the appropriate values and click "Run Calculations":

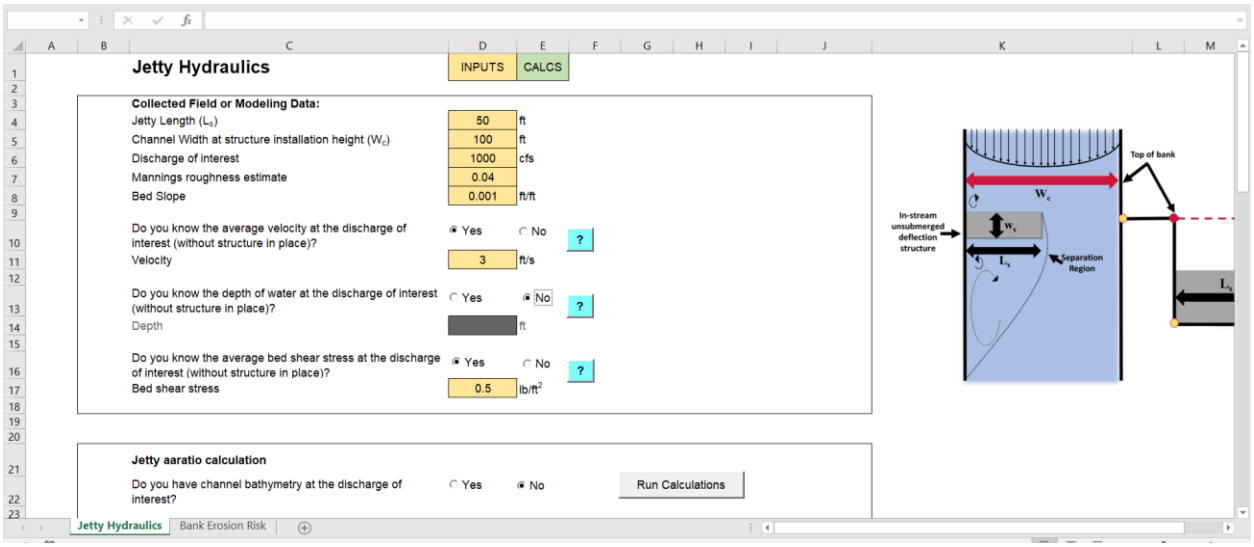


**Figure 29. Example tool application 4. Adding known velocity and shear stress.**

Another way to increase calculation accuracy is to supply channel bathymetry data. If the user selects "Yes" to this question, another worksheet appears where this data can be entered:

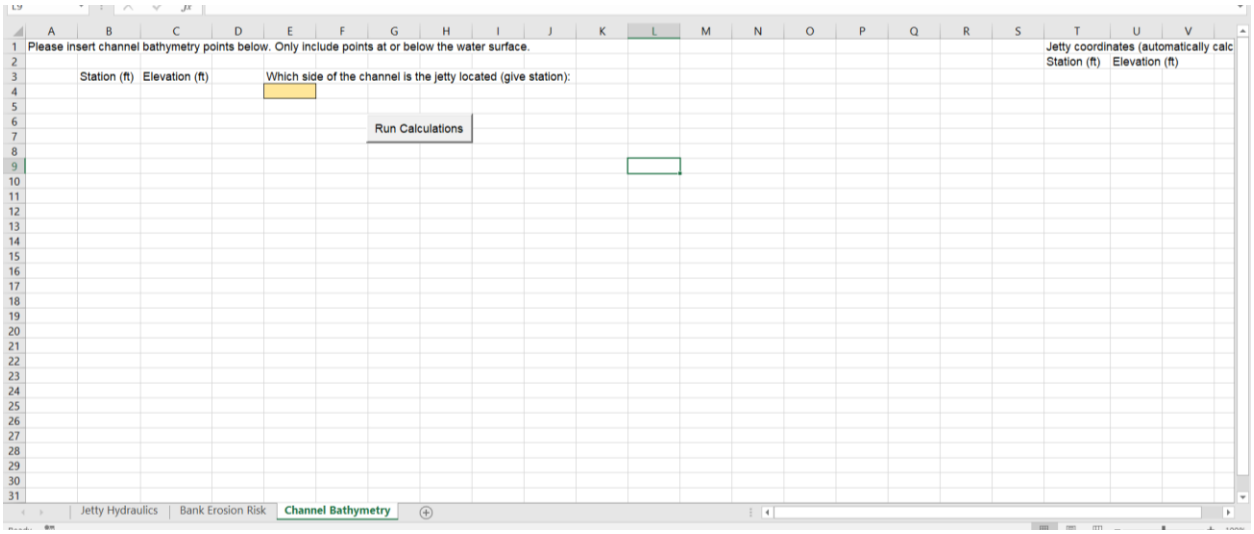


**Figure 30. Example tool application 5. Adding channel bathymetry data.**

The user should enter the station (ft) and elevation (ft) of the channel cross section. Only bathymetry points (below the water surface) should be included. Stations and elevations do not

need to be tied to any particular datum (i.e. relative elevations are acceptable). In addition to the cross section data, the user must specify which side the jetty is located on by specifying the station in the orange box. Once these are entered, the user can click “Run Calculations”, which will take them back to the “Jetty Hydraulics” tab and show the calculated results. The “Channel Bathymetry” tab will remain visible and show a graph of the channel cross section and jetty:

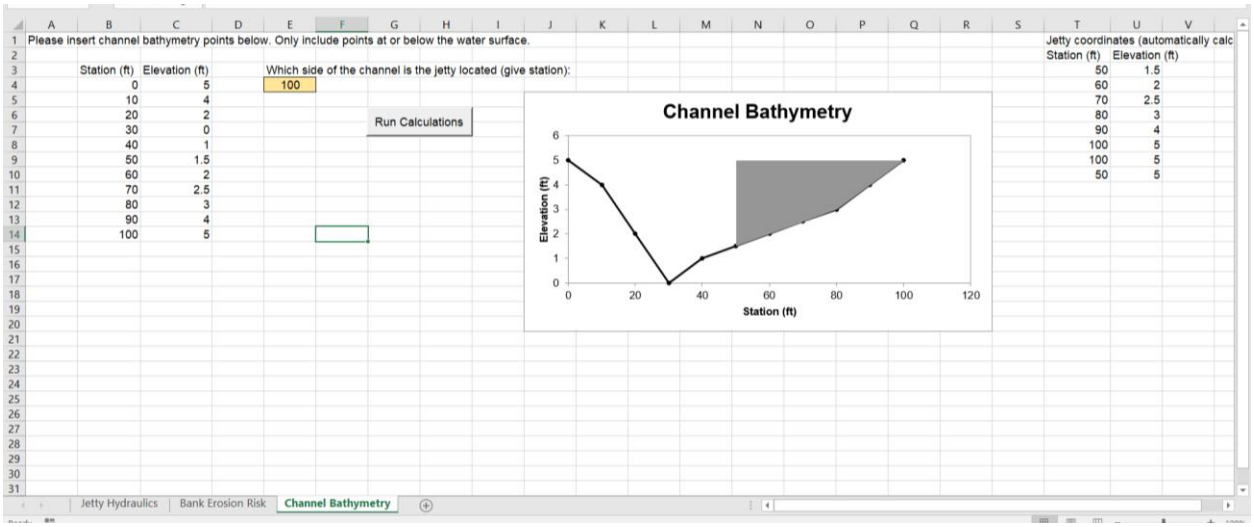


**Figure 31. Example tool application 6. Adding and calculating channel bathymetry data.**

## Bank Erosion Risk

The “Bank Erosion Risk” tab allows the user to assess bank erosion risk based on the flow chart presented above. As noted previously, this bank erosion risk should be assessed at multiple locations. However, the estimate of increased near-bank velocity is for the bank opposite the jetty. This is, therefore, a worst-case scenario and may not be directly applicable to all bank locations.

The main page of the bank erosion risk tool looks as follows:

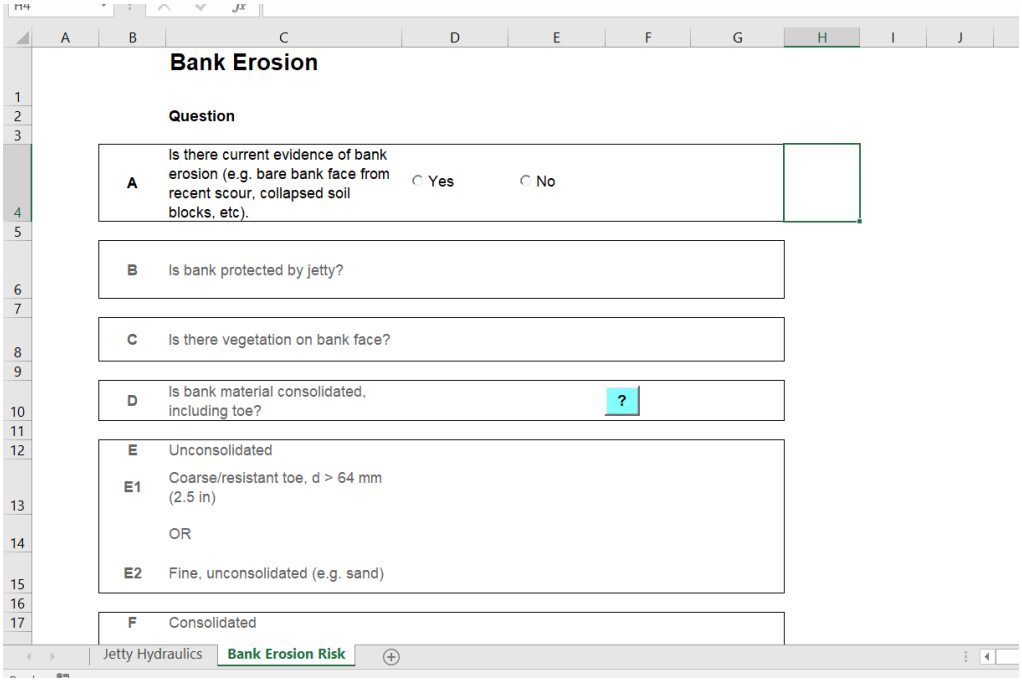


**Figure 32. Example tool application 7. Bank erosion risk tab.**

There are primarily a series of yes/no questions that the user must enter. Depending on the bank type, there may also be some quantitative data required. Questions are answered in series and based on the supplied answer, the appropriate cells for the next question are then answered. For example, we will assume that the bank location of interest is not currently eroding:

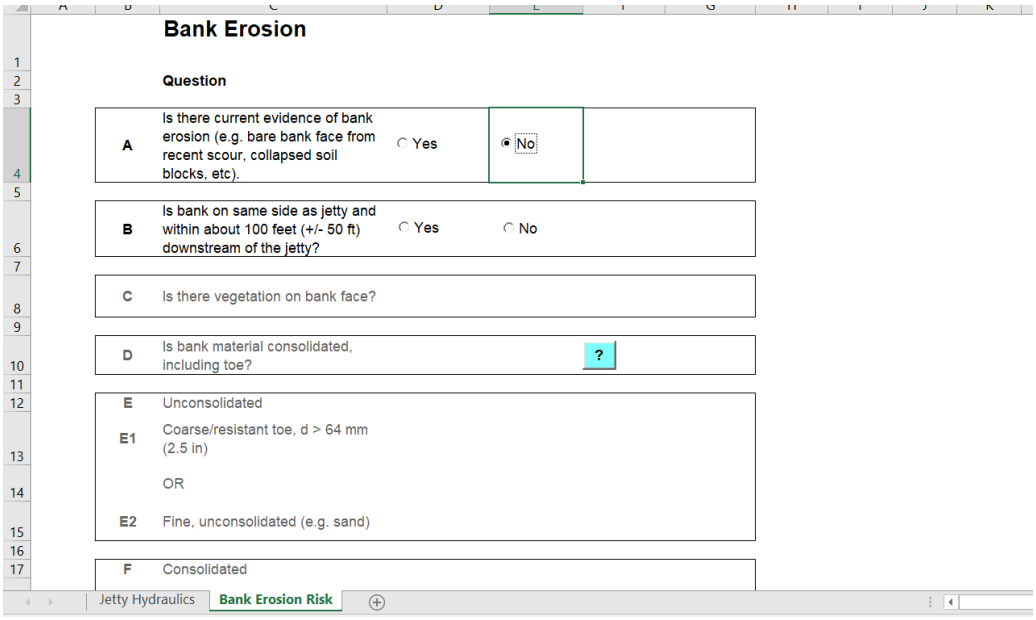


**Figure 33. Example tool application 8. Bank erosion risk tab.**

By clicking “No” for question A, the tool then proceeds to question B, which deals with bank protection downstream of the jetty. The distance downstream of the jetty with reduced velocity and reduced bank risk is estimated using the regression equation discussed in Ch. 3. Data on channel and jetty geometry must be entered in the “Jetty Hydraulics” tab for the tool to calculate the distance downstream protected by the jetty. The user must enter these data before proceeding. Selecting “No” (because the bank is not protected by the jetty) then highlights question C. If vegetation is present on the bank face, it can help stabilize the bank and make it less prone to erosion. If the user selects “Yes”, the tool increases the critical shear stress and cohesion of the bank by 50%. For this example, we will select “No” and proceed to question D.

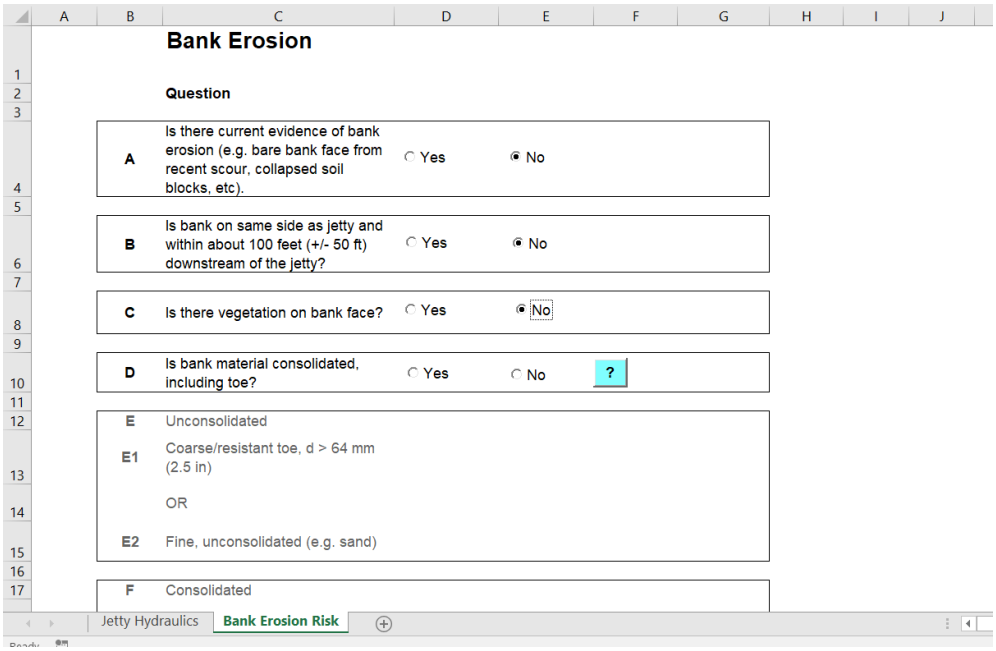


**Figure 34. Example tool application 8. Bank material.**

Question D relates to the consolidation or cohesion of the bank. Unconsolidated banks consist of loose material like sand and gravel. Consolidated or cohesive material includes silt and clay (although some sand and gravel may also be present). If the bank material is unconsolidated, erosion risk is assessed only by comparing maximum permissible velocity to estimated near-bank velocity from the Jetty Hydraulics tab. For consolidated material, erosion risk is also assessed based on the cohesion and stability of the bank. If the material is unconsolidated, clicking “No” for question D will highlight section E. Here, the user can either select “coarse” (e.g. gravel or cobbles) or “fine” (e.g. sand) for the bank material.

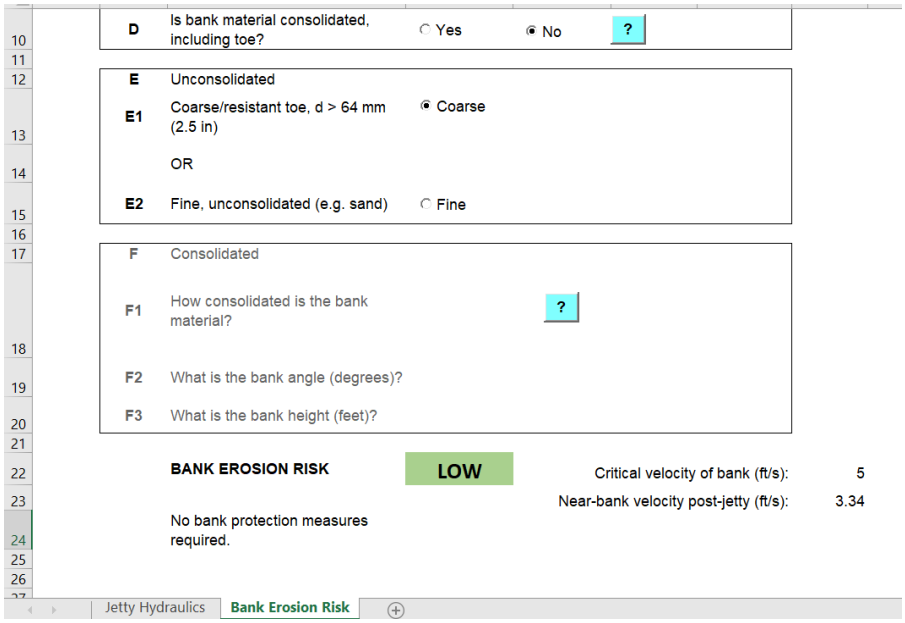


**Figure 35. Example tool application 9. Unconsolidated bank material.**

For this example, we used coarse bank material. This puts this bank in the low bank erosion risk category since the maximum permissible velocity for this material (5 ft/s) is greater than the near-bank velocity calculated from the Jetty Hydraulics tab (3.34 ft/s).

Users can click the “Reset Form” button to clear the bank erosion risk form and start over. As another example, we can look at erosion risk for a consolidated/cohesive bank:

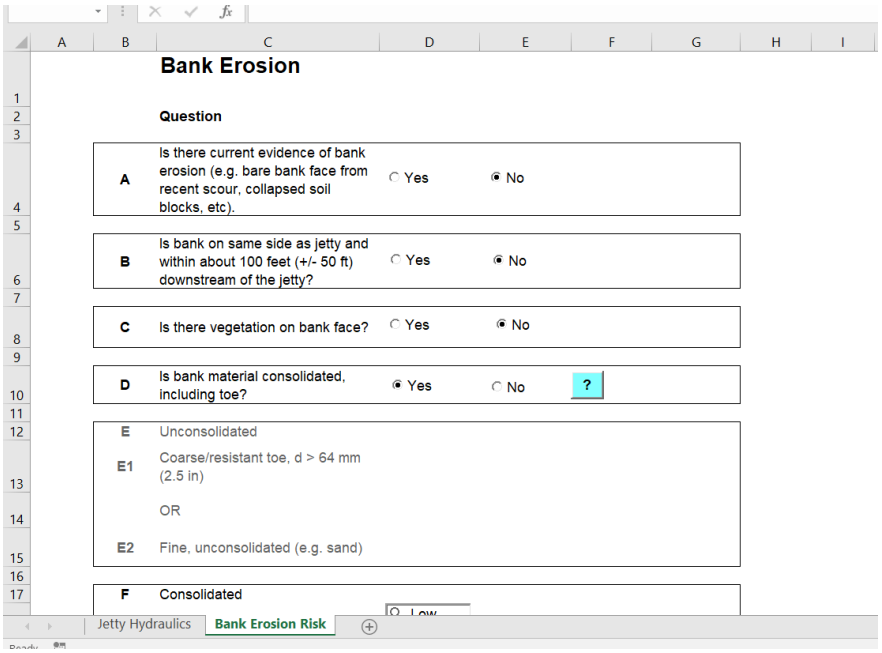


**Figure 36. Example tool application 10. Consolidation bank material.**

Selecting “Yes” for question D highlights section F, where the user enters data on the consolidated bank material. The user must select whether the bank is low, medium, or high consolidation/cohesion. The help button next to this box provides more information, but essentially lower consolidation has less clay and higher consolidation has more clay. Once the type of consolidation is selected, the user must input the bank height and angle. These should be estimated in the field and are used to assess the resistance of the bank to collapse. Once the values are entered, the user can click the “Calc Risk” button:

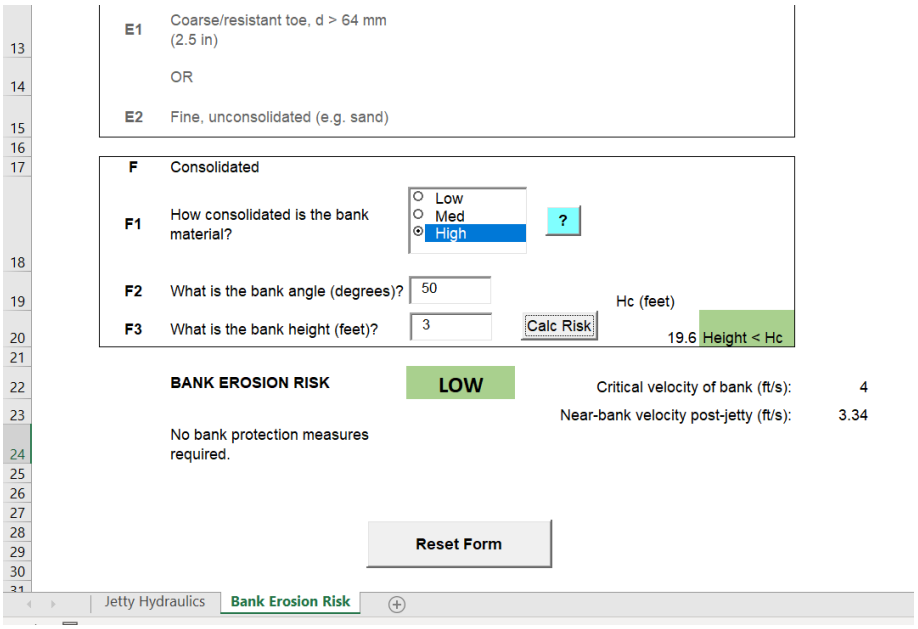


**Figure 37. Example tool application 11. Consolidation bank material 2.**

The tool calculates the critical bank height (Hc) and prints this value to the screen. Since the measured bank height (3 feet) is much less than the critical value (19.6 feet), the bank is at low risk of collapse. The maximum permissible velocity (4 ft/s) is greater than the near-bank velocity calculated from the Jetty Hydraulics sheet (3.34 ft/s), which also places the bank at low risk of erosion.

# CHAPTER 6. CONCLUSIONS AND SUMMARY OF FINDINGS

## PROJECT SUMMARY

Bridge construction often requires the placement of temporary features such as rock jetties and cofferdams in stream and river channels during the construction process. Environmental permitting agencies seek documentation, and in some cases quantification, of the potential effects of these temporary features on instream velocities, and channel bank and bed scour. The primary objective of this research was to improve the Georgia Department of Transportation's (GDOT) ability to effectively respond to environmental permitting agency concerns about the potential geomorphic and hydraulic effects of temporary in-stream jetties associated with bridge construction practices. Understanding the potential hydraulic and geomorphic impacts of jetties is essential for limiting the unintended consequences of emplacement. Abrupt flow contractions at structures can increase bed scour and bank erosion with consequent effects on channel stability and habitat. Quantitative predictions of changes in velocity and shear stress due to these structures and identification of regions at high risk for bank and bed erosion can help inform preliminary structure design, environmental management, and regulatory decision making. In this study, we performed 50,000+ 1-D HEC-RAS simulations to develop parsimonious regression models to quantify changes in velocity and shear stress in regions contracted by jetties. The regression models were compared to collected field measurements and previous experimental studies. Additionally, we conducted 42 2-D HEC-RAS simulations to examine spatial distributions of velocity and shear stress near jetties, concentrating on near-bank regions and locations of velocity and shear stress maxima.

Practical relationships to predict mean changes in velocity and shear stress due to the emplacement of jetties were developed based on 1-D modeling results to inform preliminary structure design, environmental management, and regulatory decisions. Changes in velocity and shear stress estimated with HEC-RAS for a wide range of conditions were found to be well represented by easily applied regression models based on a channel contraction area ratio for contraction percentages $\leq$ 50% and Froude numbers < 0.8. The new regression relationships for relative velocity were reasonably supported by results from a field study and previously conducted flume studies.

Two-dimensional hydraulic modeling results indicated that higher discharges and contraction percentages led to larger velocity and shear stress maxima in contracted regions, as well as longer downstream distances where velocities and shear stresses were $\geq$ 110% of unobstructed channel conditions. Maximum depth averaged relative changes in velocity and shear stress in the narrow and medium channel widths, at a 50% contraction, were higher relative to the 10% contraction and ranged from 1.7 - 2.2 times the initial velocity and 2.4 - 4.6 times the initial shear stress for a given discharge. When contraction percentages reached 30%, flows were constricted enough to lead to increases of at least 1.1 times the initial velocity and 1.5 times the initial shear stress on the opposite bank for all channel widths.

Results from this study were used to develop an Excel-based management tool that combines the predictive regression models and the results of the 2-D analysis of spatial patterns of increased velocity and shear stress resulting from jetties, which can be easily applied by DOT practitioners for planning, design, and permitting when more complex modeling is infeasible. This research

project has helped improve the understanding of the effects of temporary jetties on river channels and provided an easy to use tool that can be applied across numerous jetty and channel configurations. Additionally, this work outlined the connection between the large body of previous research on semi-permanent instream structures such as spurs, groynes, and abutments to temporary structures such as temporary riprap jetties used for bridge construction. The body of literature on semi-permanent structures is applicable to temporary jetties and can serve as a valuable resource for DOT practitioners looking for more information on the hydraulic and geomorphic effects of jetties.

The tool and regressions in this study can be applied to both temporary in-stream jetties along with other in-stream unsubmerged vertical wall structures installed perpendicular to the bank. For example, this research may also aid DOTs in understanding potential hydraulic and geomorphic effects of cofferdams attached to the channel bank that may also be used for bridge construction. This work advances the current set of tools available for preliminary jetty design and environmental management decisions. Important findings from this study are summarized below.

## FINDINGS

### State DOT Survey

1. There is no specific protocol for determining jetty height (bed to top of structure). Some state DOTs use the 2-year flood event; others use a given height above the average discharge. The longer the structure is in place, the more important designing the structure to the accurate height is to prevent overtopping. The longer the structure is in place, the larger the probability is that a large flood event may occur.
2. Jetties increase velocity the most right before the jetty overtops.
3. Jetties are not the only bridge construction option. At 4-5 ft of water depth, there is an economic breakpoint where jetties may become more expensive to construct and it may be more feasible to use a barge. Barges can be used in channels with approximately 7 ft of water and low currents. Bridge construction access is always site-dependent.
4. Jetty use and sizes are variable. Jetties are typically used on channels up to around 656 ft (200m). The maximum jetty top width of interest are typically around 50 ft, but the most common top width is 20 ft. Jetty contraction percentages (i.e. jetty length as a percent of channel width) typically range between 10% and 50%, but can be up to 70%.

### Modeling and Monitoring Hydraulic Effects of Jetties

5. Field reconnaissance indicates that jetties detectably influence hydraulic patterns compared to pre-construction conditions. The magnitude and nature of this influence are largely dependent on channel contraction percentage and discharge.

6. Jetties can be accurately modeled as blocked obstructions in 1-D HEC-RAS with ineffective flow areas and coefficients of contractions and expansions mimicking bridge abutment modeling techniques.

7. Channel contraction (represented as an area ratio) is the main variable describing the increase in velocity and shear stress due to jetties. This suggests that a jetty on one side of the river versus both sides of the river taking up the same area will likely yield the same increase in velocity. However, locations of maximum shear stress and velocity will be different.

8. Changes in velocities determined from 1-D HEC-RAS modeling results appear to be well represented by easy to use regressions developed with one variable for contraction percentages less than 50% and Froude numbers less than 0.8.

9. Analytical techniques and HEC-RAS 1-D numerical modeling regressions yield similar results when predicting changes in velocity (velocity with jetty/velocity natural conditions). Analytical techniques combine the conservation of mass equation and Manning's Equation. The resulting equations differ slightly due to differences in assumptions and the ability of HEC-RAS to include energy losses associated with contractions and expansions.

10. Regression equations to predict the absolute velocity or shear stress with a jetty in place will require one of the following variables to be known: 1) the initial value for the natural channel condition at the discharge of interest, 2) water depth at the discharge of interest, or 3) discharge of interest.

11. The maximum allowable contraction percentage of 33% permitted by the USACE regional permit is a defensible threshold. Relative increases in both velocity and shear stress increase significantly at contractions above this threshold. In addition, contraction percentage of 30%

for all channel sizes and discharges is expected to lead to increased velocities and shear stresses on the opposite bank compared to unobstructed channel conditions. The potential for bank erosion on the opposite bank is dependent on bank stability. Keeping contraction percentages below 30% is recommended when the banks opposite of the structures are susceptible to erosion and failure.

12. Higher discharges and higher contraction percentages lead to higher maximum values of velocity and shear stress and larger downstream distances impacted by increased velocities and shear stresses.

13. Jetty top width did not appear to increase the maximum velocity and shear stress in the channel.

14. Determining the most accurate estimate of the channel contraction area ratio (the main variable used in the regression models) is essential to accurate predictions of velocity and shear stress. If the actual channel bathymetry is known, it should be used to calculate the channel contraction area ratio.

.

# APPENDIX A. HYDRAULIC MODELING AND STATISTICAL ANALYSIS

## DESCRIPTION

This appendix serves as supplemental material to Chapter 2 for hydraulic modeling and regression statistical analysis.

### Tables

**Table 10. Comparison of 1-D HEC-RAS model results to flume studies.**

| Flume Study | Q (ft/s) | Contr. % | % Error Upstream Vel. | % Error Vel. at Contracted *xs* | % Error Upstream WSE |
|---|---|---|---|---|---|
| **Jeon et al. 2018 C1** | 0.982 | 33.33% | 1.45% | -5.17% | 0% |
| **Jeon et al. 2018 C2** | 1.86 | 33.33% | -1.10% | -5.96% | 4.76% |
| **Duan et al. 2009 Flat bed** | 2.05 | 32.89% | -2.39% | 16.58% | NA |

**Table 11. Selected relative velocity regression models.**

| Dependent Variable | Model | RMSE | $adjR^2$ for linear Models |
|---|---|---|---|
| **1 Variable** *aaratio* | Linear model | 0.027 | 0.991 |
| | Power function nonparametric | 0.074 | NA |
| **2 Variables** | Linear model: *aaratio and Fr* | 0.021 | 0.995 |

| | | | |
|---|---|---|---|
| *aaratio and Fr* | Power function: *aaratio and Fr* | 0.070 | NA |
| | Linear: *aaratio* and *Fr*_hydraulic geometry | 0.022 | 0.994 |
| | Linear: *aaratio* and *Fr*_darcy | 0.022 | 0.994 |
| | Linear: *aaratio* and *Fr*_ND | 0.023 | 0.994 |
| **All Independent Variables** | Linear: Inclusion of all 8 independent variables | 0.015 | 0.997 |

**Table 12. Selected relative shear stress regression models.**

| Dependent Variable | Model | RMSE | $adjR^2$ for linear Models |
|---|---|---|---|
| **1 Variable** *aaratio* | Linear model | 0.146 | 0.975 |
| | Power function nonparametric | 0.228 | NA |
| | Quadratic | 0.117 | NA |
| **2 Variables** *aaratio and Fr* | Linear Model | 0.104 | 0.988 |

**Figures**

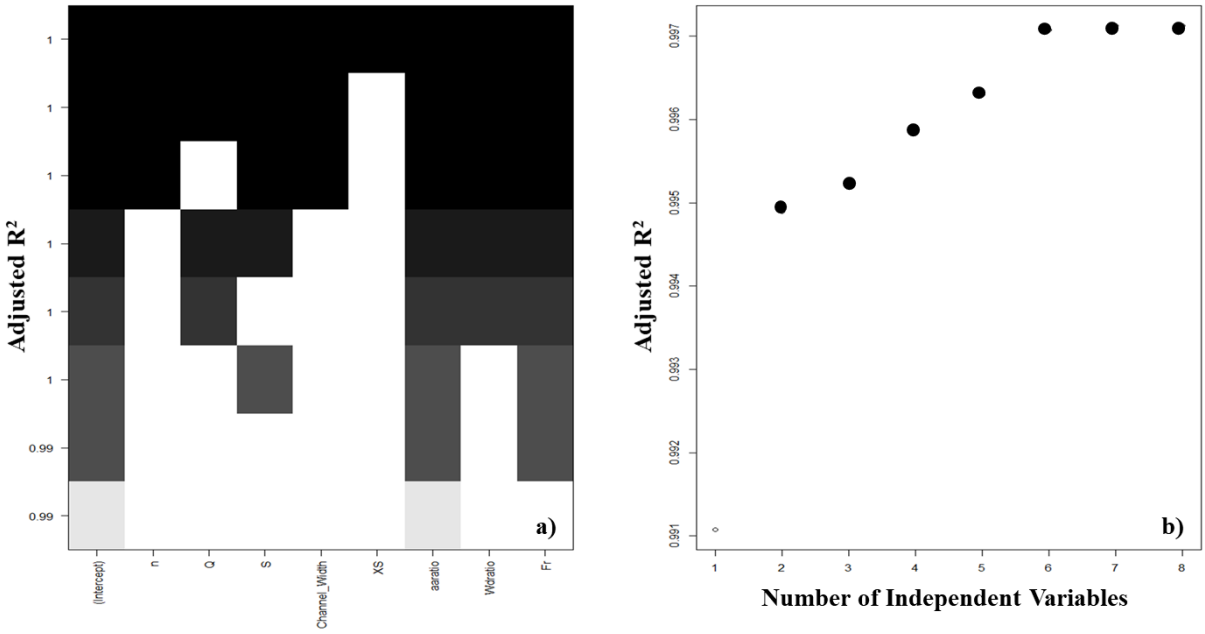


**Figure 38. Linear regression results. Results from linear regression analysis using best subsets. Figure (a) depicts the results from the best subsets analysis preformed in R using the 'Leaps' package showing the independent variables used for the best linear model for a given number of predictor variables based on $adjR^2$. Figure (b) shows that increasing the number of variables in a linear regression slightly improves the adjR$^2$, but all $adjR^2$ values are above 0.99.**

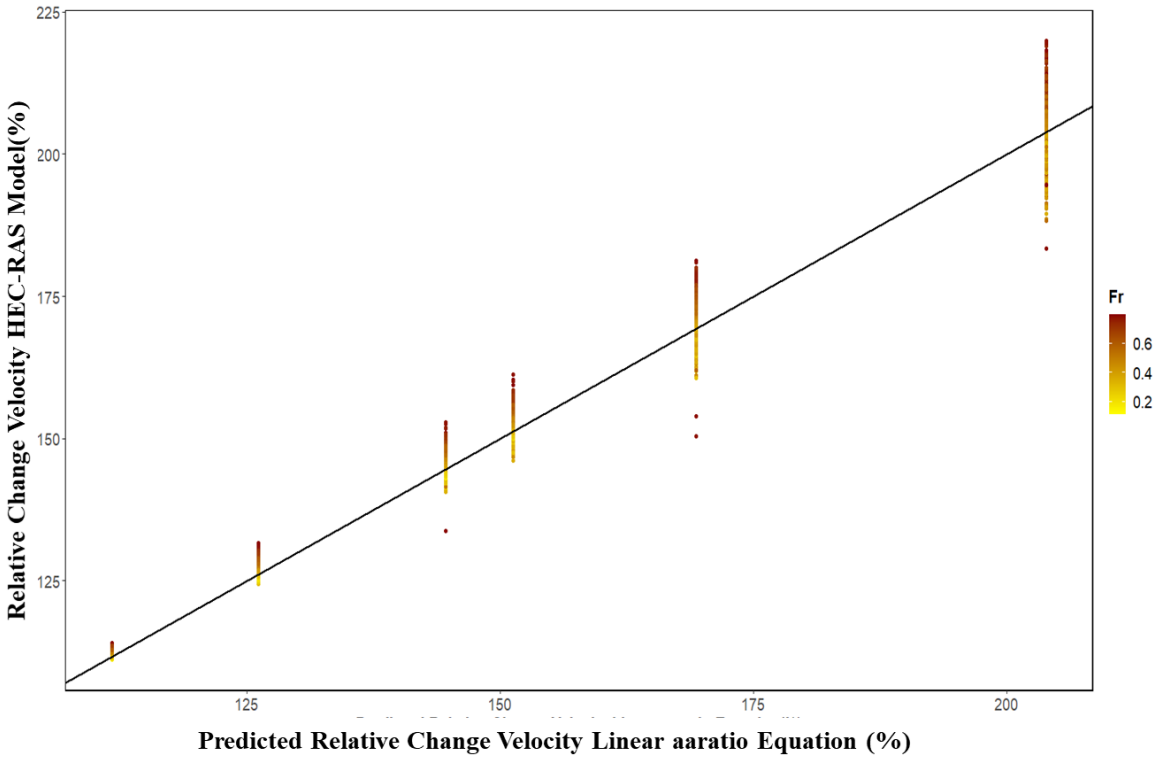


**Figure 39. Predicted and observed velocity results. Predicted relative changes in velocity using the linear *aaratio* regression versus the HEC-RAS model relative changes in velocity. The linear *aaratio* model generally underpredicts for larger Froude numbers and overpredicts for smaller Froude numbers.**

# APPENDIX B. COMPARISON OF REGRESSION MODEL PREDICTIONS TO HYDRAULICS OF COMPLEX CHANNELS

## DESCRIPTION

This appendix serves as supplemental material to Chapters 2 and 3, providing additional insight into potential errors associated with assuming rectangular channel geometries to develop *aaratios* when utilizing developed regressions for actual channel bathymetries.

## ADDITIONAL ANALYSIS

Three existing actual channel bathymetry 1-D HEC-RAS models were used to determine the absolute velocity and shear stress for six channel contraction percentages: 10%, 20%, 30%, 33%, 40% and 50%. Actual channel bathymetry 1-D HEC-RAS models were provided by the Georgia Department of Transportation for the Flint River, Chattooga River and Walnut Creek (Figure 40). The absolute values of velocity and shear stress for the actual channel bathymetries were compared to developed regressions in Chapter 2 with associated *aaratios* calculated assuming rectangular channel shape. This analysis was conducted because practitioners may utilize the developed equations for non-rectangular channels and calculate *aaratios* assuming rectangular channel conditions as described in Chapter 2 if bathymetry data is unknown.

Percent errors in predicted absolute velocity using the power regression developed in Chapter 2 generally underpredicted mean absolute velocity for actual channel bathymetries ranging from underpredicting value by 9% - 35% (Table 13). Percent errors in predicted mean absolute shear

stress utilizing the developed quadratic equation and estimating water depth utilizing the Manning equation assuming rectangular channel shape were variable. Predictions ranged between overpredicting shear stress by 59% to under predicting shear stress by 46% (Table 14). This analysis focused on a worst-case scenario, where channel bathymetry and initial velocity or depth at the discharge of interest was unknown.

Using the developed equations for relative changes with actual *aaratios* determined using channel bathymetry data is expected to increase prediction accuracy for non-rectangular channel bathymetries. Initial values can be obtained through field measurements, hydraulic modeling or estimated using the appropriate equations adjusted for channel shape. If measurements for initial velocity and *aaratio* are accurate, then predictions for absolute velocities should fall near the original estimated range of errors for the rectangular channel geometries presented in Chapter 2. The tool described in Chapter 4 uses a hierarchal approach and calculates absolute velocity and shear stress based on the best available data starting with calculating the *aaratio* using channel bathymetry then moving towards estimating *aaratio* assuming a rectangular channel condition. If measured or modeled initial values are given, these values are used for predicting absolute velocity and shear stress using the relative regressions instead of using estimated initial values or in the case of velocity, the developed power function.

## Tables

**Table 13. Velocity errors. Percent error between actual channel bathymetry absolute velocities and absolute velocities predicted using developed power regression with assumed rectangular *aaratios.***

| Percent Contraction | Rectangular *aaratio* | Chattooga Percent Error | Flint Percent Error | Walnut Percent Error |
|---|---|---|---|---|
| 10% | 0.11 | -13% | -23% | -20% |
| 20% | 0.25 | -10% | -26% | -15% |
| 30% | 0.43 | -9% | -28% | -10% |
| 33% | 0.50 | -9% | -29% | -9% |
| 40% | 0.67 | -11% | -32% | -9% |
| 50% | 1.00 | -16% | -35% | -13% |

**Table 14. Shear stress errors. Percent error between actual channel bathymetry absolute shear stress and absolute shear stress predicted using developed quadratic regression with assumed rectangular *aaratios.***

| Percent Contraction | Rectangular *aaratio* | Chattooga Percent Error | Flint Percent Error | Walnut Percent Error |
|---|---|---|---|---|
| 10% | 0.11 | 0% | -20% | 25% |
| 20% | 0.25 | 6% | -15% | 20% |
| 30% | 0.43 | 7% | -25% | 59% |
| 33% | 0.50 | 6% | -32% | 40% |
| 40% | 0.67 | -1% | -38% | 46% |
| 50% | 1.00 | -18% | -46% | 27% |

## Figures

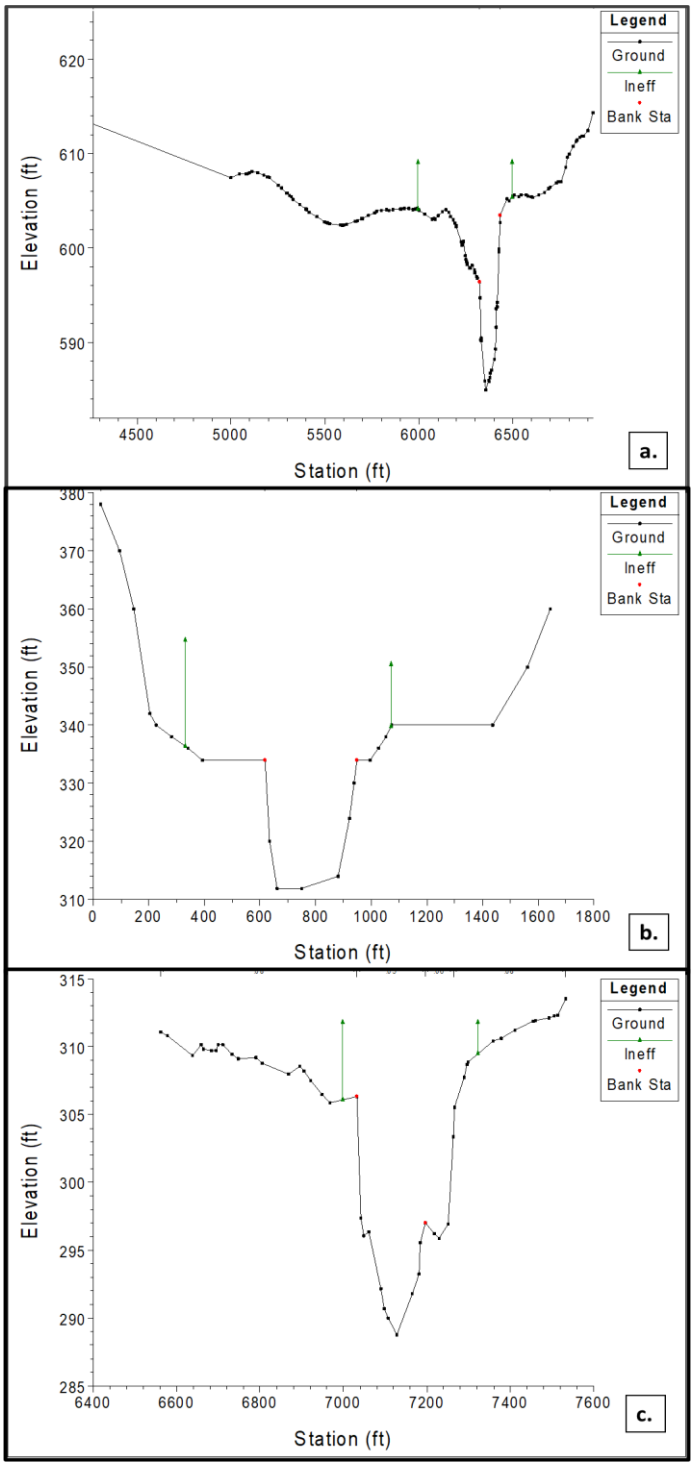


**Figure 40. Channel cross sections. One-dimensional HEC-RAS cross sections for the Chattooga River (a), the Flint River (b) and Walnut Creek (c).**

# APPENDIX C. SELECTED DOT SURVEY RESULTS

## DESCRIPTION

This appendix provides additional information about the Qualtrics Survey sent to representatives at all 50 state Departments of Transportation (DOT). Representatives were selected to include a bridge engineer, a hydraulics engineer, and an environmental representative. The survey resulted in 74 responses from 26 states and 46 fully completed surveys. Survey results were used to supplement information provided by the Georgia Department of Transportation (GDOT) to gain insight about temporary riprap construction platform implementation across the United States. Most respondents responded to the survey as individuals; however, seven responses were submitted as groups. One state could respond with multiple surveys if multiple individuals chose to respond. Survey respondents were asked if they were familiar with structure design, structure permitting or construction and provided questions relevant to their knowledge.

### Survey Results

#### *Question 1*

What **name or names** does your state Department of Transportation commonly call the temporary in-stream access structure used for bridge construction shown in the previous photo? Select all that apply.

**Figure 41. Survey photo. Photo shown in survey. Photo curtesy of GDOT.**

***Response 1***

Responses to Question 1 (Figure 42) indicated that there are numerous names for the structure shown in the provided photo (Figure 41). Information obtained from GDOT is not shown in Figure 42, as information from GDOT was obtained from in person meetings. However, GDOT refers to the structure shown in the provided photo as a riprap jetty. The multiple names for these structures may make it challenging to compile information regarding structure design and implementation. For the remainder of this appendix, the structure will be referred to as a temporary riprap construction platform.

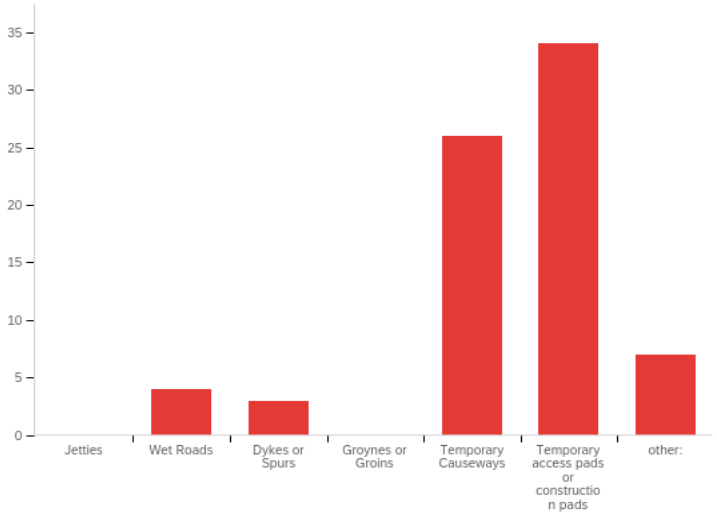


**Figure 42. Response to survey question 1. Response to Question 1 about the name of temporary access construction structures used for bridge construction based on the provided photo.**

***Question 2***

How often are the temporary access structures of interest used by your state DOT during bridge construction projects?

***Response 2***

Responses to Question 2 (Figure 43) indicated that the frequency of use of temporary riprap construction platforms varies between DOTs. Implementation of these structures is highly site and project dependent.

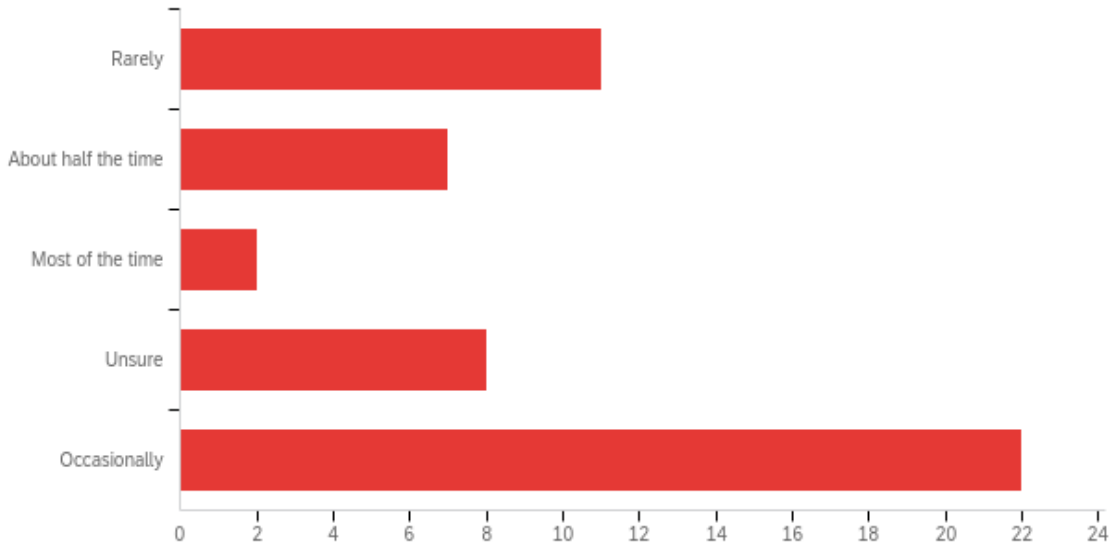


**Figure 43. Response to survey question 2. Response to Question 2 about the frequency of use of temporary riprap construction platforms.**

***Question 3***

Does your state DOT have design guidelines or a design manual that provides guidelines on the design or implementation of temporary bridge construction access structures?

***Response 3***

Responses to Question 3 (Figure 44) indicated that more respondents were unaware of design manuals or guidelines for implementation of temporary riprap construction platforms then respondents that were aware of design guidelines. This suggests there may be a need for improved design guidelines or manuals for these structures.

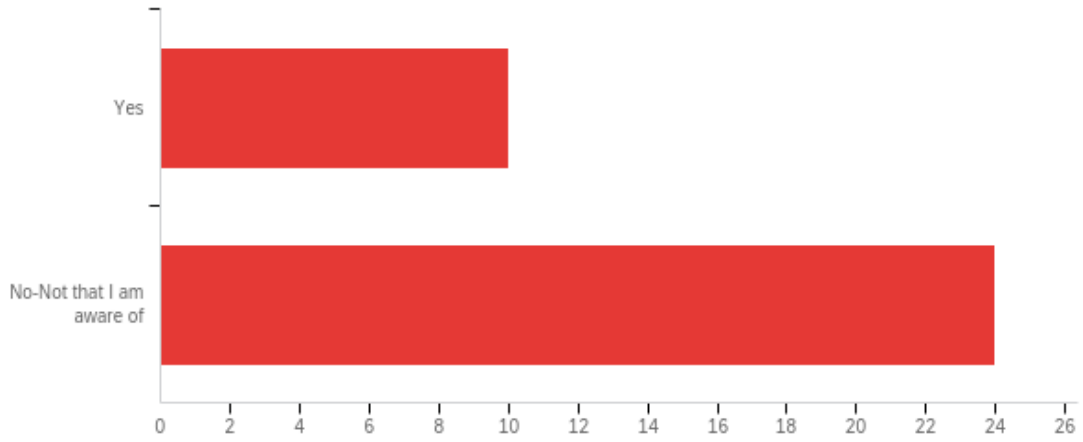


**Figure 44. Response to survey question 3. Response to Question 3 about availability of design guidelines and manuals for temporary riprap construction platforms.**

***Question 4***

Based on your experience please estimate the maximum and minimum percent of a channel width that could be blocked by these temporary structures. You can SKIP this question if you would not like to provide an estimate. (Include the case where 2 temporary structures could be in the channel at the same time from either side of the channel.)

***Response 4***

Responses to Question 4 (Figure 45) indicated that channel contraction percentages for temporary riprap construction platforms range between 10% - 70% with the most common maximum contraction being 50%.

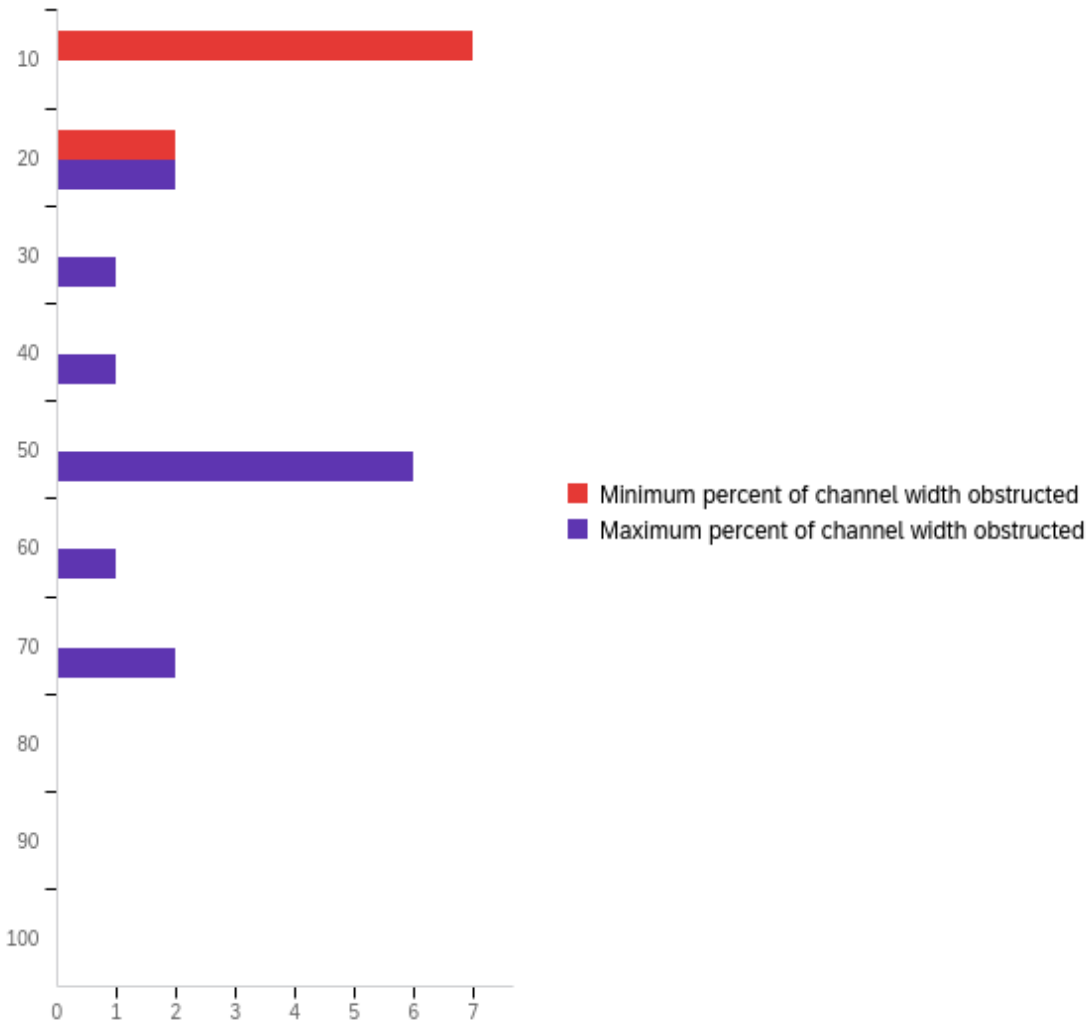


**Figure 45. Response to survey question 4. Response to Question 4 about the range of channel contraction percentages caused by temporary riprap construction platforms.**

***Question 5***

Based on your experience please estimate the maximum and minimum temporary access structures width in FEET (top width NOT the length the structure protrudes into the stream). You can SKIP this question if you would not like to provide an estimate.

***Response 5***

Responses to Question 5 indicated that the top width of temporary riprap construction platforms ranges between 10ft - 250ft. The most common maximum listed was 20ft, which is large enough for most construction vehicles to drive on.

- Minimum =10ft
- Maximum= 250ft
- Most common max=20ft

***Question 6***

How often are the temporary construction structures overtopped/flooded during the bridge construction period?

***Response 6***

Responses to Question 6 (Figure 46) indicated that installed structures usually do not overtop. Respondents indicated in related questions that determining the height to install temporary riprap construction platforms is dependent on site conditions and potential risk. Some DOTs base the height of the installed structure based on the average water depth, where others base it on a specified height above a given flood event.

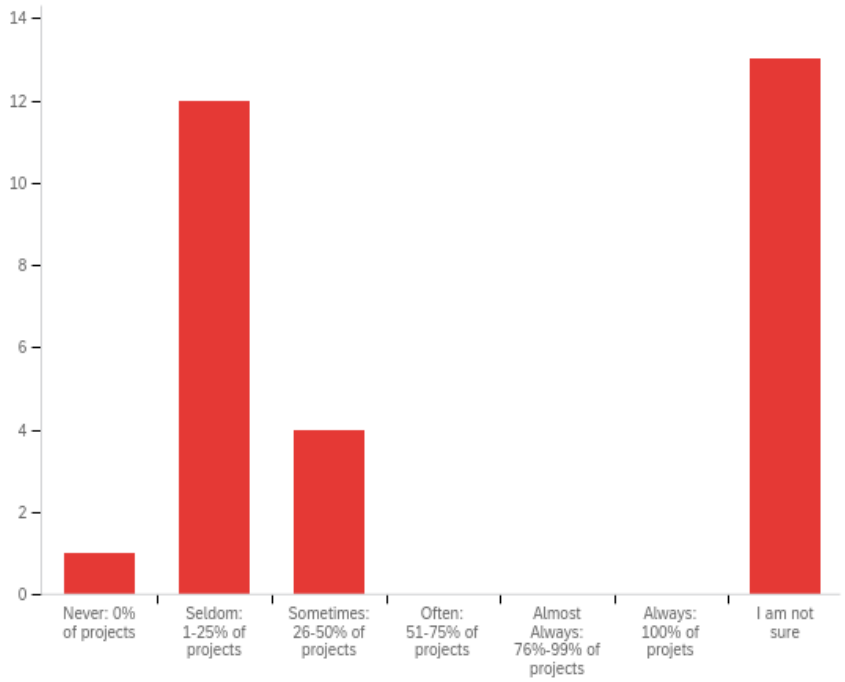


**Figure 46. Response to survey question 6. Response to Question 6 about the frequency that temporary riprap construction platforms overtop while installed in river channels for bridge construction.**

***Question 7***

On a scale of 1 to 5 how satisfied is your state DOT with the time it currently takes to respond to environmental permitting questions related to hydraulic and environmental effects of temporary bridge construction access features? 1=Inefficient/ Room for improvement 5=Very Efficient/Doesn't need improvement

***Response 7***

Responses to Question 7 (Figure 47) indicated that the majority of respondents believed the time it takes their state DOTs to respond to permitting agency questions related to hydraulic and environmental effects of temporary bridge construction access features to be average (score of 3). Only two respondents believed there was no room for improvement.

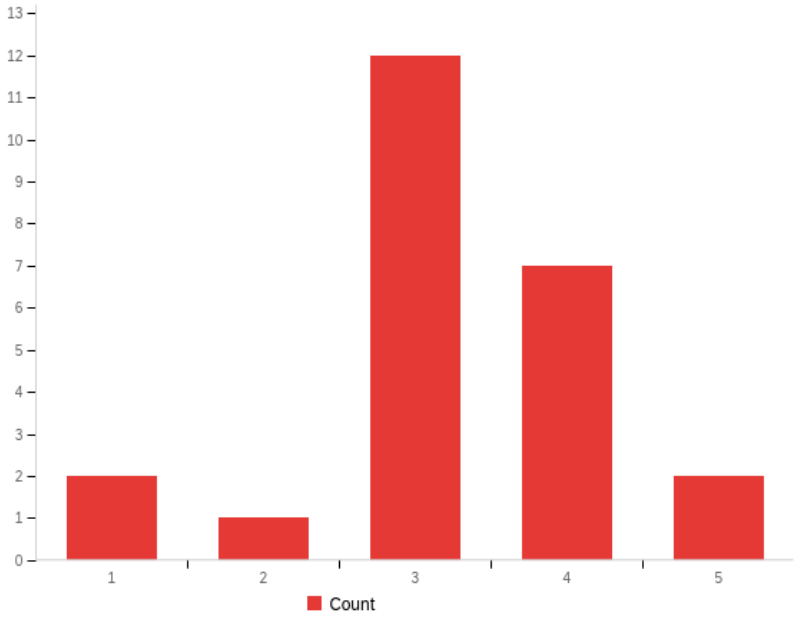


**Figure 47. Response to survey question 7. Response to Question 7 where respondents ranked on a scale of 1 to 5 how satisfied they were with their state DOTs time to respond to environmental permitting questions related to hydraulic and environmental effects of temporary bridge construction access features. 1=Inefficient/ Room for improvement 5=Very Efficient/Doesn't need improvement.**

***Question 8***

How effective are your current state DOT responses at addressing all environmental permitting questions about temporary in-stream structures used for bridge construction?

***Response 8***

Responses to Question 8 (Figure 48) indicated that the majority of respondents found their state DOTs to be moderately effective at addressing all environmental permitting agency questions about temporary bridge construction access features.

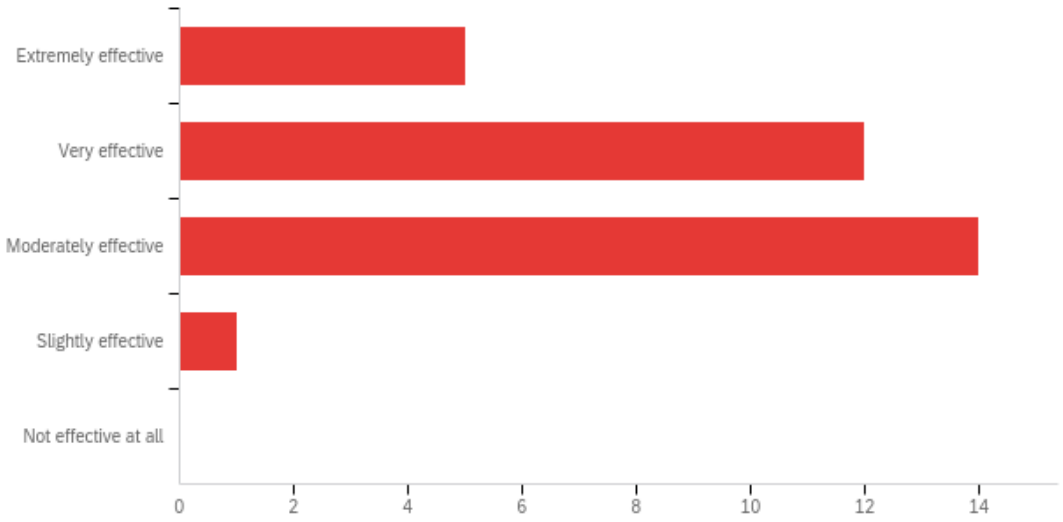


**Figure 48. Response to survey question 8. Response to Question 8 about the effectiveness of state DOTs in addressing all environmental permitting questions about temporary in-stream structures used for bridge construction.**

***Question 9***

Does your State DOT have a specific protocol, tool, or guidelines for responding to permitting agency concerns about the temporary structures used for bridge construction?

***Response 9***

Responses to Question 9 (Figure 49) indicated most respondents have a specific protocol, tool or guidelines for responding to permitting agency concerns about temporary riprap construction platforms. However, seven respondents indicated they did not have specific methods to respond to permitting agencies, suggesting some DOTs may still need assistance developing tools and guidelines.

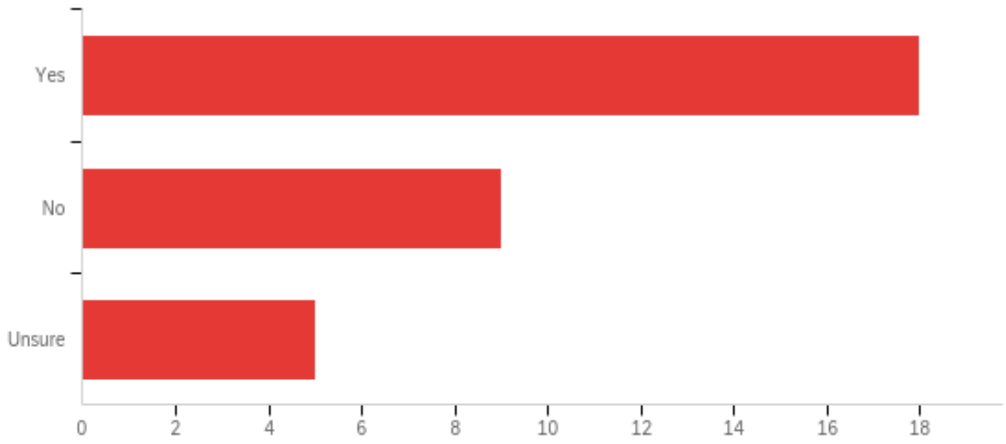


**Figure 49. Response to survey question 9. Response to Question 9 about the availability of a specific protocol, tool, or guidelines for responding to permitting agency concerns about temporary in-stream structures used for bridge construction.**

***Question 10***

Do you think there is room for improvement on how your State DOT responds to environmental permitting agency concerns about temporary in-stream structures?

***Response 10***

Responses to Question 10 (Figure 50) indicated that the majority of respondents believe there is room for improvement on how their state DOTs respond to environmental permitting agency concerns about temporary riprap construction platforms.

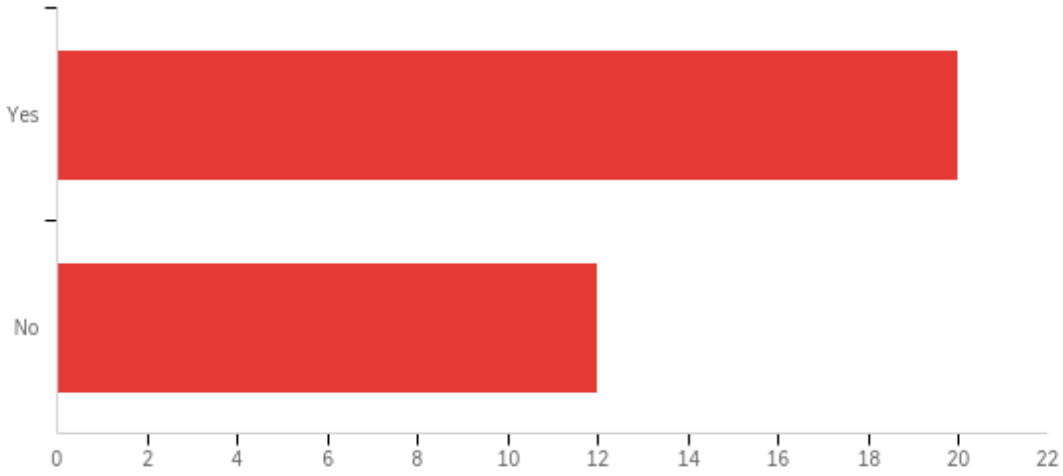


**Figure 50. Response to survey question 10. Response to Question 10 about the respondent's opinion on room for improvement on how their state DOTs respond to environmental permitting agency concerns about temporary riprap construction platforms.**

***Question 11***

How do you think your State DOT could improve on answering environmental permitting concerns? Select ALL that apply.

*This question was only asked to respondents that believed there was room for improvement in Question 10.

***Response 11***

Respondents to Question 11 most commonly selected that the development of a standard tool to estimate potential impacts due to temporary riprap construction platforms would help their state DOT improve on answering environmental permitting agency concerns (Figure 51). Results from this thesis are being used to develop such a tool to fill this need.

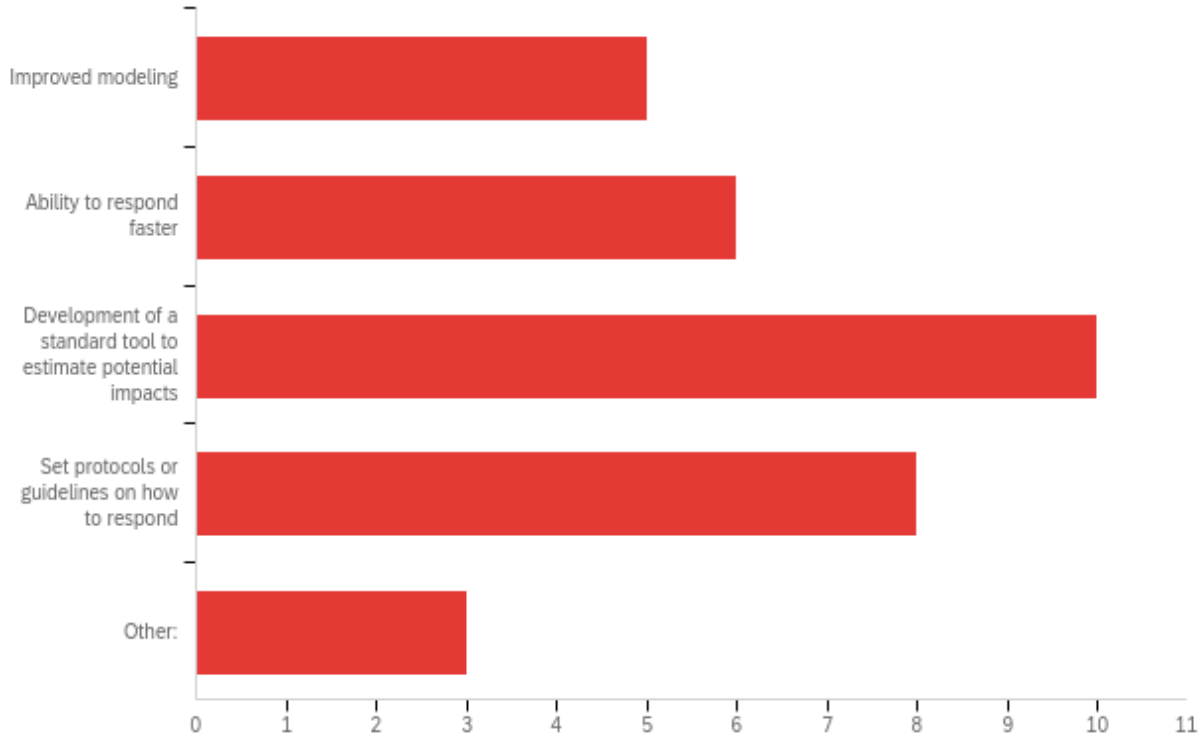


**Figure 51. Response to survey question 11. Response to Question 11 about the respondent's opinion on how to improve upon their state DOTs ability to respond to environmental permitting agency concerns about temporary riprap construction platforms.**

***Question 12***

What do you think are the main concerns of the permitting agencies regarding environmental impacts from temporary-in stream bridge construction access structures? Drag and drop the issues into the box you think best describes the level of importance/concern.

***Response 12***

Responses to Question 12 suggested shear changes and maximum scour depth are not typically the main concerns of environmental permitting agencies when implementing temporary riprap construction platforms for bridge construction (Figure 52). Shear changes (bed shear stress) were listed most commonly as sometimes a concern. Velocity changes, bank erosion, endangered

species, general habitat quality and quantity and water quality were all selected as most commonly being the main concern.

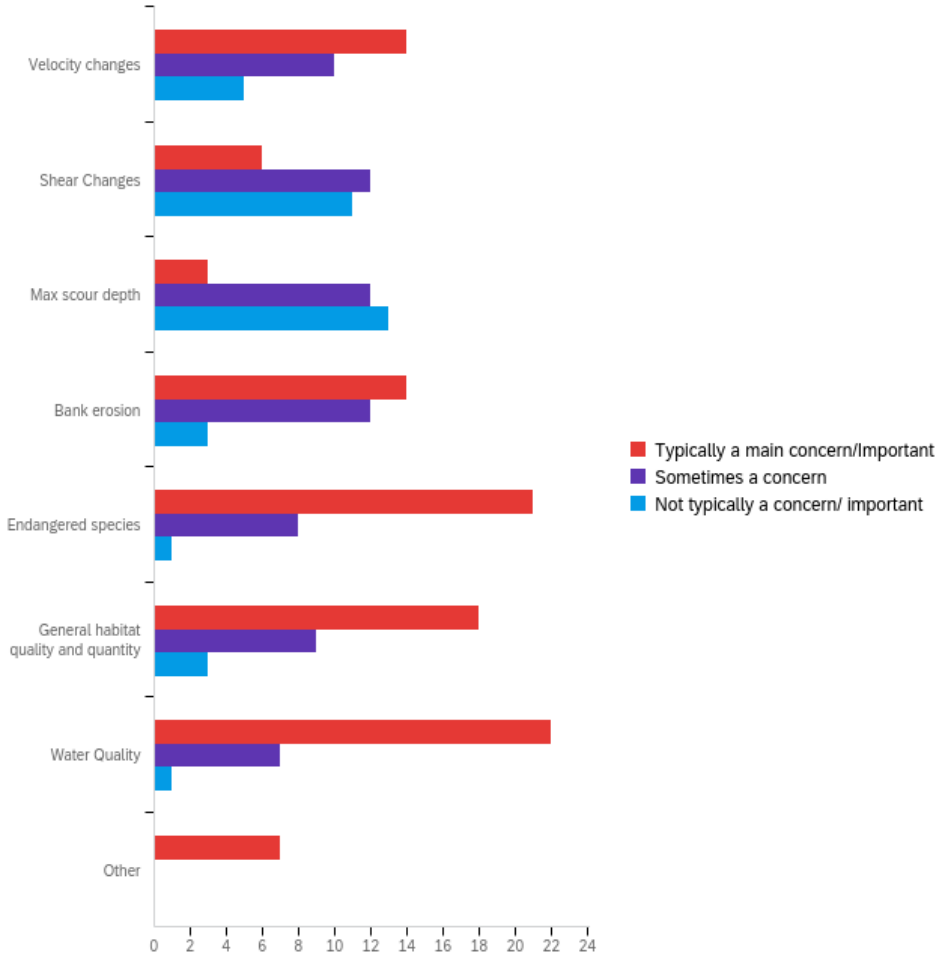


**Figure 52. Response to survey question 12. Response to Question 12 about the respondent's opinion on the main concerns of permitting agencies regarding environmental impacts from temporary in-stream bridge construction access structures.**

## APPENDIX D. EXAMPLE FIELD DATA COLLECTION FORM

**River Name/Location: _____**

**Date: _____ Time: _____**

**Observers: _____**

**Channel Description:**

Manning's n estimate: _____

**Basic Channel Geometry:**

Jetty Length (perpendicular to flow direction): _____ft

Channel Width (at location of jetty): _____ft

Discharge (estimate or from gage): _____$ft^3/s$

Channel slope (estimate or survey): _____ft/ft

Water Depth (optional): _____ft

Size of dominant bed material (optional): _____ in or mm (circle one)

**Bank #1 Condition and Geometry:**

Location (e.g., 100 ft downstream of jetty, right bank):

Current condition (e.g. evidence of erosion):

Vegetation on bank face (if yes, describe type and density):

Bank material type (e.g. gravel, sand, silt, clay, or mixture):

Size of bank material (if sand or gravel): _____in or mm (circle one)

Bank height (from top of bank to channel bed): _____ft

Bank angle: _____ degrees or H:V (circle one)

**Bank #2 Condition and Geometry:**

Location (e.g., 100 ft downstream of jetty, right bank):

Current condition (e.g. evidence of erosion):

Vegetation on bank face (if yes, describe type and density):

Bank material type (e.g. gravel, sand, silt, clay, or mixture):

Size of bank material (if sand or gravel): _____ in or mm (circle one)

Bank height (from top of bank to channel bed): _____ft

Bank angle: _____ degrees or H:V (circle one)

# REFERENCES


Ali, Md. Shahjahan., M.M. Hasan, and M. Haque. 2017. "A Two-Dimensional Simulation of Flows in an Open Channel with Groin-Like Structures by IRIC Nays2DH." *Math*, 1–10.

American Road and Transportation Builders Association (ARTBA). 2020. *Bridge Report*. https://artbabridgereport.org/

American Society of Civil Engineers (ASCE). 2017. *Infrastructure Report Card.* https://www.infrastructurereportcard.org/

Bledsoe, B.P., Stein, E.D., Hawley, R.J., Booth, D. 2012. "Framework and Tool for Rapid Assessment of Stream Susceptibility to Hydromodification." *Journal of American Water Resources Association* 48, 788–808.

Brown, S. 1985. *Design of Spur-Type Streambank Stabilization Structures*. U.S. DOT Federal Highway Administration, FHWA/RD-84/101, McLean, Virginia.

Brunner, G.W. 2016a. *HEC-RAS River Analysis System User's Manual.* U.S. Army Corps of Engineers, Davis, California. https://www.hec.usace.army.mil/software/hec-ras/documentation/HEC-RAS 5.0 Users Manual.pdf.

Brunner, G.W. 2016b. *HEC-RAS River Analysis System Hydraulic Reference Manual Version 5.0.* U.S. Army Corps of Engineers, Davis, California.

Chow, V. Te. 1959. *Open-Channel Hydraulics*. McGraw Hill Book Company, Inc.

Church, M. 2006. "Bed Material Transport and the Morphology of Alluvial River Channels." *Annual Review of Earth and Planetary Sciences* 34, 325–354.

Dey, S. and A.K. Barbhuiya. 2005. “Flow Field at a Vertical-Wall Abutment.” *Journal of Hydraulic Engineering* 131, 1126–1135.

Duan, J.G. 2009. “Mean Flow and Turbulence around a Laboratory Spur Dike.” *Journal of Hydraulic Engineering* 135, 803–811.

Duan, J.G., L. He, X. Fu, and Q. Wang. 2009. “Mean Flow and Turbulence around Experimental Spur Dike.” *Advances in Water Resources* 32, 1717–1725.

Ettema, R. and M. Muste. 2004. “Scale Effects in Flume Experiments on Flow around a Spur Dike in Flatbed Channel.” *Journal of Hydraulic Engineering* 130, 635–646.

Fischenich, C. and M. Landers. 2000. *Computing Scour*. ERDC TN-EMRRP-SR-05. Vicksburg, MS. https://sav.el.erdc.dren.mil/elpubs/pdf/sr05.pdf

Goodell, C. 2014. *Breaking the HEC-RAS Code: A User’s Guide to Automating HEC-RAS*. H2ls, Portland, OR.

Haschenburger, J.K. 1999. “A Probability Model of Scour and Fill Depths in Gravel-Bed Channels*.” Water Resources Research* 35:2857–2869.

Ho, J., H.K. Yeo, J. Coonrod, and W.-S. Ahn. 2007. “Numerical Modeling Study for Flow Pattern Changes Induced by Single Groyne.” *Proceedings of the Congress-International Association for Hydraulic Research.* http://66.221.229.18/pdfs/tp/wat_env_tp/numerical-modeling-study-for-flow-pattern-changes-induced-by-single-groyne-25-07.pdf.

Jeon, J., J.Y. Lee, and S. Kang. 2018. “Experimental Investigation of Three-Dimensional Flow Structure and Turbulent Flow Mechanisms Around a Nonsubmerged Spur Dike With a Low Length-to-Depth Ratio.” *Water Resources Research* 54, 3530–3556.

Karim, O.A. and K.H.M. Ali. 1999. “Simulation of the Flow Pattern Around Spur Dykes Using FLUENTS.” *Jurnal Kejuruteraan* 11, 3–19.

Knighton, D. 1998. *Fluvial Forms & Processes.* Oxford University Press Inc., New York, NY.

Koken, M. and G. Constantinescu. 2008. “An Investigation of the Flow and Scour Mechanisms Around Isolated Spur Dikes in a Shallow Open Channel: 1. Conditions Corresponding to the Initiation of the Erosion and Deposition Process.” *Water Resources Research* 44:1–19.

Koken, M. 2011. “Coherent Structures around Isolated Spur Dikes at Various Approach Flow Angles.” *Journal of Hydraulic Research* 49:736–743.

Kuhnle, R.A., Jia, Y., Alonso, C. V. 2008. “Measured and Simulated Flow Near a Submerged Spur Dike.” *Journal of Hydraulic Engineering* 134, 916–924.

Lagasse, P.F., P.E. Clopper, J.E. Pagan-Ortiz, L.W. Zevenbergen, L. A. Arneson, J.D. Schall, and L.G. Girard. 2009a. *Bridge Scour and Stream Instability Countermeasures: Experience, Selection, and Design Guidance-Volume 1, Third Edition*. U.S. DOT Federal Highway Administration, FHWA NHI HEC-23.

Lagasse, P.F., P.E. Clopper, J.E. Pagan-Ortiz, L.W. Zevenbergen, L. A. Arneson, J.D. Schall, and L.G. Girard. 2009. *Bridge Scour and Stream Instability Countermeasures: Experience, Selection, and Design Guidance-Volume 2, Third Edition.* U.S. DOT Federal Highway Administration, FHWA NHI HEC-23.

Li, G., L. Lang, and J. Ning. 2013. *3D Numerical Simulation of Flow and Local Scour around a Spur Dike.* IAHR World Congress.

Lumley, T. 2020. *Package "Leaps": Regression Subset Selection*. https://cran.r-project.org/package=leaps.

Melville, B.W. 1992. "Local Scour at Bridge Abutments." *Journal of Hydraulic Engineering* 118, 615–631.

Molinas, A., K. Kheireldin, and B. Wu. 1998. "Shear Stress around Vertical Wall Abutments." *Journal of Hydraulic Engineering* 124:822–830.

Molls, T., M. Hanif Chaudhry, and K. Wasey Khan. 1995. "Numerical Simulation of Two-Dimensional Flow near a Spur-Dike." *Advances in Water Resources* 18:227–236.

Mueller, D.S. and C.R. Wagner. 2009. "Measuring Discharge with Acoustic Doppler Current Profilers from a Moving Boat." *U. S. Geological Survey Techniques and Methods* 3-A22. Reston, Virginia, p. 72.

Federal Highway Administration (FHA). 2019. *National Bridge Inventory ASCII Files 2019*. https://www.fhwa.dot.gov/bridge/nbi/ascii2019.cfm.

Oullion, S. and D. Dartus. 1997. "Three-Dimensional Computation of Flow Around Groyne." *Journal of Hydraulic Engineering* 123, 962–970.

Pandey, M., Z. Ahmad, and P.K. Sharma. 2018. "Scour Around Impermeable Spur Dikes: A Review." *ISH Journal of Hydraulic Engineering* 24, 25–44.

Parker, G., P.R. Wilcock, C. Paola, W.E. Dietrich, and J. Pitlick. 2007. "Physical Basis for Quasi-Universal Relations Describing Bankfull Hydraulic Geometry of Single-Thread Gravel Bed Rivers." *Journal of Geophysical Research* 112, F04005.

Pollen-Bankhead, N., Simon, A. 2010. “Hydrologic and Hydraulic Effects of Riparian Root Networks on Streambank Stability: Is Mechanical Root-Reinforcement the Whole Story?” *Geomorphology* 116, 353–362. https://doi.org/10.1016/j.geomorph.2009.11.013

R Core Team. 2019. *R: A Language and Environment for Statistical Computing.* Vienna, Austria. https://www.R-project.org/

Radspinner, R.R., P. Diplas, A.F. Lightbody, and F. Sotiropoulos. 2010. “River Training and Ecological Enhancement Potential Using In-Stream Structures.” *Journal of Hydraulic Engineering* 136, 967–980.

Rajaratnam, N. and B.A. Nwachukwu. 1983a. “Erosion Near Groyne-Like Structures.” *Journal of Hydraulic Research* 21, 227–287.

Rajaratnam, N. and B.A. Nwachukwu. 1983b. “Flow Near Groin-Like Structures.” *Journal of Hydraulic Engineering* 109, 463–480.

SAS Institute Inc. 2018. *JMP 14 Basic Analysis.*

Seed, D.J. 1997. *Guidelines on the Geometry of Groynes for River Training.* HR Wallingford, Report SR 493.

Shields, F. 1983. “Design of Habitat Structures for Open Channels.” *Journal of Water Resources Planning and Management* 109, 331–344.

Simon, A., Curini, A., Darby, S.E., Langendoen, E.J. 2000. “Bank and Near-Bank Processes in an Incised Channel.” *Geomorphology* 35, 193–217. https://doi.org/10.1016/S0169-555X(00)00036-2

Simon, A., Pollen-Bankhead, N., Thomas, R.E. 2011. “Development and Application of a Deterministic Bank Stability and Toe Erosion Model for Stream Restoration” In: Simon,

A., Bennett, S., Castro, J. (Editors) *Stream Restoration in Dynamic Fluvial Systems: Scientific Approaches, Analyses, and Tools*. American Geophysical Union, Washington, D.C. 453–474.

Federal Transit Administration (FTA). 2019. *Status of the Nation's Highways, Bridges and Transit: Conditions and Performance, 23rd Edition*. Report to Congress. https://www.fhwa.dot.gov/policy/23cpr/pdfs/23cpr.pdf

Terzaghi, K. 1943. *Theoretical Soil Mechanics*. Wiley, New York.

Thorne, C.R. 1982. "Processes and Mechanisms of Bank Erosion." In: Hey, R., Bathurst, J., Thorne, C, editors, *Gravel Bed Rivers*. Wiley, Chichester, pp. 227–271.

Tingsanchali, T. and S. Maheswaran. 1990. "2-D Depth-Averaged Flow Computation Near Groyne." *Journal of Hydraulic Engineering* 116, 71–86.

USACE. 2018. *Regional Permits 30, 31, 32, 33, 34, and 35 For Public Transportation Projects Within the State of Georgia.* Savannah District of the U.S. Army Corps of Engineers.

Yazdi, J., H. Sarkardeh, H.M. Azamathulla, and A.A. Ghani. 2010. "3D Simulation of Flow around a Single Spur Dike with Free-Surface Flow." *International Journal of River Basin Management* 8, 55–62.

Yeo, H.-K., J.-G. Kang, and S.-J. Kim. 2005. "An Experimental Study on Tip Velocity and Downstream Recirculation Zone of Single Groyne Conditions." *KSCE Journal of Civil Engineering* 9, 29–38.

Zhang, H. and H. Nakagawa. 2008. "Scour around Spur Dyke: Recent Advances and Future Researches." *Annuals of Disaster Prevention Res. Institute.* Kyoto University, 633–6 52.

Zhang, H., H. Nakagawa, K. Kawaike, and Baba Yasuyuki. 2009. “Experiment and Simulation of Turbulent Flow in Local Scour around a Spur Dyke.” *International Journal of Sediment Research* 24, 33–45.